

DETERMINATION OF THE PRECONSOLIDATION PRESSURE  
FOR A SENSITIVE MARINE CLAY.

by

MONA BECHAI

Submitted in partial fulfillment  
of the requirements for the degree of  
Master of Applied Science

Department of Civil Engineering  
School of Graduate Studies  
University of Ottawa  
Ottawa, Canada

1974

### ACKNOWLEDGMENTS

The author wishes to express her gratitude to Professor D. H. Shields, under whose direction and supervision the project was carried out, for his constant help and guidance throughout.

Financial assistance by the N.R.C. Grant No. A7376 is gratefully acknowledged.

The author also wishes to thank her husband, N. R. Bechai for designing, building and testing the automatic control system used to carry out the controlled gradient consolidation tests, and for supplying Appendix B.

Sincere thanks are also due to Mr. C. V. Trites of the Ontario Housing Corporation for the permission to obtain clay samples from lands belonging to the corporation, to Professor J. D. Scott of the Civil Engineering Department, University of Ottawa, for his advice and valuable suggestions; to Mr. N. S. Verma, graduate student, for his help and advice concerning the testing techniques; and to Messrs. R. Toombs and E. Moniz, for their kind help during the field work. Finally, the author wishes to thank Mrs. W. Storto for her patience in typing the manuscript.

## PREFACE

The exact determination of the preconsolidation pressure,  $p_c$ , is often a main factor in the design of structures on clay. The conventional oedometer test, based on the Terzaghi theory of one dimensional consolidation, is the most widely used basis for the determination of  $p_c$ . In this test,  $p_c$  is not determined directly but is estimated by means of the Casagrande or Schmertmann constructions.

New methods of consolidation testing have been introduced in the past few years, each presenting some advantages over the conventional method.

One of these new methods, the controlled gradient consolidation test, seems to have an important advantage over the others. This is an easy, direct way of determining  $p_c$  from a time-effective stress plot.

The intent of this research program is to investigate the applicability of the controlled gradient consolidation test for the measurement of the preconsolidation pressure of a sensitive marine clay. The results are compared to those from conventional tests.

Tests are performed on block samples of Leda clay, using 3 in. and 6 in. diameter Rowe cells.

The results show that the controlled gradient consolidation test on a sensitive marine clay results in a

better defined strain-log effective stresses plot than the conventional tests. It is found that the  $p_c$  value obtained from the time-effective stress plot always compares favourably to the value obtained from the strain-log effective pressure plot. It is also found that the  $p_c$  is easily obtained from a stress-strain curve plotted to natural scale that results from a controlled gradient test on Leda clay.

From the analysis of the results it seems that the breakdown of the structure of Leda clay begins to occur when the applied stress reaches 75 to 90% of the difference between the preconsolidation pressure and the in situ overburden pressure.

Considerable difference is found between the  $p_c$  values obtained from 3 in. and the 6 in. diameter samples. The reason for this is investigated and it is found to be due to the membrane of the Rowe cell whose stiffness affects the 3 in. diameter cell results. Calibration difficulties, which are not resolved, are also found with the Rowe cells. Modification of the cells appears in order before test results can be used with confidence for engineering design.

TABLE OF CONTENTS

	<u>Page</u>
ACKNOWLEDGMENTS	i
PREFACE	ii
TABLE OF CONTENTS	iv
LIST OF TABLES AND ILLUSTRATION	vii
CHAPTER 1	1
INTRODUCTION	1
CHAPTER 2	3
REVIEW OF PREVIOUS WORK ON THE SUBJECT	3
2.1. Theory of Consolidation	3
2.2. Conventional Consolidation Test	9
2.2.1 Interpretation of Test Results	9
2.2.2 The Influence of Load Increment Ratio	17
2.2.3 The Influence of Load Increment Duration	23
2.3. Constant Rate of Strain Test	26
2.4. Constant Rate of Loading Tests	28
2.5. Controlled Gradient Consolidation Test	29
2.6. Summary	32
CHAPTER 3	33
RESEARCH PROGRAM	33
3.1. Research Proposal	33
3.2. Testing Program	34

	<u>Page</u>
3.2.1 The Controlled Gradient Consolidation Tests	34
3.2.2 The Conventional Consolidation Tests	35
3.3 Testing Equipment	36
3.3.1 The Consolidation Cells	36
3.3.2 The Automatic Control Unit	38
3.4 The Soil	39
3.4.1 Geological Review	39
3.4.2 Properties of the Leda Clay	41
3.4.3 Location and Description of the Site	43
3.4.4 Sampling and Storage	46
3.4.5 Index Properties	46
3.5 Testing Method	47
3.5.1 Sample Preparation	47
3.5.2 Testing Procedure	49
CHAPTER 4	51
TEST RESULTS AND DISCUSSION OF RESULTS	51
4.1 Calibration of the Rowe Cells	51
4.2 The Controlled Gradient Consolidation Tests	54
4.2.1 General Comments	54
4.2.2 Effect of Sample Size	66
4.2.3 Effect of the Hydraulic Gradient	81

	<u>Page</u>
4.2.4 Effect of the Variation in $p_o$ and $p_c$	86
4.3 The Conventional Consolidation Tests	93
4.3.1 Effect of the Load Duration	99
4.3.2 Effect of the Load Increment Ratio	99
4.3.3 Effect of the Variation in $p_o$ and $p_c$	99
4.4 Comparison of Results from the Controlled Gradient Consolidation Tests and the Con- ventional Tests	107
4.4.1 The $\epsilon$ - $\log p'$ curve	107
4.4.2 The $\epsilon$ - $p'$ curve	113
4.4.3 The $c_v$ - $\log p'$ and $k_v$ - $\log p'$ relation- ships	113
4.5 Comments Concerning the Clay	116
CHAPTER 5	119
CONCLUSIONS AND RECOMMENDATIONS FOR FURTHER RESEARCH	119
LIST OF REFERENCES	123
APPENDIX A: ADDITIONAL REFERENCES	128
APPENDIX B: OTHER TESTS PERFORMED	129
APPENDIX C: AUTOMATIC CONTROL SYSTEM	133
APPENDIX D: PHOTOGRAPHS	139

LIST OF TABLES AND ILLUSTRATION

<u>Figure</u>		<u>Page</u>
2.1	Double-drained consolidation test	6
2.2	Theoretical time consolidation curve for one dimensional consolidation	8
2.3	Effect of sampling disturbance on the "e-log p" curve	10
2.4	Casagrande construction for the determination of $p_c$	12
2.5	Schmertmann's method for the determination of $p_c$	14
2.6	Casagrande "log of time" curve fitting method	16
2.7	Taylor "square root of time" curve fitting method	18
2.8	Change in void ratio-log pressure relationship, for incremental loading tests	20
2.9	Effect of load-increment ratio on shape of dial reading-time curves	22
2.10	Compression log pressure curves for normal and long term incremental loading	25
2.11	Comparison of hydrostatic excess pressure during conventional test and controlled gradient test	31
3.1	The consolidation cell	37

<u>Figure</u>		<u>Page</u>
3.2	The Champlain Sea	40
3.3	Lambe's schematic diagram for one-dimensional consolidation	42
3.4	Ottawa-Hull Region	44
3.5	Test pit log	45
3.6	Particle size distribution curve	48
4.1	Attempts to calibrate a Rowe cell	52
4.2	Attempts to calibrate a Rowe cell	53
4.3	$\epsilon$ -log $p'$ plot-controlled gradient consolidation tests	55
4.4	$\epsilon$ - $p'$ plot-controlled gradient consolidation tests	56
4.5	$t$ - $p'$ plot. Controlled gradient consolidation tests	57
4.6	$c_v$ -log $p'$ and $k_v$ -log $p'$ plots. Controlled gradient consolidation tests	58
4.7a	Values of $m_v$ from controlled gradient tests on samples from 5 ft depth	61
4.7b	Values of $m_v$ from controlled gradient tests on samples from 7 ft depth	62
4.8	Summary of results of controlled gradient tests on samples from 5 ft depth	64
4.9	Summary of results of controlled gradient tests on samples from 7 ft depth	65

<u>Figure</u>		<u>Page</u>
4.10	Effect of sample size. Controlled gradient consolidation test	67
4.11	Effect of sample size. Controlled gradient consolidation test	69
4.12	Controlled gradient consolidation tests using a mechanical loading system	71
4.13	Controlled gradient consolidation tests using a mechanical loading system	72
4.14	Controlled gradient consolidation tests using a mechanical loading system	73
4.15	Effect of sample size. Controlled gradient consolidation tests	75
4.16	Effect of sample size. Controlled gradient consolidation tests	76
4.17	Effect of sample size. Controlled gradient consolidation tests	77
4.18	Effect of sample size. Controlled gradient consolidation tests	78
4.19	Effect of sample size. Controlled gradient consolidation tests	79
4.20	Effect of sample size. Controlled gradient consolidation tests	80
4.21	Effect of $i$ . Controlled gradient consolidation tests	82
4.22	Effect of $i$ . Controlled gradient consolidation tests	83

<u>Figure</u>		<u>Page</u>
4.23	Effect of $i$ : Controlled gradient consolidation tests	84
4.24	Effect of $i$ : Controlled gradient consolidation tests	85
4.25	Effect of $i$ : Controlled gradient consolidation tests	87
4.26	Effect of $i$ : Controlled gradient consolidation tests	88
4.27	Variation of $p_c$ with depth for different controlled gradient tests	90
4.28	Effect of the depth of the sample. Controlled gradient consolidation tests	91
4.29	Effect of the depth of the sample. Controlled gradient consolidation tests	92
4.30	$\epsilon$ -log $p'$ curve. Conventional consolidation tests	94
4.31	$\epsilon$ - $p'$ plot. Conventional consolidation tests	95
4.32	$\epsilon$ -log $p'$ curve for a short duration test before and after correction	98
4.33	Summary of results of incremental loading tests on samples from 5 ft	100
4.34	Summary of results of incremental loading tests on samples from 7 ft	101
4.35	Effect of load duration. Conventional consolidation tests	102

<u>Figure</u>		<u>Page</u>
4.36	Effect of load duration. Conventional consolidation tests	103
4.37	Effect of load increment ratio and duration. Conventional consolidation tests	104
4.38	Effect of load increment ratio and duration. Conventional consolidation tests	105
4.39	Variation of $p_c$ with depth for incremental loading tests	106
4.40	Comparison between controlled gradient and conventional consolidation tests	108
4.41	Comparison between controlled gradient and conventional consolidation tests	109
4.42	Range of variation of results for samples from 5 ft depth	111
4.43	Range of variation of results for samples from 7 ft depth	112
4.44	Comparison between controlled gradient and conventional consolidation tests	114
4.45	Comparison between controlled gradient and conventional consolidation tests	115
4.46	Correlation between $\frac{p_c}{p_o}$ ratio and the P.I. for normally consolidated clays	117
B.1	Plasticity chart	130
C.1	Timing diagram	134
C.2	Block diagram of the automatic control system	137

## CHAPTER 1

### INTRODUCTION

The exact determination of the preconsolidation pressure,  $p_c$ , is often of primary importance for the design of structures on clay. The conventional oedometer test, based on the Terzaghi theory of one dimensional consolidation, is the most widely used basis for the determination of  $p_c$ . Many investigators have pointed out that variations in the testing procedure result in variations in the estimated value of  $p_c$ .

New methods of consolidation testing have been introduced in the past few years. Because the  $p_c$  value is affected by the testing procedure, it is expected that the  $p_c$  obtained from different testing methods will be different. A comparison is necessary in order to evaluate each method. The new consolidation methods, together with the conventional method, are reviewed in Chapter 2.

One of these new methods, the controlled gradient consolidation test, seems to have one important advantage over the others. This is an easy, direct way for the determination of the preconsolidation pressure.

A research proposal is presented in Chapter 3. The intent is to investigate experimentally the applicability of the controlled gradient test for testing a sensitive

marine clay, and to compare the results to those from conventional tests.

Tests were performed on specimens from block samples of soft, Leda clay. Results and comparisons are given in Chapter 4; conclusions and recommendations will be found in Chapter 5.

In this thesis, only one new method of consolidation testing is investigated in detail. The findings are intended to be a contribution towards the overall study of all current methods of consolidation testing, in particular, as they apply to a sensitive marine clay.

## CHAPTER 2

### REVIEW OF PREVIOUS WORK ON THE SUBJECT

Strictly speaking the determination of the pre-consolidation pressure does not involve consolidation theory provided that the average effective stress within the sample can be determined and a plot made of strain versus effective stress. However, in practice, the porewater pressure is usually not measured. Instead the effective stress is assumed to be equal to the applied load, i.e., the average excess porewater pressure is equal to zero, after 100% consolidation has occurred under a particular load increment. It was felt necessary, therefore, to review and discuss the theory of consolidation in some detail, as well as to review previous work on the prediction of preconsolidation pressure per se.

#### 2.1 Theory of Consolidation

An increase in the magnitude of compressive stresses acting on a soil mass will generally result in a decrease in volume. This volume decrease will cause settlement of structures founded on the soil.

The settlement of structures founded on clay is due to four different phenomena: (22)

1. Shear strains developing simultaneously with the change in load with no volume change (immediate or initial settlement).

2. Time dependent shear strains with no volume change (creep).
3. Time dependent volume changes occurring during dissipation of porewater pressures (consolidation).
4. Time dependent volume changes after excess pore pressures are dissipated (secondary compression).

Consider the third phenomenon for a saturated clay mass. The compressibility of the soil skeleton is large compared to the compressibility of water. Consequently any increase in applied pressure is immediately transformed into an increase in porewater pressure, which results in an hydraulic gradient. If drainage is permitted, the porewater will flow out of the soil mass and the mass will begin to compress. In the same time a portion of the newly applied pressure is transferred to the soil skeleton, due to the gradual reduction in the excess porewater pressure. The process continues until all the applied pressure is finally carried by the soil skeleton. This process is called consolidation.

Terzaghi's 1923 theory of one dimensional consolidation, (see for example reference 39), is based on the following assumptions:

- The soil is homogeneous, isotropic and completely saturated.
- The porewater flow and the compression of the clay take place in only one direction.
- The soil particles and the water are incompressible.
- Darcy's law is valid.
- The permeability ( $k_v$ ) and the coefficient of compressibility ( $a_v$ ) of the soil are constant for any particular load increment.

- The time lag of consolidation is entirely due to the low permeability of the soil.
- At any time during consolidation, the intergranular pressure in the soil structure, plus the porewater pressure, are equal to the applied load.
- Deformations are small compared to the initial thickness of the clay layer.

The differential equation for one dimensional consolidation according to these assumptions is expressed as:

$$c_v \frac{d^2 u}{dz^2} = \frac{du}{dt} \quad (2.1)$$

where

$c_v$  = coefficient of consolidation =  $\frac{k_v}{\gamma_w m_v}$  = a constant

$k_v$  = coefficient of permeability

$\gamma_w$  = unit weight of water

$m_v$  = coefficient of volume compressibility

$u$  = porewater pressure varying with the time,  $t$  and with the depth,  $z$ .

The solution of this equation for the case of a soil sample of thickness  $2H$ , confined in a ring, and draining from both sides (Fig. 2.1) is:

$$u_z = \sum_{m=0}^{\infty} \frac{2u_0}{M} \left( \sin \frac{Mz}{H} \right) E^{-M^2 T_v} \quad (2.2)$$

where

$u_z$  = porewater pressure at any depth  $z$ , at any time  $t$

$u_0$  = initial porewater pressure

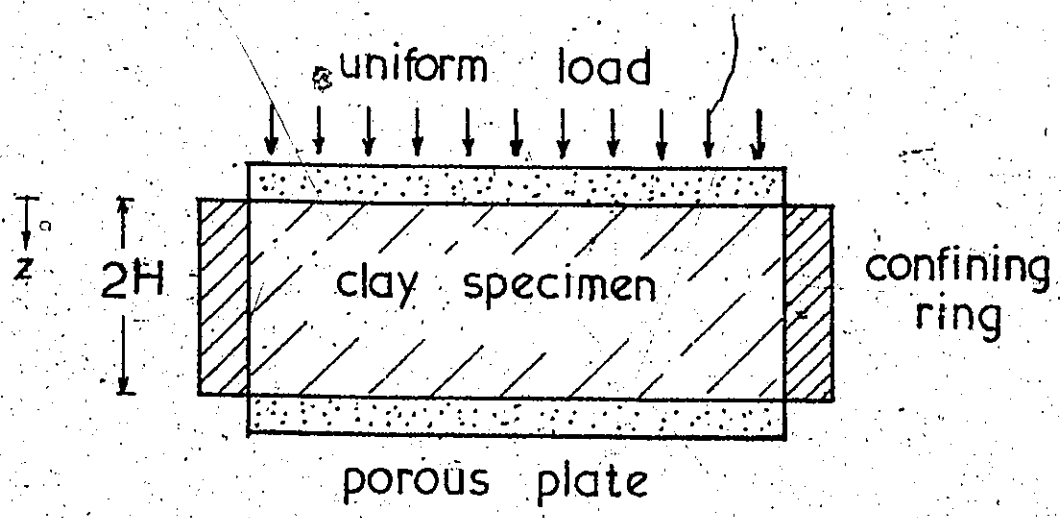


FIGURE 2.1

Double-drained consolidation test

$$M = \frac{2m+1}{2} \pi \quad \text{where } m = 0, 1, 2, 3, \dots$$

$$T_v = \text{time factor} = \frac{c_v t}{H^2}$$

e = base of the natural logarithm.

For a small element within the sample at depth z,  $u_z$  at any time is expressed as the degree of consolidation,  $U_z$ , where

$$U_z = \frac{u_o - u_z}{u_o} \% \quad (2.3)$$

which is also equal to the change in height of the element at time t divided by the total change in height of the element for the load increment.

The average degree of consolidation for the sample is expressed as  $\bar{U}$ . A plot of  $\bar{U}$  vs  $T_v$  can be made (Fig. 2.2) which permits the determination of the time rate of settlement.

Many investigators have attempted to add refinements to the Terzaghi theory. For example, Taylor in 1948 (38) introduced the concept of plastic structural resistance; Schiffman in 1958 (32), tried to solve the problem for time dependent loading and variable permeability; Hansbo in 1960 (16) accounted for the non-linearity of Darcy's law at small gradients; Janbu's approach to the problem in 1965 (17) was to consider a non-linear stress-strain relationship; and Barden in 1965 (2) assumed a non-linear viscosity.

However, these refinements added complications to the problem while the accuracy of the solution was not

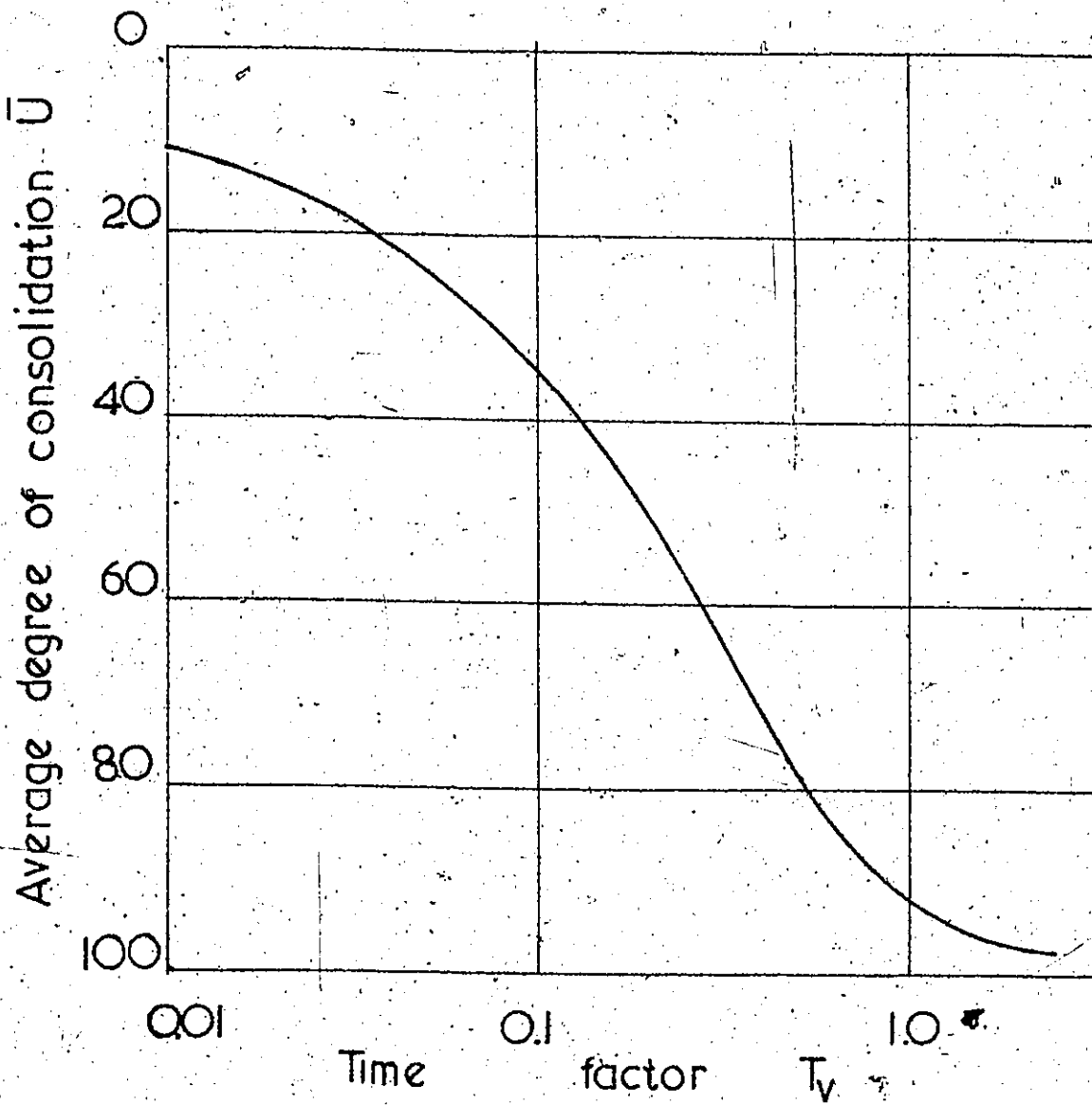


FIGURE 2.2

Theoretical time consolidation curve for one dimensional consolidation

greatly improved. For this reason, the Terzaghi theory is still the most widely used.

## 2.2 Conventional Consolidation Test

The consolidation test provides a means for the determination of parameters such as  $m_v$ ,  $c_v$ ,  $C_c^*$  necessary for settlement calculations.

Based on earlier studies, (Taylor (38), Van Zelst (40), Casagrande (6)), certain standard procedures for carrying out the test and interpreting the data have been adopted. These procedures require samples about 3/4 ins. thick (2 cm) and 2 ins. in diameter (5 cm). The loads are applied in increments to the top of the sample, and compression is measured by means of a dial indicator. Each increment equals the previous consolidation pressure and is kept on for 24 hours. Dial readings are taken at certain specified time intervals.

### 2.2.1 Interpretation of test results

Using the data obtained from a consolidation test, the results can be represented graphically. A semi-log plot is generally used where the void ratios,  $e$ , are plotted vertically to a natural scale, and the effective stresses,  $p'$ , are plotted horizontally to a logarithmic scale. The result is an  $e$ -log  $p'$  curve, (Fig. 2.3). This curve is

---

\*  $C_c$  - Compression Index

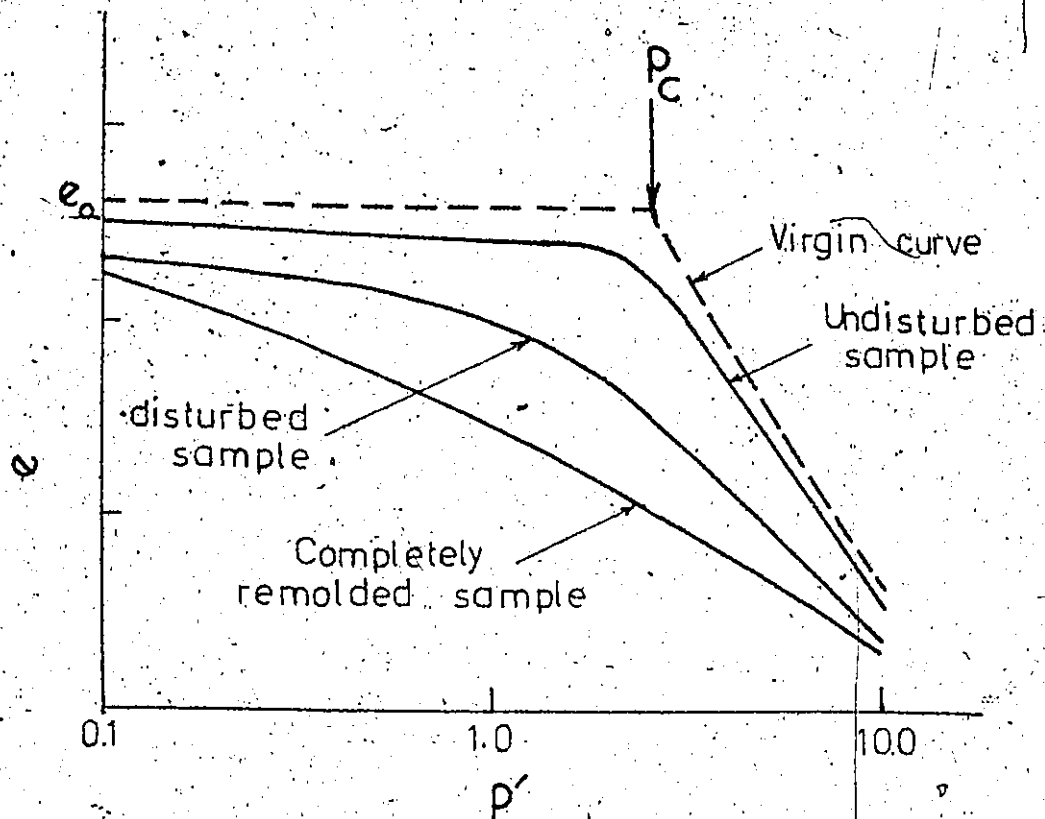


FIGURE 2.3

Effect of sampling disturbance on the "e-log p'" curve.

(After Léonards.)

used for the calculation of the magnitude of consolidation settlements which are likely to occur under certain loads. The void ratios in this plot are usually those corresponding to 100% consolidation under each load increment. (The methods of determination of 100% consolidation will be explained later). But according to A.S.T.M. standards (1973, part 11, Designation D.2435-70), "as an alternate" void ratios (or strains) using values obtained "after a selected time interval which shall include some of the secondary compression, and which shall be kept the same for each load increment" can also be used for such a plot.

For an undisturbed sample, the  $e$ -log  $p'$  curve usually starts with a nearly horizontal line; then after a sharp bend, it continues as a straight line of much steeper slope. The bend occurs when the stresses reach the preconsolidation pressure. This is equal to the overburden pressure in the case of normally consolidated clays. For overconsolidated clays it is equal to the maximum pressure the clay has even been subjected to in its geological history. (Under certain conditions the bend occurs at higher stresses than the true  $p_c$ , and a "quasi-preconsolidation pressure" is obtained - this is discussed later).

An empirical procedure was developed by Casagrande in 1936 (6) to determine the preconsolidation pressure from an  $e$ -log  $p'$  curve (Fig. 2.4). This method involves selecting the point of maximum curvature on the  $e$ -log  $p'$

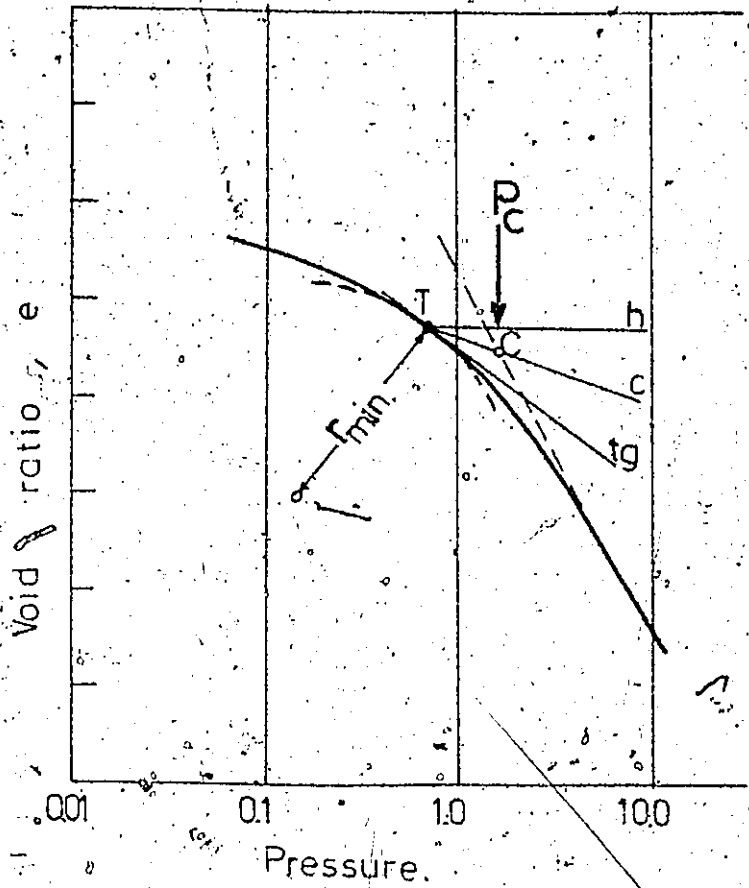


FIGURE 2.4

Casagrande construction }  
for the determination of  $P_c$   
(1936)

curve, drawing horizontal and tangent lines to the curve at this point, and bisecting the angle between them. The projection of the straight line portion of the curve intersects the bisector at a point corresponding to the preconsolidation pressure. But the shape of the  $e$ -log  $p'$  curve is strongly influenced by the amount of disturbance during sampling, storage, sample preparation, etc., (Fig. 2.3), and this in turn affects the  $p_c$  value obtained by the Casagrande method.

Schmertmann in 1955 (33) estimated that the true field virgin curve and the laboratory virgin curve meet at a void ratio equal to about  $0.42 e_0^*$ . Schmertmann's method for the determination of  $p_c$  involves unloading the specimen in steps in order to obtain a rebound curve (Fig. 2.5). The point  $p_0$  representing the actual overburden pressure is determined, and a line parallel to the rebound curve is drawn from this point. An assumed value of  $p_c$  is then selected on this line, and joined to the laboratory curve at  $0.42 e_0$  by a straight line. A void ratio reduction curve ( $\Delta e$ -log  $p'$  curve) is drawn where  $\Delta e$  is the difference in void ratios between the assumed virgin curve and the laboratory curve. Other values of  $p_c$  are assumed, and the procedure repeated until a symmetrical void ratio reduction curve is obtained. The corresponding  $p_c$  is then representative of the preconsolidation pressure, and the virgin curve obtained is considered to be the in-situ compression curve,

\*  $e_0$  - initial void ratio.

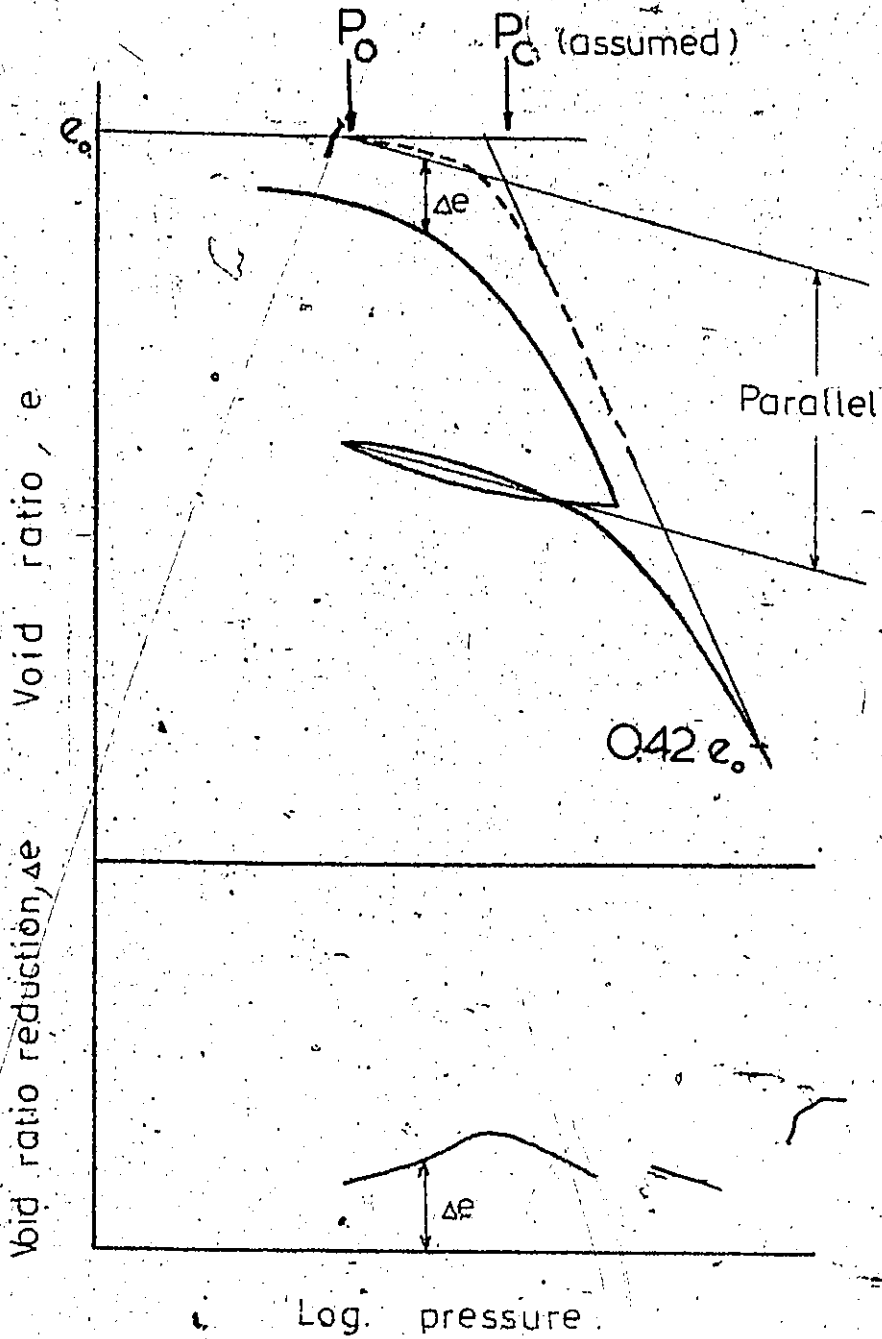


FIGURE 2.5

Schmertmann's method for the  
determination of  $P_c$

(1955)

The coefficient of consolidation is also determined by the use of curve-fitting methods.

The Casagrande log of time method requires a plot of dial readings versus log of time for each increment of load (Fig. 2.6). The first portion of the plot being parabolic, the dial reading corresponding to zero time can be determined. It may not coincide with the actual initial reading due, for example, to the possibility of air bubbles delaying the consolidation process. The dial reading corresponding to 100% consolidation is estimated to correspond to the intersection of the tangent to the curve at the point of contraflexure and the extension of the straight line portion. The dial reading,  $R_{50}$  at 50% consolidation is then equal to  $\frac{R_{100}-R_0}{2}$ , and the corresponding time  $t_{50}$  can be found from the plot.

Then

$$H_{50} = \frac{2H-R_0}{2} \quad (\text{for the case of double drainage}) \quad (2.4)$$

or

$$H_{50} = 2H-R_{50} \quad (\text{for single drainage}) \quad (2.5)$$

where

$2H$  is the original thickness of the sample.

Then

$$c_v = \frac{T_{v50}(H_{50})^2}{t_{50}} \quad (2.6)$$

For the Taylor square root of time method, the dial readings are plotted against the root of time,  $\sqrt{t}$ ,

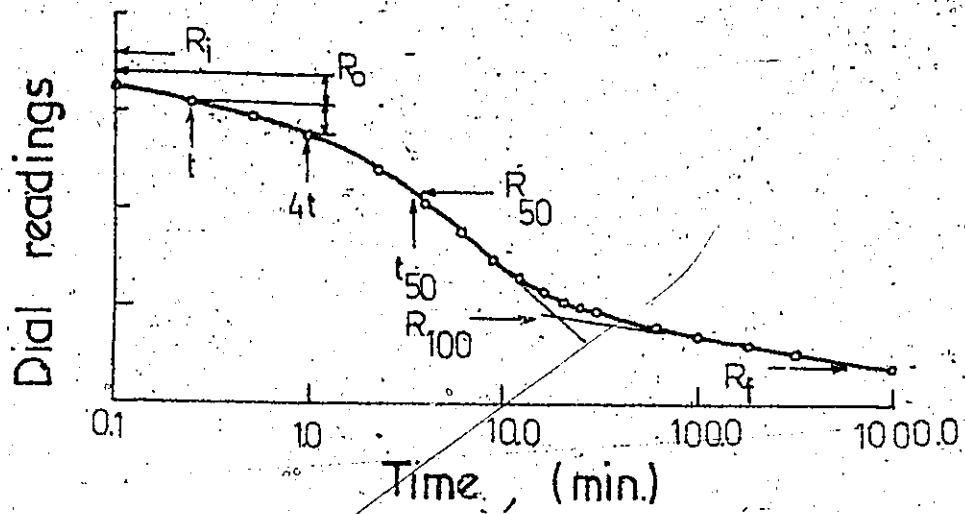


FIGURE 2.6

Casagrande "log of time"  
curve fitting method.

(Fig. 2.7). The straight line portion projected back to zero time gives  $R_0$ . It is assumed that a straight line with abscissa 1.15 times that of the straight line portion intersects the curve at  $R_{90}$ .

$H_{90}$  is then calculated:

$$H_{90} = \frac{2H - R_{90}}{2} \quad (\text{for double drainage}) \quad (2.7)$$

or

$$H_{90} = 2H - R_{90} \quad (\text{for single drainage}) \quad (2.8)$$

Then

$$c_v = \frac{T_{v90} (H_{90})^2}{t_{90}} \quad (2.9)$$

Also the dial readings corresponding to 100% consolidation can be calculated

$$R_{100} = R_0 - \frac{10}{9} (R_0 - R_{90}) \quad (2.10)$$

### 2.2.2 The Influence of Load Increment Ratio

Deviations from the Terzaghi theory have always been recognized. Some of them can be due to the arbitrary nature of the consolidation test (for example: sample size, load increment ratio, load duration, which fitting method is used, etc.). Of these, the two main factors are:

- 1) the load increment ratio and
- 2) the load increment duration.

Only the first of these is discussed in this section. The duration of load will be considered in the next section.

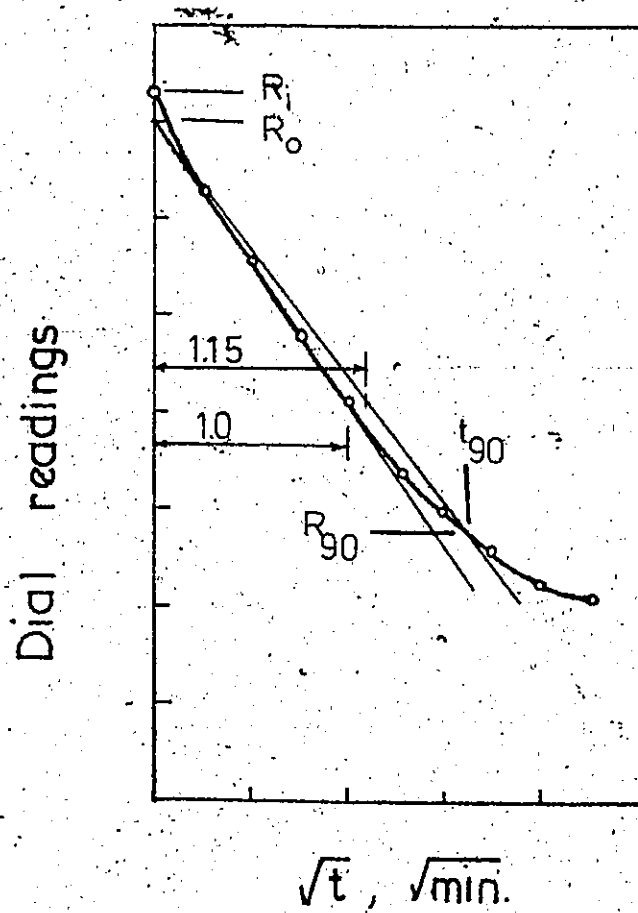


FIGURE 2.7

Taylor "square root of time"  
curve fitting method.

The load increment ratio is the ratio of the pressure increment to the preceding consolidation pressure. As mentioned previously, this ratio is equal to one in the conventional procedure. However, smaller ratios are needed usually to better define the  $e$ -log  $p'$  curve

Langer in 1936 (19) used very small incremental loads ( $40 \text{ kg/cm}^2$ ,  $70 \text{ kg/cm}^2$  and  $700 \text{ kg/cm}^2$ ) daily. Compared with conventional tests, it appeared that soft clays and slimes gave almost the same  $e$ -log  $p'$  curves. For stiff clays, the smaller the load increment, the less compressible the soil appeared to become.

Hamilton and Crawford in 1959, (15) tested Leda clay using load increment ratios of 1,  $1/2$ ,  $1/3$  and  $1/10$ . Comparing their results, they concluded that the size of increment has practically no effect on the  $e$ -log  $p'$  curve (Fig. 2.8). However, when the load increment ratio was decreased, the point of 100% consolidation could not be determined by any of the curve-fitting methods. They used a modified Casagrande method in which they considered 100% consolidation to occur when the compression of the sample reduced to the rate of 0.08% per hour.

Leonards and Ramiah in 1959 (20), testing remolded samples of residual clays, stated that after a period of rest, "at small pressure increments, a quasi-preconsolidation pressure is observed, that is considerably larger than the maximum previous consolidation pressure." No explanation was offered at that time.

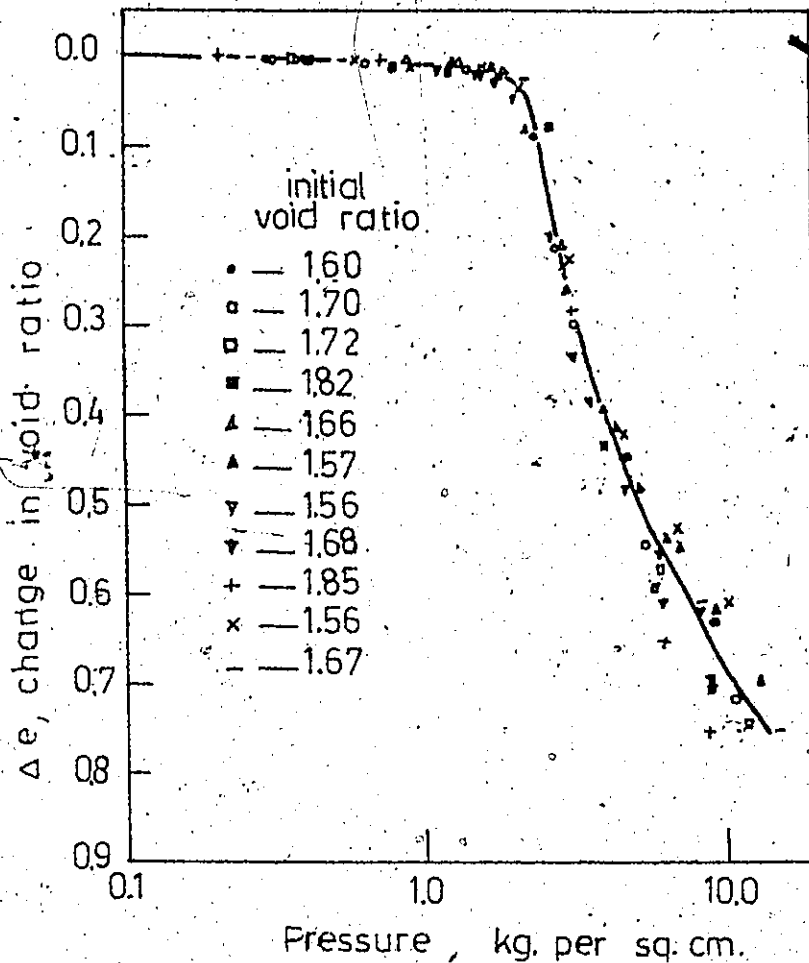


FIGURE 2.8,  
Change in void-ratio—log pressure  
relationship  
for incremental loading tests.

( After Hamilton & Crawford )

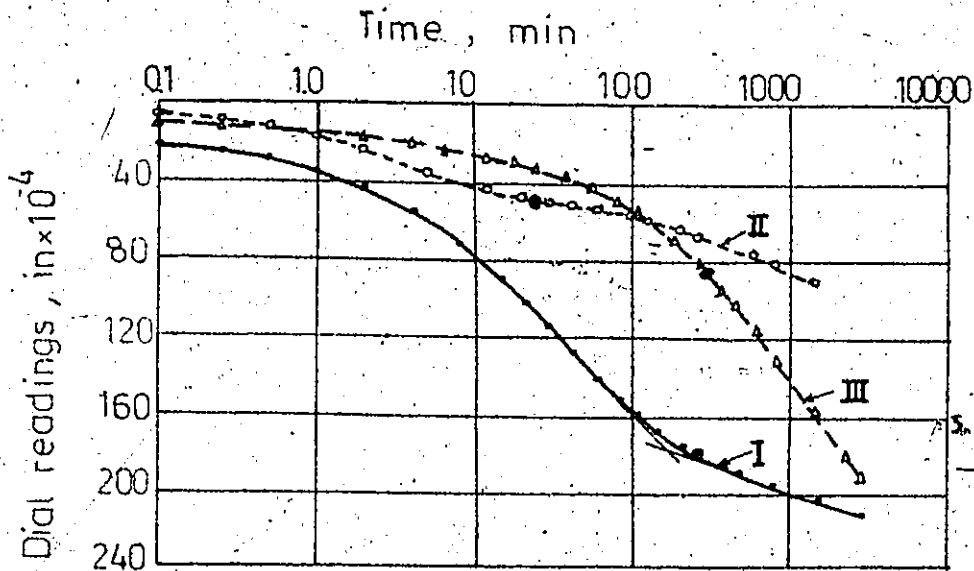
( 1959 )

Bjerrum and Wu in 1960 (3) and later Sangrey in 1972 (31) attributed the "quasi-preconsolidation pressure" in sensitive clays to natural cementation.

Leonards and Girault in 1961 (21) classified the compression-log time curves according to three types (Fig. 2.9): Type I obtained at large increment ratios and for which the Casagrande method yields the dial reading corresponding to 100% consolidation to a good approximation, and Types II and III characteristic of the load increments that straddle the preconsolidation pressure. Type III is also obtained for small increment ratios. They concluded that the Terzaghi theory can predict the rate of pore pressure dissipation only for large increment ratios, and that for each clay there exists a critical value of load increment ratio, smaller than which the Terzaghi theory cannot be used.

This was also pointed out by Wahls in 1962 (41).

Leonards and Alstchaeffl in 1964 (22) related the "quasi-preconsolidation pressure" to the orientation of water molecules in the vicinity of the contact points in the clay mass, during and after deposition of the clay. This phenomenon, which appears to be stress level dependent, increases the strength of the clay so that a net pressure  $\Delta p$  can be sustained by the mineral skeleton before sliding of the particles occurs. This means that the "quasi-preconsolidation pressure" is related to the previous over-



• measured pore pressure  $\approx 0$

Designation	Curve type	P kg/cm <sup>2</sup>	$\Delta P$ kg/cm <sup>2</sup>	$\frac{\Delta P}{P}$
—	I	0.20	0.20	1.00
○-○	II	0.40	0.10	0.25
△-△	III	7.30	1.60	0.22

Effect of load-increment ratio on shape of dial reading-time curves

(After Leonards & Girault)

(1961)

FIGURE 2.9

burden load. For various types of normally consolidated soils, they found that the ratio  $\frac{p_{cq} - p_o}{p_o}$  is approximately equal to 0.4; where

$p_{cq}$  = Quasi-preconsolidation pressure

$p_o$  = Overburden pressure.

This is in agreement with Narain and Singh's 1969 conclusions concerning normally consolidated soils (24), except that their ratios of  $\frac{p_{cq}}{p_o}$  varied with the load increment ratio and with the duration of the sustained load.

In his Rankine Lecture in 1967 (4) Bjerrum related the quasi-preconsolidation pressure to delayed consolidation which depends on the magnitude of the overburden, the age of the clay deposit, as well as to the chemical bonding.

Considering the effect of the load increment ratio on the rate of consolidation, it appears that as the load increment ratio reduces, the compressibility reduces, and hence, the pore pressure dissipation, (i.e., the primary consolidation process) is accelerated (22,35).

### 2.2.3 The Influence of Load Increment Duration

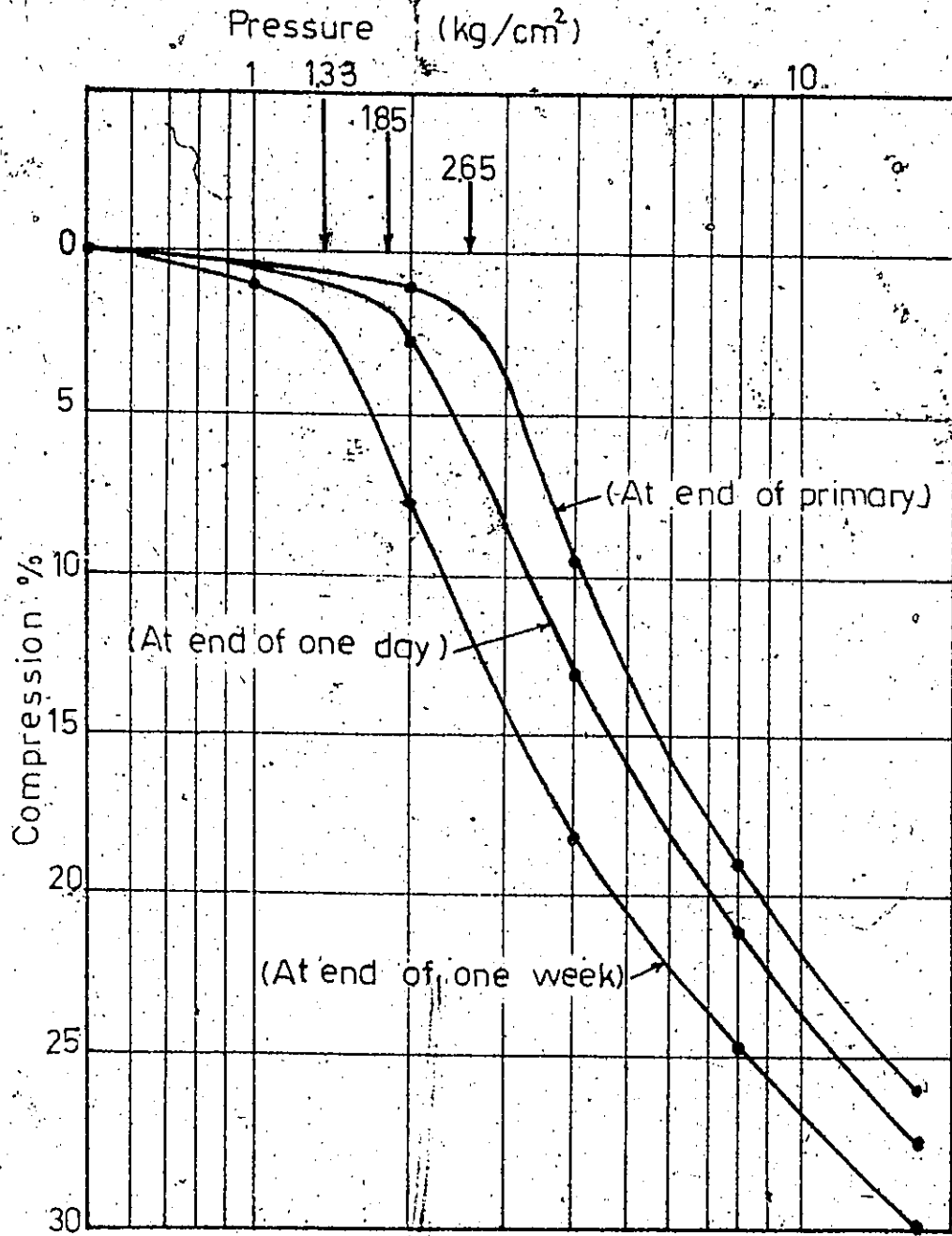
In the conventional test, each load increment is kept on for 24 hours. This makes the test time-consuming, especially for soils of high preconsolidation pressure. Taylor in 1942 (38) proposed that there exists a primary e-log p' curve obtained by allowing just enough time for primary consolidation alone. Below and parallel to it are curves of successively longer duration.

Northey in 1956 (26), using an increment ratio of 1 and a 20 min load duration for each increment, found good agreement with the 24-hour tests for soils of  $p_c$  higher than  $\frac{1}{4}$  ton/sq ft ( $1/4$  kg/cm<sup>2</sup>) and  $c_v$  of about 10 in<sup>2</sup>/min (65 cm<sup>2</sup>/min). He suggested that, since the total compression under each load is approximately the same for the two types of test, only the ratio of primary to secondary compression must vary.

The same argument was given by Newland and Alleley in 1960 (25), although they noticed a tendency for the  $e$ -log  $p'$  curves of long increment duration tests to lie below those of short duration tests. It is interesting to note that some eleven years later, in 1971, Okumara and Ogawa (37) made the same remark concerning the relative positions of the curves in their tests.

Leonards and Ramiah in 1959 (20) stated that, provided the load increment has been kept on long enough for primary consolidation to occur, and provided the soil does not exhibit abnormally high secondary compression, the duration of the load increment does not significantly affect the pressure-void ratio relationship.

Crawford in 1964 (8), testing Leda clay, found that the load duration greatly affects the  $e$ -log  $p'$  curves and consequently the value of  $p_c$  (Fig. 2.10). This effect is accentuated if one load increment happens to be in the vicinity of the preconsolidation pressure (9).



Compression log pressure curves for normal and long term incremental loading

(After Crawford)

(1964)

FIGURE 2.10

Altschaeffl<sup>1</sup>, discussing Crawford's results, suggested that a plot of compression resulting from primary consolidation alone should be used for the determination of  $p_c$ .

Okumara and Ogawa (37) did not notice any significant difference in the values of  $c_v$  obtained from short duration tests as compared with values from conventional tests.

### 2.3 Constant Rate of Strain Tests

The conditions applied to the sample in an incremental loading test can differ greatly from the field conditions where the loads are usually increased rather gradually. If a soil sample were compressed at a constant rate rather than the widely varying rates in a conventional test, three significant advantages could be achieved:

1. a better defined  $e$ - $\log p'$  curve based on a large number of points would result.
2. there could be a considerable saving in testing time
3. automation would be simpler.

Hamilton and Crawford in 1959 (15) reported on tests carried out at rates of strain varying from 0.3%/hr.

---

<sup>1</sup>Altschaeffl's discussion is contained in the National Research Council of Canada publication mentioned in reference (8).

to 9%/hr. The values of  $p_c$  seemed to increase as the rate of testing increased. However the porewater pressure was not measured in these tests so that the effective stress at any time could not be determined, at least for the tests at faster rates.

More data were reported by Crawford in 1965 (9), where the porewater pressures were measured and the effective stresses calculated. Again, the value of  $p_c$  increased as the rate of strain was increased.

This was in agreement with the results obtained by Wahls and Degodoy<sup>1</sup>, who also found that for rates of strain of 0.053%/min to 0.23%/min the  $e$ -log  $p'$  curves obtained from constant rate of strain tests were all located above those from conventional tests.

For the above-mentioned attempts,  $c_v$  could not be calculated. That is, the rate of consolidation could not be determined by this test.

Smith and Wahls in 1969 (36) developed a mathematical model for the constant strain rate tests, which permits the determination of the rate as well as the magnitude of consolidation. Their  $e$ -log  $p'$  curves for various rates compared quite closely to the conventional test except when the porewater pressures exceeded 50% of the applied load. Values of  $c_v$  were slightly higher than those obtained from the conventional test.

---

<sup>1</sup> Wahls and Degodoy's comments are contained in the National Research Council of Canada publication mentioned in reference (8).

Wissa et al in 1971 (42) developed another mathematical solution applicable to linear (constant  $m_v$ ), as well as non-linear (constant  $C_c$ ) soils. Their test results were in agreement with those of Smith and Wahls.

#### 2.4 Constant Rate of Loading Tests

This test has the same advantages over the conventional incremental test as the constant rate of strain test.

Hamilton and Crawford (15), testing Leda clay at various rates of stress application, found that  $p_c$  increases with an increase in the rate. Generally the values of  $p_c$  from the constant rate of stress tests were higher than those from conventional tests. These results agree with those obtained by Jarret in 1967 (18). Jarret suggested that there is a minimum rate of loading for each type of clay, below which, essentially the same 'e-log p' curves are obtained. He found this rate to be  $0.225 \text{ kg/cm}^2/\text{day}$  ( $0.225 \text{ t/ft}^2/\text{day}$ ) for Leda clay.

Aboshi, Yoshikumi and Maruyana in 1970 (1) based their theoretical model on Schiffman's solution for an external load increasing with time (32). Their solution enables the determination of the time factor  $T_v$  if the ratio of the porewater pressure at the base to the applied total pressure is known. Their experiments proved that  $c_v$  values for constant rate of loading tests are comparable to

those from conventional tests only at stresses above the preconsolidation pressure. They pointed out that the rate of stress application should be rapid enough to enable the porewater pressure at the base to be sufficiently large to be measured accurately, but it should not be too rapid so that the condition of uniformity of stresses within the sample remains satisfied.

### 2.5 Controlled Gradient Consolidation Test

Lowe et al in 1969 (23) developed the controlled gradient consolidation test, to fulfill three basic objectives.

1. To have the stress conditions throughout the sample as uniform as possible.

2. To have a more or less uniform rate of compression throughout the test.

3. To be able to run tests at different slow rates of compression; so that extrapolation of data to the field conditions can be made.

The test is performed on a cylindrical specimen similar to the one used in the conventional test. The specimen is drained vertically, to the upper face only. At the bottom face, a small hydrostatic excess pressure,  $u$ , is maintained constant by gradually applying axial loads to the specimen. The value of  $u$  is chosen in advance.

The pattern of the hydrostatic excess pore pressure in the sample is parabolic and constant throughout the test (except at the beginning of loading and at the end of the test). In the conventional test, this pattern varies from the beginning to the end of each load duration (Fig. 2.11).

An indefinite number of points define the  $e$ - $\log p'$  curve so that the value of  $p_c$  can be determined more accurately by the Casagrande or Schmertmann method. On the other hand, a plot of applied stress versus elapsed time to a natural scale, gives two straight lines with a short curved transition. The intersection of the extension of these lines also indicates the preconsolidation pressure for the tests carried out by Lowe et al.

In deriving a formula for the rate of consolidation, Lowe et al used Terzaghi's assumptions and obtained a simple formula for  $c_v$

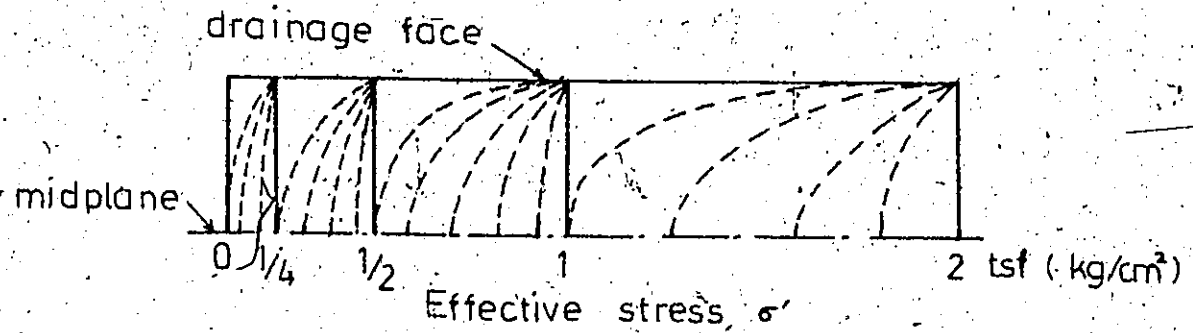
$$c_v = \frac{\Delta p \cdot H^2}{\Delta t \cdot 2u} \quad (2.11)$$

when  $\Delta p$  = change in stress during the time interval  $\Delta t$ .

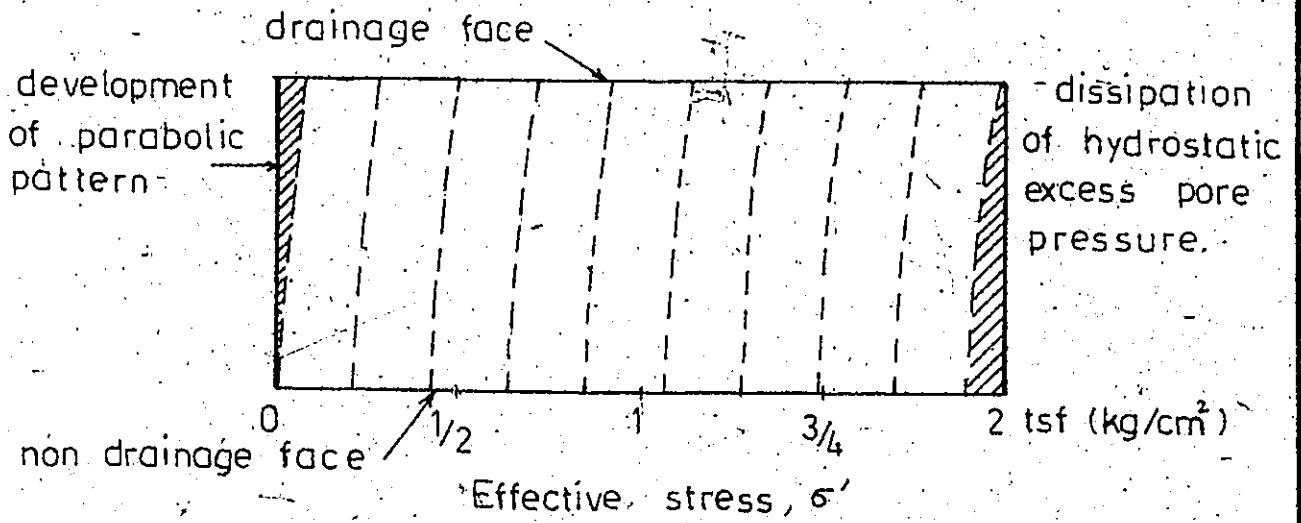
$H$  = total thickness of the specimen at time  $t$ .

$u$  = excess porewater pressure at the base.

Their results did not show any trend in the  $e$ - $\log p'$  curves or in the  $c_v$ - $\log p'$  curves due to a variation in  $u$  between the limits of 1.21 psi and 3.05 psi. All curves fell within a narrow range and were quite close to the conventional test results.



Isochrones - conventional test.



Isochrones - controlled gradient test.

Comparison of hydrostatic excess pressure during conventional test & controlled gradient test.

(After Lowe et al)

( 1969 )

FIGURE 2.11

## 2.6 Summary

Examining the different test procedures, it appears that the controlled gradient consolidation test is the only one that permits the determination of the pre-consolidation pressure by a simple plot not requiring a complicated empirical method or a curve fitting procedure.

The controlled gradient test also has the hydraulic gradient as the independent variable during the test. The hydraulic gradient in the conventional test can often exceed the field gradient by orders of magnitude. While more reasonable gradients are possible in the constant rate of strain and constant rate of stress tests, the gradient is a dependent value in each case. In the extreme, large gradients could lead to fracturing of the soil.

CHAPTER 3

3.1 Research Proposal

A reliable determination of the preconsolidation pressure can be of great importance in the design of foundations on clay, in particular in the estimation of settlement. As outlined in the previous chapter, various methods have been used in consolidation testing, each having probably its own influence on the value of  $p_c$  that is measured. The controlled gradient test is the only one which seems to present two methods for the determination of  $p_c$ , one from strain-log effective stress plot ( $\epsilon$ -log  $p'$ ) and the other from the time effective stress plot ( $t$  -  $p'$ ). It was decided to investigate this test, and find out experimentally if the ( $t$  -  $p'$ ) plot defines the  $p_c$  for Leda clay as it did for the Portland (Maine) clay tested by Lowe.

As the incremental test is still the most widely used, a comparison between the controlled gradient test results and incremental test results was thought to be necessary. Indeed Lowe et al also used the conventional test results for comparison, with a load increment ratio of one and a duration of 24 hrs for each load. But as shown in the previous chapter, the  $p_c$  value changes with the

change in those variables. For this reason, it was decided to run a number of incremental tests with different load increment ratios and durations and find out how far from, or close to, the results are to those of the controlled gradient test.

In addition to a comparison of  $p_c$  values, a comparison will be made, where feasible, of  $c_v$ ,  $k_v$  and  $m_v$ .

### 3.2 Testing Program

#### 3.2.1 The Controlled Gradient Consolidation Tests

The following variables were considered:

- The size of the consolidation cell and the thickness of the sample. Two sizes were used: standard size of 3 in (7.62 cm) inside diameter with samples 1 in (2.54 cm) thick and 6 in (15.2 cm) inside diameter with samples 2 in (5.09 cm) thick. Details of the cells will be given later.
- The actual  $p_c$  and  $p_o$  values of the clay tested. It was decided to test samples at two different levels: at 5 feet (1.5 m) depth and at 7 feet (2.1 m) depth.
- The porewater pressure maintained at the base. Preliminary tests were run in order to find out some rough correlations between the time required for testing until a certain stress level was

reached—and the porewater pressure maintained at the base for the two cell sizes. Two values of  $u$  were used, namely, 1.5 psi (10.4 KN/m<sup>2</sup>) and 3 psi (20.8 KN/m<sup>2</sup>).

The following program was arrived at:

---

Size of the sample	Porewater pressure at the base
3 in dia x 1 in thick (7.62 cm dia x 2.54 cm thick)	1.5 psi (10.4 KN/m <sup>2</sup> )
3 in dia x 1 in thick (7.62 cm dia x 2.54 cm thick)	3 psi (20.8 KN/m <sup>2</sup> )
6 in dia x 2 in thick (15.24 cm dia x 5.08 cm thick)	3 psi (20.8 KN/m <sup>2</sup> )

---

This program was to be followed for the samples from 5 feet (1.5m) depth and for those from 7 feet (2.1m) depth. A minimum of 3 tests of each kind was performed, totalling 18 controlled gradient consolidation tests.

### 3.2.2 The conventional Consolidation Tests

The variables considered in this test were:

- The size of the consolidation cell:  
3 in (7.62 cm) internal diameter cells were used.
- The actual  $p_o$  and  $p_c$  values of the clay tested:  
Samples from 5 feet (1.5 m) depth and from 7 feet (2.1 m) depth were also used.

- The load increment ratio and the load duration:  
A combination of load increment ratios and load durations was selected as follows:

Load increment ratio	Load duration
0.5	24 hr
1	1 hr
0.5	30 min
0.25	15 min

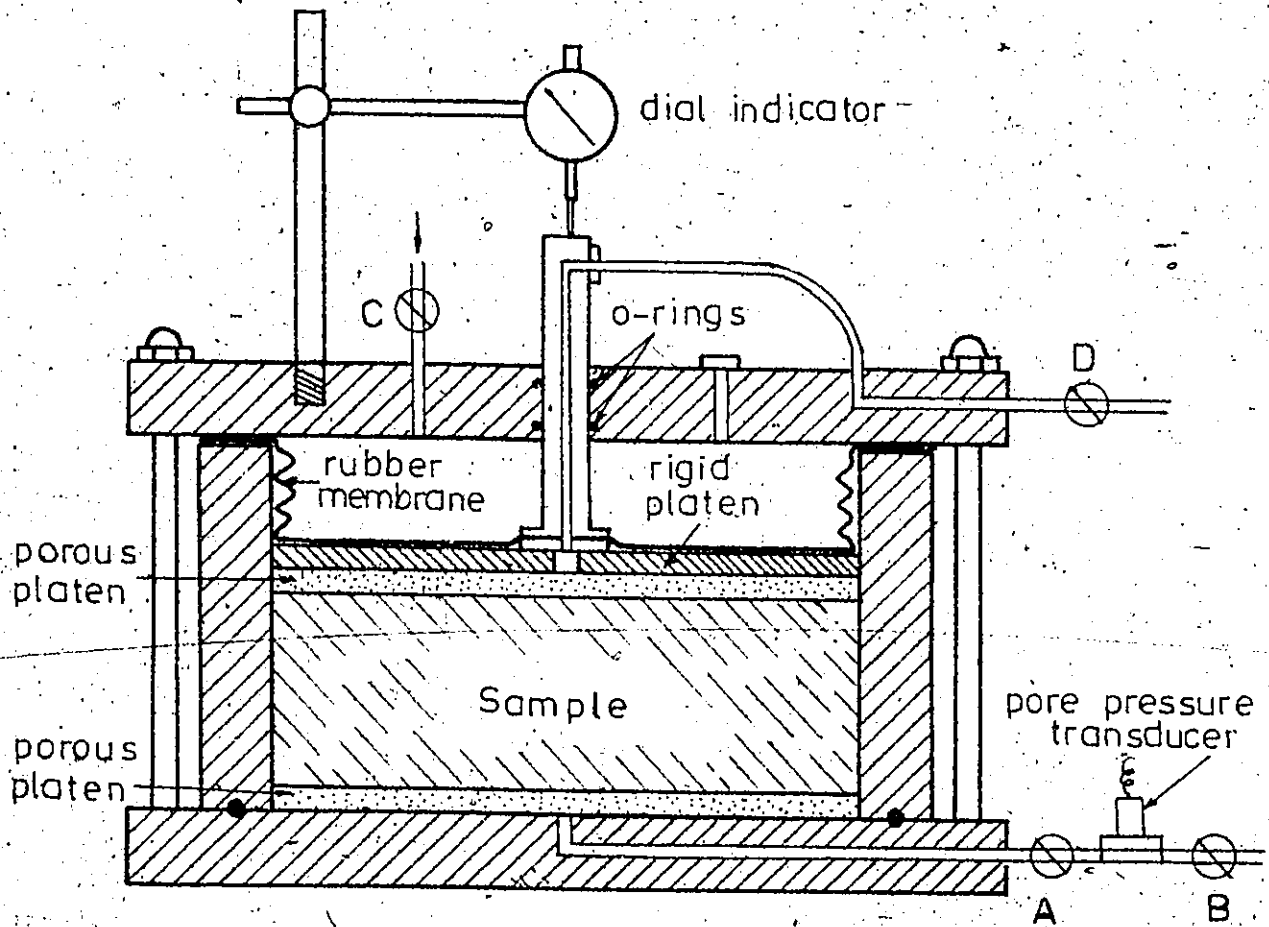
This program was repeated for the samples from 5 feet (1.5 m) depth and for those from 7 feet (2.1 m) depth. A minimum of three tests of each kind was also performed totalling 24 incremental loading tests.

### 3.3 Testing Equipment

#### 3.3.1 The Consolidation Cells

Rowe consolidation cells were chosen because they are essentially closed systems. They can be adapted readily to the requirements of the controlled gradient consolidation test and lend themselves relatively easily to automation.

The main features of the cell are shown in Fig. 3.1. The design and various details of the cell were given by Shields and Rowe in 1965 (34) and by Rowe and



Rowe consolidation cell

FIGURE 3.1

Barden in 1966 (29). The cells used were 3 ins (7.62 cm) diameter by 2-1/4 ins (5.71 cm) deep, and 6 ins (15.24 cm) diameter by 4-1/2 ins (11.42 cm) deep. They were made of steel and chrome plated. One 3-in cell was purchased commercially (cell #1). A second 3-in cell (cell #2) and one 6-in cell were manufactured in the University workshops using commercially obtained strain followers and rubber membranes. The loads were applied hydraulically using a Bishop's mercury control system. A rigid top platten made of stainless steel was inserted below the rubber membrane to maintain equal strain conditions. Silicone grease was applied to the inside of the ring to minimize side friction. Filter papers and porous plates were used on top and bottom of the sample.

Double drainage was permitted during the conventional tests. For the controlled gradient tests, top drainage alone was permitted, and a pressure transducer was connected to the bottom drainage outlet to measure the base porewater pressure.

### 3.3.2 Automatic Control Unit

For the controlled gradient test, an automatic control unit was designed to maintain the porewater pressure at the base within  $\pm 0.1$  psi ( $\pm 0.7$  KN/m<sup>2</sup>) of the set value. When the porewater pressure drops due to consolidation, below the fixed limit, a motor automatically raises the mercury pots, allowing more pressure to be applied to the sample, until the pore pressure at the base reaches the set value. The motor then stops automatically. Details of the control unit are given in Appendix B.

### 3.4 The Soil

The clay used in this study was of the type called Leda clay.

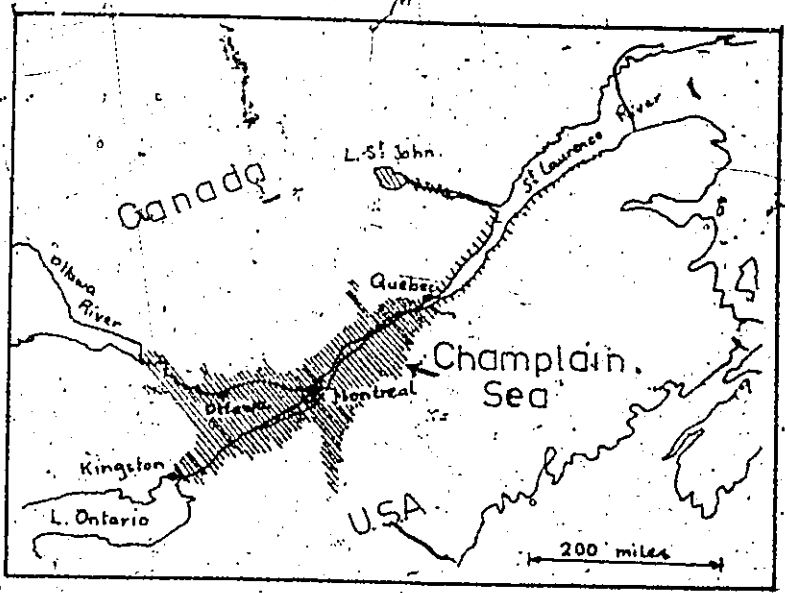
#### 3.4.1 Geological review

The term Leda clay was first used by the Canadian geologist Dr. J. W. Dawson. It is used to designate the clays of Eastern Canada which cover large areas of the Ottawa and St. Lawrence valleys.

For many years, the Leda clay was considered to be a marine deposit of the Champlain Sea which covered the area 10,000 years ago (Fig. 3.2). However, the possibility that these clays are not uniquely marine was strengthened by some evidence (11), mainly:

- That the porewater is generally low in salt concentration.
- That the marine shells occur in layers as half shells, without the orientation expected in natural marine deposits.
- That these clays are generally low in carbonates which is the reverse of what is expected in a marine deposit.

Gadd in 1962 (12) suggested that the area has been subjected to a sudden influx of fresh water, (probably from the Great Lakes region). The currents created eroded much of the marine clays from the scarps and



# The Champlain Sea

FIGURE 3.2

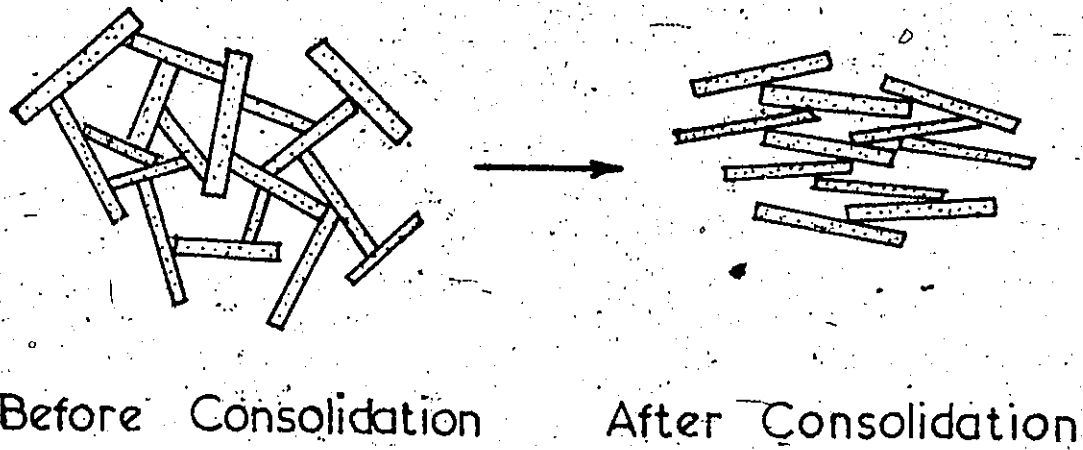
terraces and redeposited it. This resulted in two types of clays: the older, deposited in a marine or brackish water environment, covered by the younger, deposited in a fresh water or fluvial environment. Gadd described the older, marine clay as being "very soft, blue grey, silty clay and the younger, fluvial clay as being "stiff, grey to brownish grey, rust mottled silty clay." This explanation is generally accepted today.

#### 3.4.2 Properties of Leda clay

Minerology: The mineralogical composition of Leda clay consists of high amounts of illite, chlorite and mica, with lesser amounts of quartz and feldspar (7,10).

Structure: It is known that the particles of Leda clay are flaky and assume a card-house arrangement. Quigley and Thompson, in 1966 (28), used an x-ray diffraction technique to examine the changes in the structure of Leda clay during one dimensional consolidation. They found no particular particle orientation for pressures up to the preconsolidation pressure. Beyond this pressure, as is shown in Lambe's schematic diagram (Fig. 3.3), the structure begins to break down, and the particles orient towards parallelism.

Sensitivity: Leda clays are known to be very sensitive. Their sensitivity ranges from 20 to hundreds. While the sensitivity of the Norwegian marine clays has



Lambe's schematic diagram for  
one-dimensional consolidation.

FIGURE 3.3

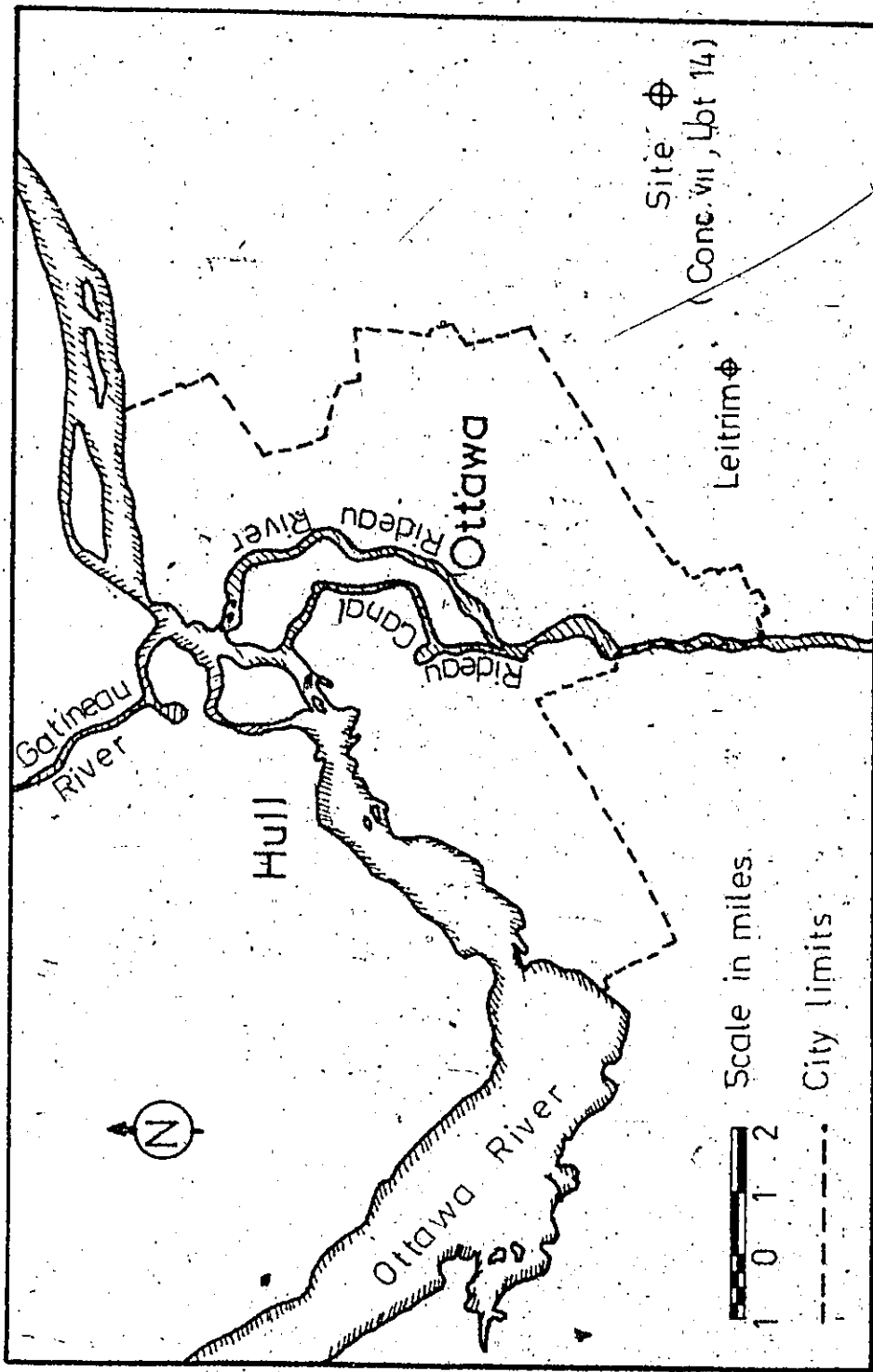
been related to the porewater salt concentration, that of the Leda clay has been related to cementation (31), or to the electrokinetic potential (27).

Porewater: The porewater of Leda clay is generally low in salt content (less than 2 gm/l) (7,11), but its chemical composition supports Gadd's hypothesis, showing the older clay porewater to be higher in sodium, iron and manganese (characteristics of marine environment), while the younger clay porewater is higher in calcium and magnesium (characteristic of fresh water environment). This was reported by Sangrey and Paul in 1971 (30).

#### 3.4.3 Location and Description of the Site

The clay samples needed for this research program were taken from an excavation made in a field in Gloucester Township, South East of Ottawa, Concession VII, Lot 14. The location is shown in Fig. 3.4. A bore hole log of the soil profile is given in Fig. 3.5. The clay showed no signs of desiccation, or the formation of a crust, and it seems reasonable to conclude that the groundwater level has always remained in the overlying sand.




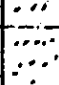
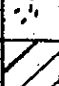
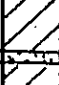
From the Ottawa map prepared by Gadd (12) it can be concluded that the area where this site is located has a core of marine clay capped by a fluvial sediment of medium to fine sand. The soil profile in Fig. 3.5 conforms with this description. Also the clay from this location is



Ottawa-Hull Region

FIGURE 3.4

Elev. 260

depth, ft.	soil profile	
0'		
1'	Topsoil & sand.	
1'7"	Fine, brown sand	
3'		
4'	Fine, yellow, silty sand	
5'	silt layer (1/2")	
	Soft, grey, silty clay	
9'	End of pit	

W.T. (May, 1973)

### Test pit log

FIGURE 3.5

soft, grey, silty, as in Gadd's description of the marine clays. Based on those facts, it can be said that the clay tested in this program is representative of the old, marine clay. However, a chemical analysis of the porewater would have given a better indication of its origin.

#### 3.4.4 Sampling and Storage

Crawford and Eden in 1965 (11) stressed the influence of disturbance on the  $p_c$  values. They obtained a higher  $p_c$  from block samples than from tube samples.

It was decided to use block samples for this study. The blocks were obtained from two test pits which measured 3 ft by 5 ft in plan. The clay at the chosen site being very soft, it was possible to cut the blocks using a sharp knife. The blocks were then immediately wrapped in saran wrap to prevent any change in moisture content. After marking and labelling, the blocks were carefully set on a foam pad in a truck. This was done to minimize the disturbance during the drive to the laboratory. Once in the laboratory, the samples were wrapped in foil paper over the saran wrap, and coated with wax. They were then stored in a cool room maintained at a constant temperature: 50°F - 53°F (10°C - 12°C).

#### 3.4.5 Index Properties

Tests were performed to determine some properties of the clay used in this study. The results are given below:

	at 5'0"	at 7'0"
- Unit weight $\gamma$	100 pcf	95 pcf
$\omega$	70%	85%-95%
$\omega_P$	25	27
$\omega_L$	60	73
$I_P$	35	46

Specific gravity,  $G = 2.79$

Degree of saturation,  $s_r = 100\%$

% clay size particles = 74% at 5 ft depth  
and 78% at 7 ft depth

Activity = 0.46 at 5 ft depth and 0.59 at  
7 ft depth

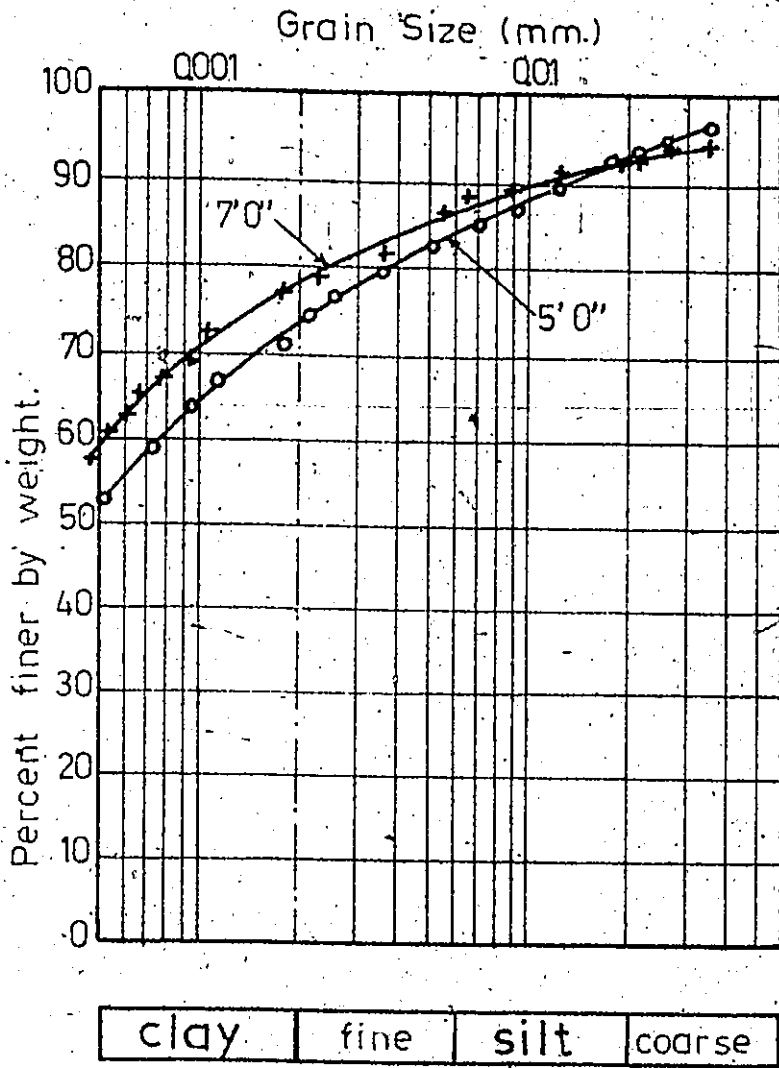
Salt content in porewater = 1.17 g/l

A grading curve is shown in Fig. 3.6.

### 3.5 Testing Method

#### 3.5.1 Sample Preparation

To prepare undisturbed samples, a sharp edged cutter ring of inside diameter equal to the cell inside diameter, was smeared internally with silicone grease, to minimize the side resistance, and was pressed into the specimen. The top and bottom were trimmed, and the sample was carefully transferred to the consolidation ring. This was done by mounting the cutting ring concentric with the cell body and pushing the sample from the cutting ring into the cell body. The cell body was lubricated before-



Particle size distribution curves

FIGURE 3.6

hand using silicone grease. As no back pressure was to be used during testing, care was taken to saturate the cell with water. Before each test, the cell was disassembled, placed in a basin and flooded with water. The porous stones were boiled. The ring containing the sample was slid over the base, and the cell was reassembled under water.

For the controlled gradient test, the pore pressure system was carefully de-aired by flushing water through the transducer housing (Fig. 3.1) until no air bubbles could be detected coming out from the opening in the centre of the base. The cell was then flooded, the sample placed in the ring and the cell reassembled under water.

### 3.5.2 Testing Procedure

For the conventional tests, a small bedding pressure of about 0.5 psi ( $3.9 \text{ KN/m}^2$ ) was first applied to the sample, and drainage was allowed for a few minutes. This permitted the surplus water between the top of the sample and the membrane to be driven out through the top drain. It also allowed good contact to be established between the surface of the sample, the filter papers and the porous stones. The drainage lines were kept open while valve C was closed. The first load was then created by raising the mercury pots until the pressure, as indicated by a pressure gauge or a mercury manometer, reached the

required value. Valve C was then opened so that the load was applied instantaneously to the sample simulating the normal procedure using dead weight apparatus. Readings of the dial gauge were taken at the specific time intervals. Before the next load was applied, valve C was closed and the process repeated.

For the controlled gradient test, a small bedding pressure was also applied in the same manner. The top drainage line was then closed, and a pressure equal to the desired base porewater pressure was applied. The transducer response was monitored through a digital voltmeter. When the pore pressure at the base reached the set value, the top drainage line was opened, and the test commenced. The automatic control unit allowed more pressure to be applied to the sample when needed, so that the pore pressure at the base was maintained constant. Readings of the dial gauge were taken at convenient time intervals, and the corresponding applied pressures were measured. For greater accuracy, a mercury manometer was used to measure the applied pressures up to about 30 psi ( $207 \text{ KN/m}^2$ ), and a pressure gauge was used for higher pressures.

CHAPTER 4

TEST RESULTS AND DISCUSSION OF RESULTS

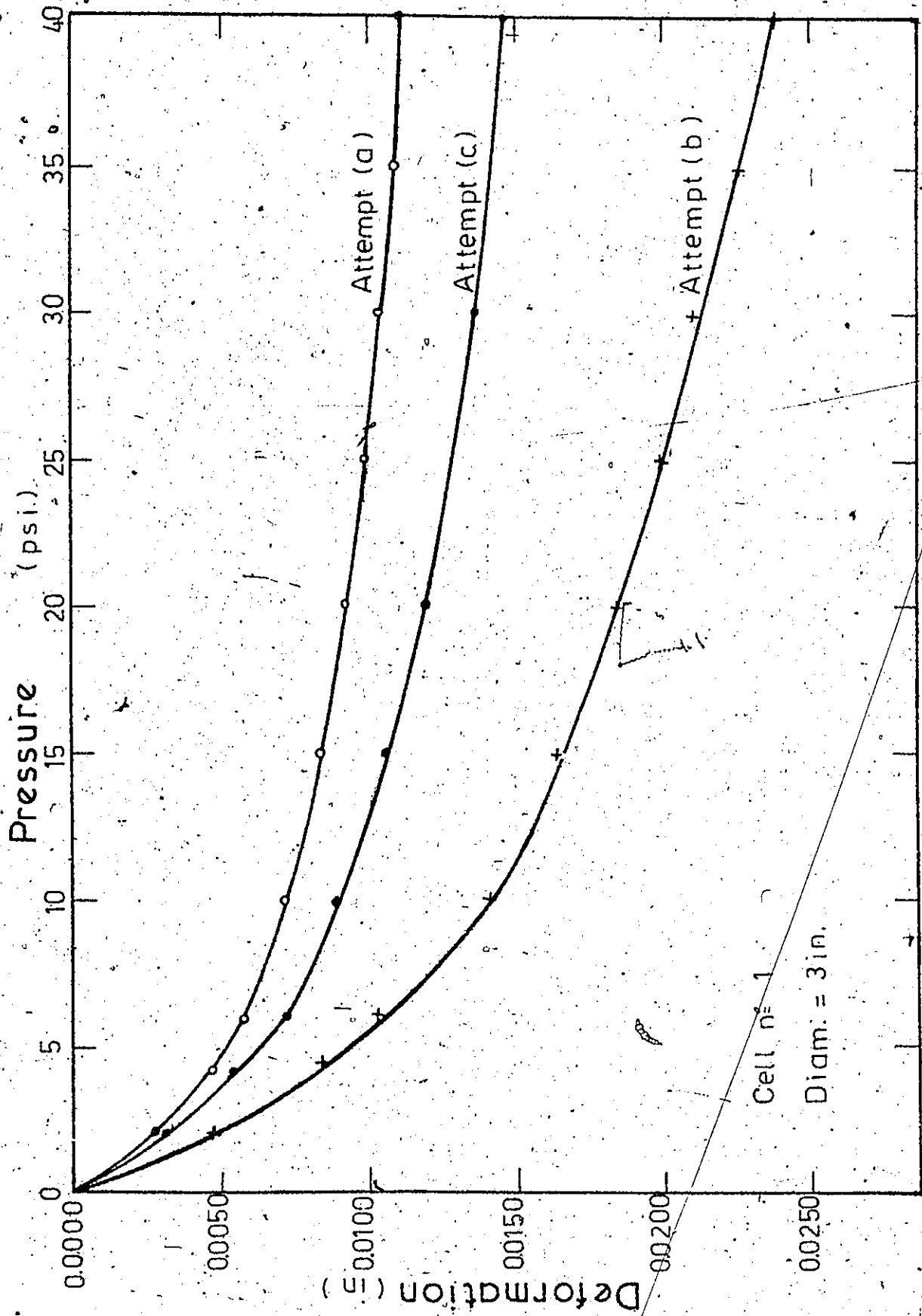
4.1 Calibration of the Rowe Cells

Figures 4.1 and 4.2 give the results of attempts to calibrate two 3-inch diameter Rowe cells. It should be noted that there was considerable difference in the results of repeat tests on either cell. The compressibility and/or deformation of the cells was appreciable in any event.

As subsequent actual test results will show the calibration factors will be of considerable importance to the recompression phase of the stress strain curves for the marine clay. They will not alter significantly the determination of  $p_c$  nor the  $m_v$  of the virgin portions of the curves.

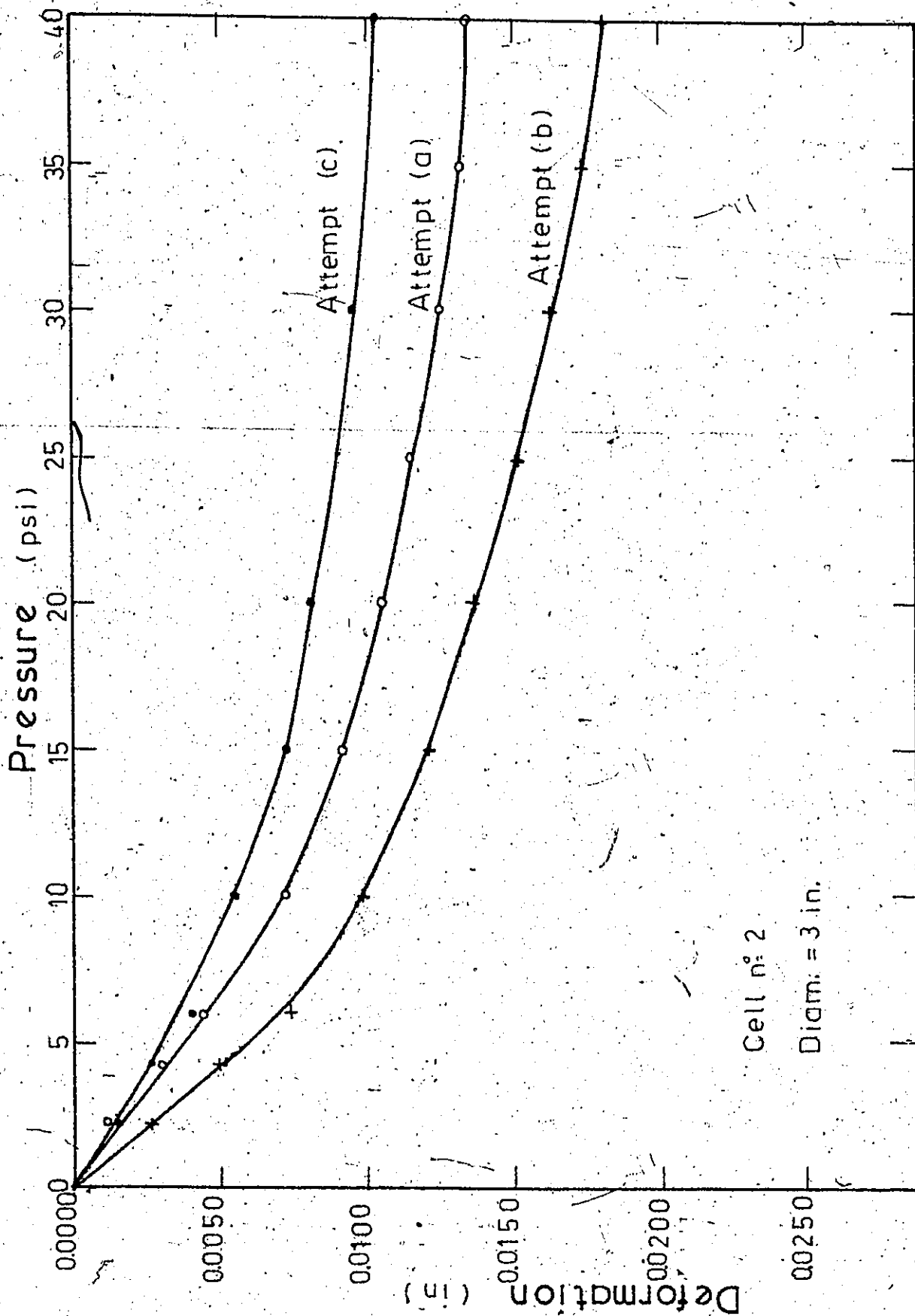
Because no particular calibration curves could be measured for the cells and because calibration was not necessary for the main purpose of the thesis no further attempts at calibration were pursued. In addition, calibration corrections were not made to any of the test results.

The reasons for the appreciable calibration factors for Rowe cells and the poor repeatability of the calibration results should be investigated at the first opportunity.



Attempts to calibrate a Rowe cell.

FIGURE 4.1



Attempts to calibrate a Rowe cell.

FIGURE 4.2

## 4.2 The Controlled Gradient Consolidation Tests

### 4.2.1 General Comments

As stated in the previous chapter, a minimum of three tests of each kind was performed. Figures 4.3, 4.4, 4.5 and 4.6 represent the results obtained from one set of tests on 6-in. diameter, 2-in. thick samples. The samples were from 5 feet (1.5 m) depth and were tested with a 3 psi porewater pressure at the base. These figures are given as an example of the repeatability which was generally obtained, and because they are representative of the shapes of the different curves irrespective of sample size and base porewater pressure.

#### 4.2.1.1 Stress-Strain Curves

Figure 4.3 is an  $\epsilon$ - $\log p'$  plot<sup>1</sup> and it can be observed that a sharp bend occurs at the  $p_c$  level, this is followed by an almost vertical segment and then at higher strains, the curves bend slightly outwards. Because of this sharp bend, the point of maximum curvature could be defined easily and so the Casagrande construction was used to determine the preconsolidation pressure. On the other hand, the shape of the curve in the normally consolidated range made the Schmertmann method of accounting for sample disturbance difficult to apply.

---

<sup>1</sup>In this thesis strain,  $\epsilon$ , rather than void ratio,  $e$ , is used for the ordinate of the stress strain curves.

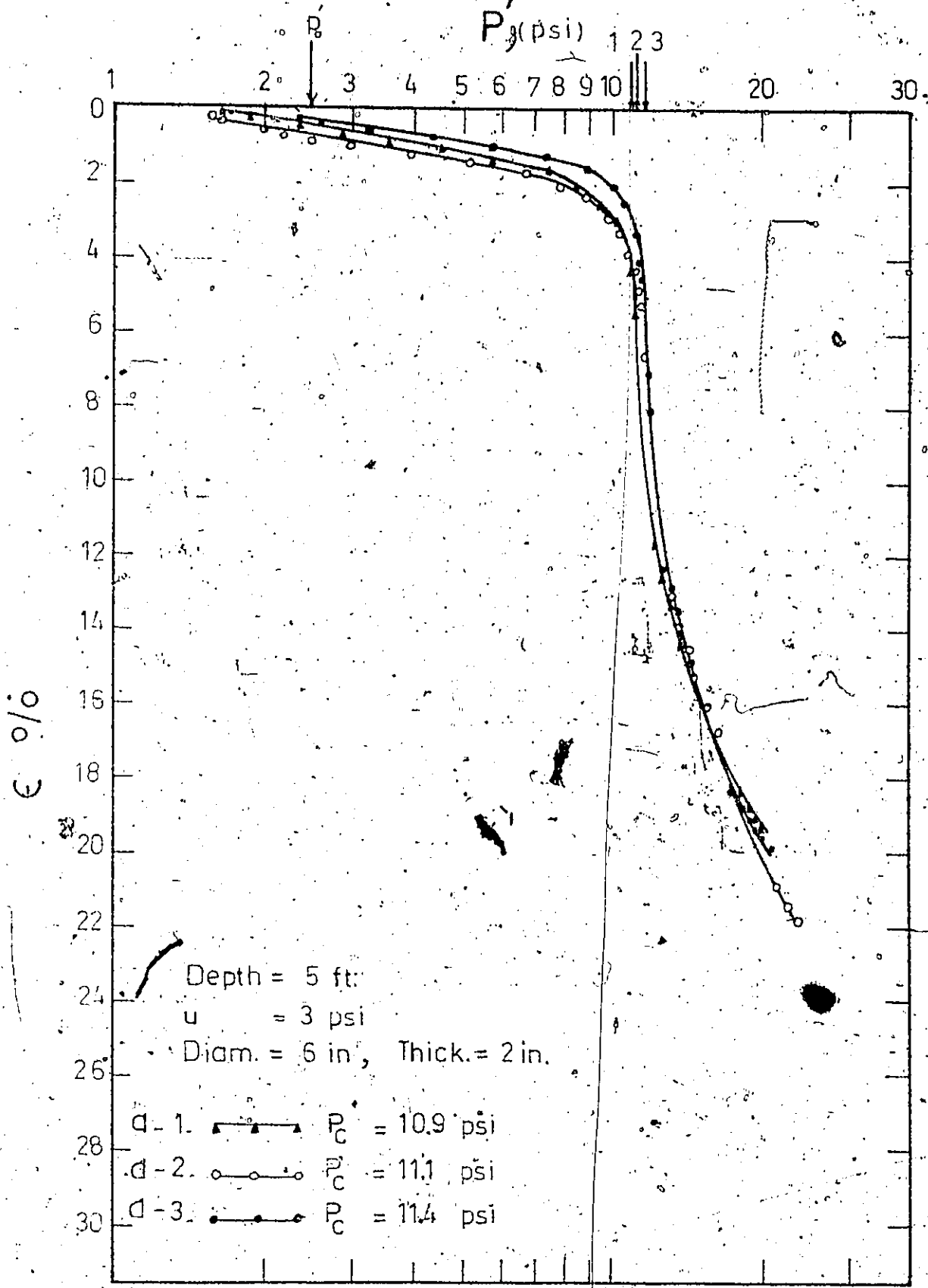
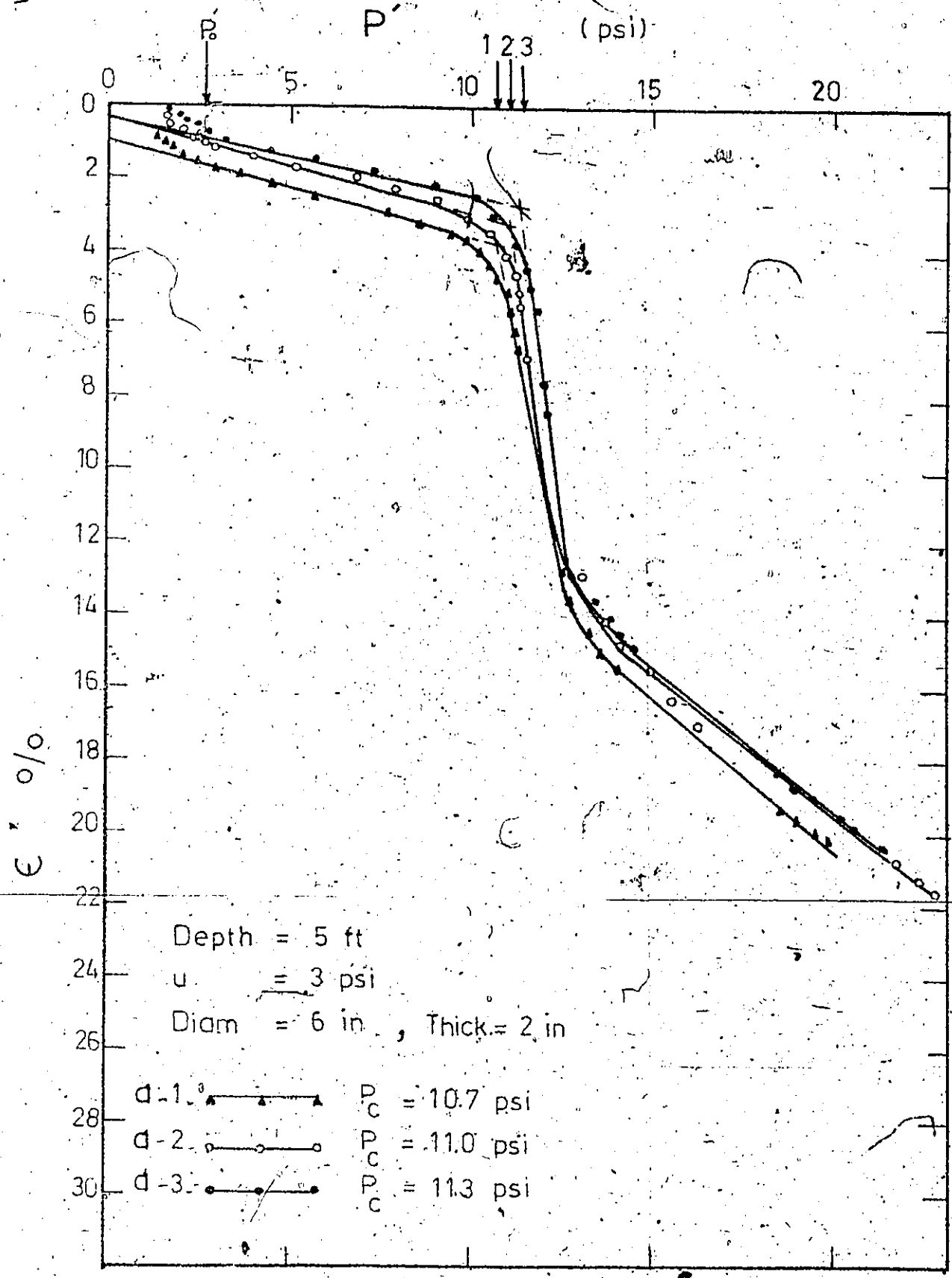


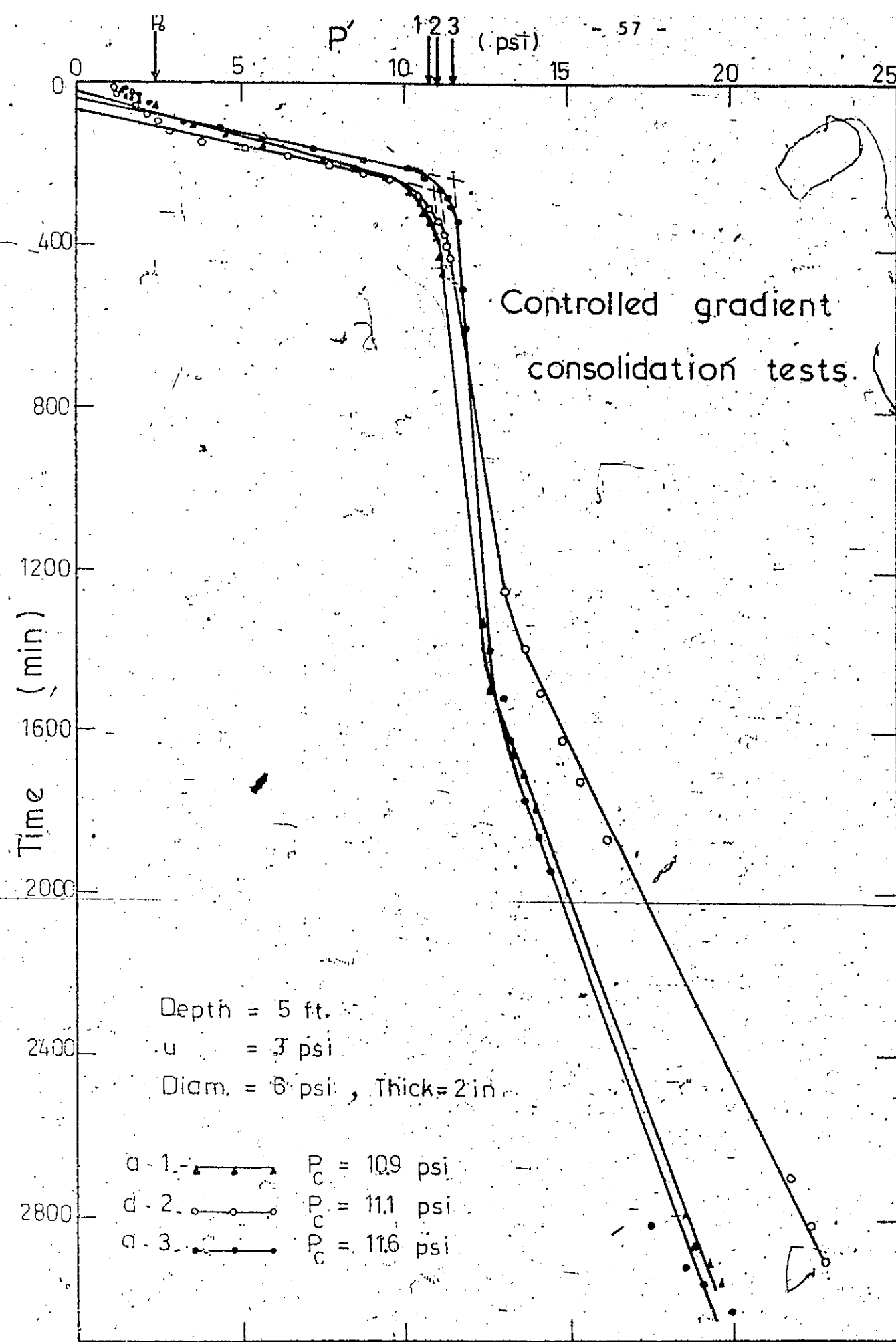
FIGURE 4.3

$e - \log P'$  plot  
Controlled gradient consolidation tests

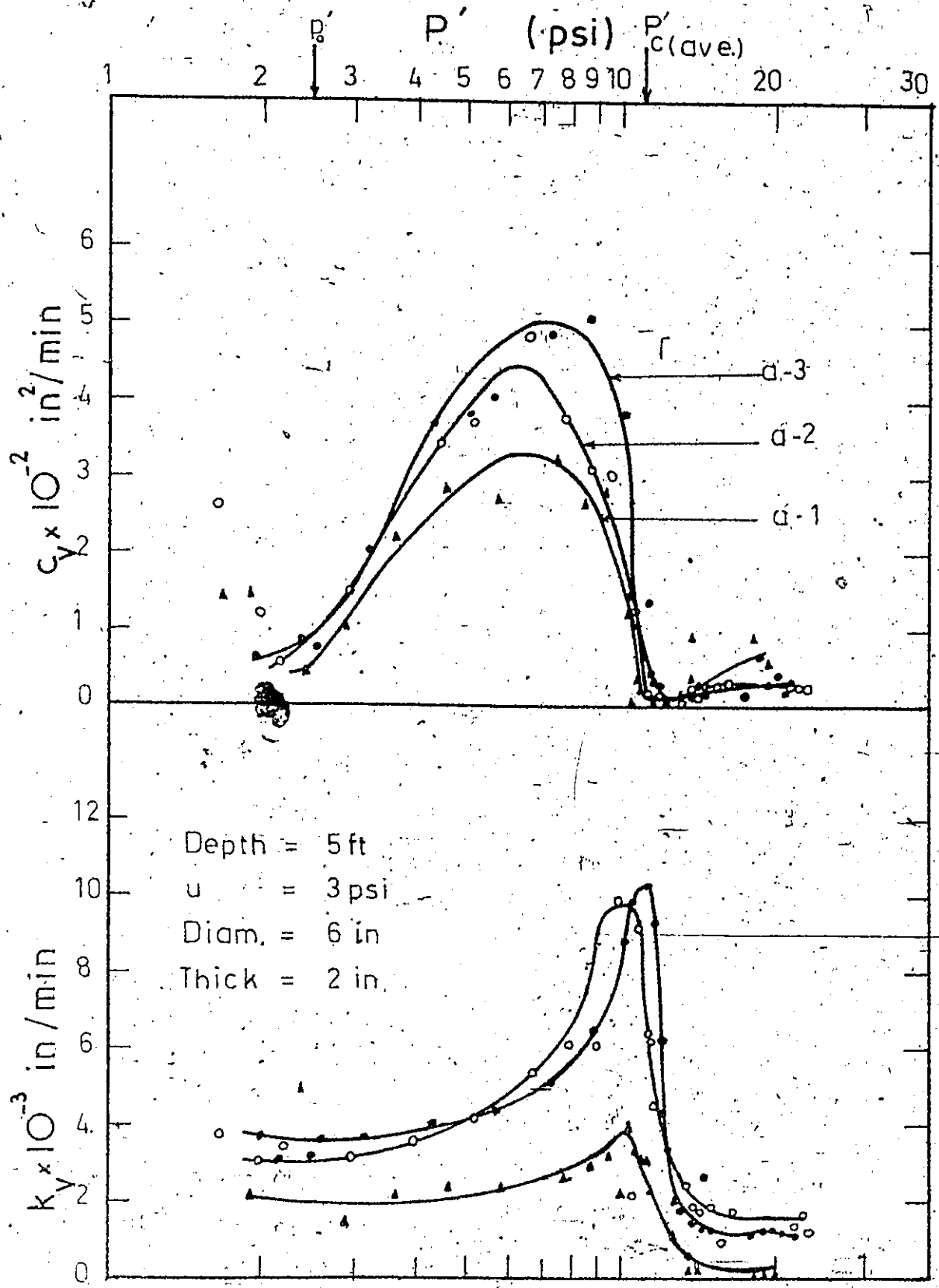


$e \sim P'$  Plot  
Controlled gradient consolidation tests

FIGURE 4.4



t-p' plot  
 FIGURE 4.5



$c_v$ -log  $p'$  &  $k_v$ -log  $p'$  plots.  
Controlled gradient consolidation tests.

FIGURE 4.6

The shape of the  $\epsilon$ -log  $p'$  curves agrees with Jarret's description of the consolidation process in Leda clay (18) mainly that it passes through three phases.

- "An elastic deformation phase, with little settlement, extending up the preconsolidation area.

- Breakdown of the initial bond between the particles, followed by a collapse of the flocculated clay structure,

- Development of a more normal form of consolidation behaviour with the void ratio being the prime criterion for settlement as might occur in a normal clay without a highly flocculated structure."

Figure 4.4, is a  $\epsilon$ - $p'$ , natural scale plot and it shows that the stress-strain relationship is linear, with little strain, up to the preconsolidation pressure, (phase I), where a break followed by considerable yielding occurs (phase II). A strength rebuild or a strain hardening phenomenon follows and corresponds to phase III.

The three phases of the consolidation process seem to be more clearly defined on an  $\epsilon$ - $p'$  plot than on an  $\epsilon$ -log  $p'$  plot for the controlled gradient consolidation test, and sensitive marine clay. In addition the two straight lines corresponding to the first two phases seem to intersect at the preconsolidation level.

The point of departure from linearity in the recompression phase (phase I) of the  $\epsilon$ - $p'$  plot is of interest

in settlement studies. It was found that this part occurred generally 0.7 to 2.0 psi before  $p_c$ . This may mean that loads of almost 75 to 90% the difference between  $p_c - p_o$  can be applied in the field before appreciable creep should be expected.

#### 4.2.1.2 Time-Effective Stress Plot

Figure 4.4 can also be used to study the variation of  $m_v$  during one test, by examining the slopes of the various parts of the plot ( $m_v = \frac{\text{strain}}{\text{stress}}$ ). It can be seen that during one test, essentially three values of  $m_v$  exist corresponding to the three phases of consolidation. Figure 4.7(a) and (b) lists the values of  $m_v$  that were obtained during each test for the straight line portions of the three phases.

Figure 4.5 is a  $t-p'$  plot. As described by Lowe et al. (23) the plot traces two straight lines joined by a short curved transition which occurs in the region of  $p_c$ . The intersection of these two lines in all cases indicates a stress close to the  $p_c$  value as determined from the  $\epsilon - \log p'$  or the  $\epsilon - p'$  plots. But it is interesting to note that in addition, a third straight line defining an increased rate of stress application, seems to correspond to phase III as defined by the two other plots. However, greater variation is noticed in this plot among the three repeat tests as far as the slope of this third line is

FIGURE 4.7(a)

Values of  $m_v$  from controlled gradient.  
tests on samples from 5' depth

Test No	sample size (in)		u (psi)	$m_v$ (in <sup>2</sup> /lb) x 10 <sup>-2</sup>		
	diam	thick		Phase I	Phase II	Phase III
a-1	6	2	3	0.30	7.80	0.75
a-2	"	"	"	0.20	7.50	0.86
a-3	"	"	"	0.31	5.00	0.80
b-1	3	1	3	0.28	4.50	1.23
b-2	"	"	"	0.22	4.20	1.10
b-3	"	"	"	0.24	3.0	1.07
c-1	3	1	1.5	0.25	8.00	0.74
c-2	"	"	"	0.26	8.6	0.65
c-3	"	"	"	0.20	3.0	0.85

FIGURE 4.7(b)  
 Values of  $m_v$  from controlled gradient  
 tests on samples from 7' depth

Test No	sample size (in)		u (psi)	$m_v$ (in <sup>2</sup> /lb) x 10 <sup>-2</sup>		
	diam	thick		Phase I	Phase II	Phase III
d-1	6	2	3	0.25	6.20	2.00
d-2	"	"	"	0.19	7.00	
d-3	"	"	"	0.26	5.00	0.80
e-1	3	1	3	0.33	5.10	1.00
e-2	"	"	"	0.26	3.50	
e-3	"	"	"	0.25	3.30	0.76
f-1	3	1	1.5	0.27	7.50	1.00
f-2	"	"	"	0.27	4.20	
f-3	"	"	"	0.22	4.50	1.00

concerned. This could be explained by the fact that the transducer used to measure the base porewater pressure was measuring "absolute" pressures. For this reason, any change in the atmospheric pressure may have resulted in a change in the "gage" value of the porewater pressure set at the base. This in turn would have resulted in a variation in the rate of stress application, as defined by the slope of the lines in the  $t-p'$  plot. (The effect of variation of  $u$  on the  $t-p'$  plot will be discussed later). As a change in atmospheric pressure occurs gradually its effect is more noticeable in the long term portion of the test.

#### 4.2.1.3 Preconsolidation Pressure

Figures 4.8 and 4.9 summarize the results obtained for the  $p_c$  values from samples from 5 feet (1.5 m) and 7 feet (2.1 m) respectively. For one test, three values of  $p_c$  are given which represent the values from the  $\epsilon-\log p''$ , the  $\epsilon-p'$ , and the  $t-p'$  plots. Generally, good agreement between those values for one test was obtained, as shown. Average values for each set are also given. These values were arrived at by drawing average curves for each set and finding the  $p_c$  for these curves. For this reason, the average  $p_c$  does not necessarily coincide with the arithmetic average.




FIGURE 4.8

Summary of results of controlled gradient tests on samples from 5 ft depth

Test No	sample size		$\Delta u$ base	$p_c$ (psi) E-log $p'$ curves	average (psi)	$p_c$ (psi) t-p' curves	average (psi)	$p_c$ (psi) e-p' curves	average (psi)
	diam	thick							
a-1	6	2	3	10.9	11.0	10.9	10.9	10.7	11.0
a-2	"	"	"	11.1	11.0	11.1	11.0	11.0	11.0
a-3	"	"	"	11.4	11.0	11.6	11.3	11.3	11.0
b-1	3	1	3	13.2	13.1	13.0	12.8	12.8	12.9
b-2	"	"	"	13.1	13.1	13.1	13.1	13.1	12.9
b-3	"	"	"	13.0	13.1	13.3	12.8	12.8	12.9
c-1	3	1	1.5	12.5	12.2	12.2	12.2	12.2	12.1
c-2	"	"	"	12.5	12.2	13.0	12.5	12.7	12.1
c-3	"	"	"	12.1	12.2	12.1	12.0	12.0	12.1

FIGURE 4.9

Summary of results of controlled gradient tests on samples

from 7 ft depth

Test No	diam	sample size (in)	thick psi	$\Delta u$ base	$P_{\epsilon-\log p}$ (psi)	average (psi)	$P_{c-t-p}$ (psi)	average (psi)	$P_{c-\epsilon-p}$ (psi)	average (psi)
					curves	(psi)	curves	(psi)	curves	(psi)
d-1	6	2	3		10.8	11.0	11.0	11.0	10.5	10.9
d-2	"	"	"		11.2	11.0	11.2	11.0	11.0	10.9
d-3	"	"	"		10.8	10.8	10.8	10.8	10.5	10.9
e-1	3	1	3		14.8	14.8	14.8	14.6	14.3	14.1
e-2	"	"	"		13.8	14.5	14.2	14.6	13.4	14.1
e-3	"	"	"		14.7	14.7	14.7	14.7	14.3	14.1
f-1	3	1	1.5		13.2	13.7	13.7	13.7	13.2	12.8
f-2	"	"	"		12.2	12.8	12.2	13.1	12.4	12.8
f-3	"	"	"		12.2	12.5	12.5	12.5	12.1	12.8

#### 4.2.1.4 $c_v$ and $k_v$ Plots

Figure 4.6 represents a  $c_v$ -log  $p'$  and a  $k_v$ -log  $p'$  plot for the same set of tests. Values of  $c_v$  were calculated using the formula given by Lowe et al.

$$c_v = \frac{\Delta p}{\Delta t} \frac{H^2}{2u} \quad (2.11)$$

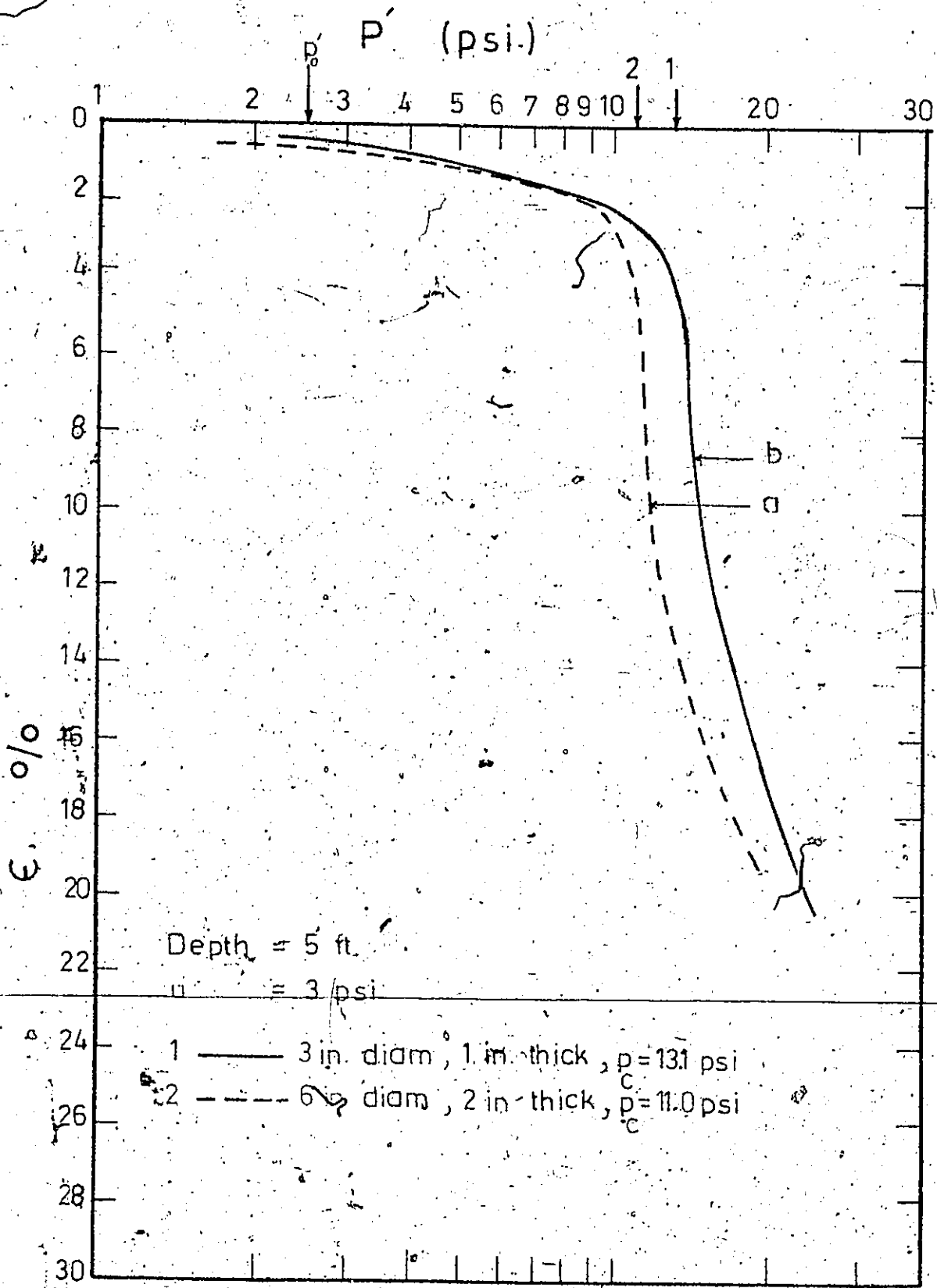
and  $k_v$  values were calculated using the formula.

$$k_v = c_v \cdot \gamma_w \cdot m_v \quad (4.1)$$

Since the permeability should be proportional to the void ratio, one would expect a continuous drop in  $k_v$  as the consolidation process takes place. But from the  $k_v$ -log  $p'$  plot, it is observed that  $k_v$  increases, reaches a peak approximately at the  $p_c$  level, then drops sharply afterwards. This increase in  $k_v$  can be due to an error introduced by the simplifying assumptions of the Terzaghi theory, for example, the assumption that  $k_v$  is constant. The sharp decrease in  $k_v$  at the  $p_c$  level can be explained by the fact that the break down of the structure at the level in addition to decreasing the void ratio, orients the particles perpendicular to the direction of the flow and so greatly decreases the permeability.

#### 4.2.2 Effect of the Sample Size

Figure 4.10 compares the average  $e$ -log  $p'$  curves for the 6 in. diameter, 2 in. thick, and the 3 in. diameter, 1 in. thick samples, all tested with 3 psi porewater pressure



Effect of sample size

Controlled gradient consolidation test:

FIGURE 4.10.

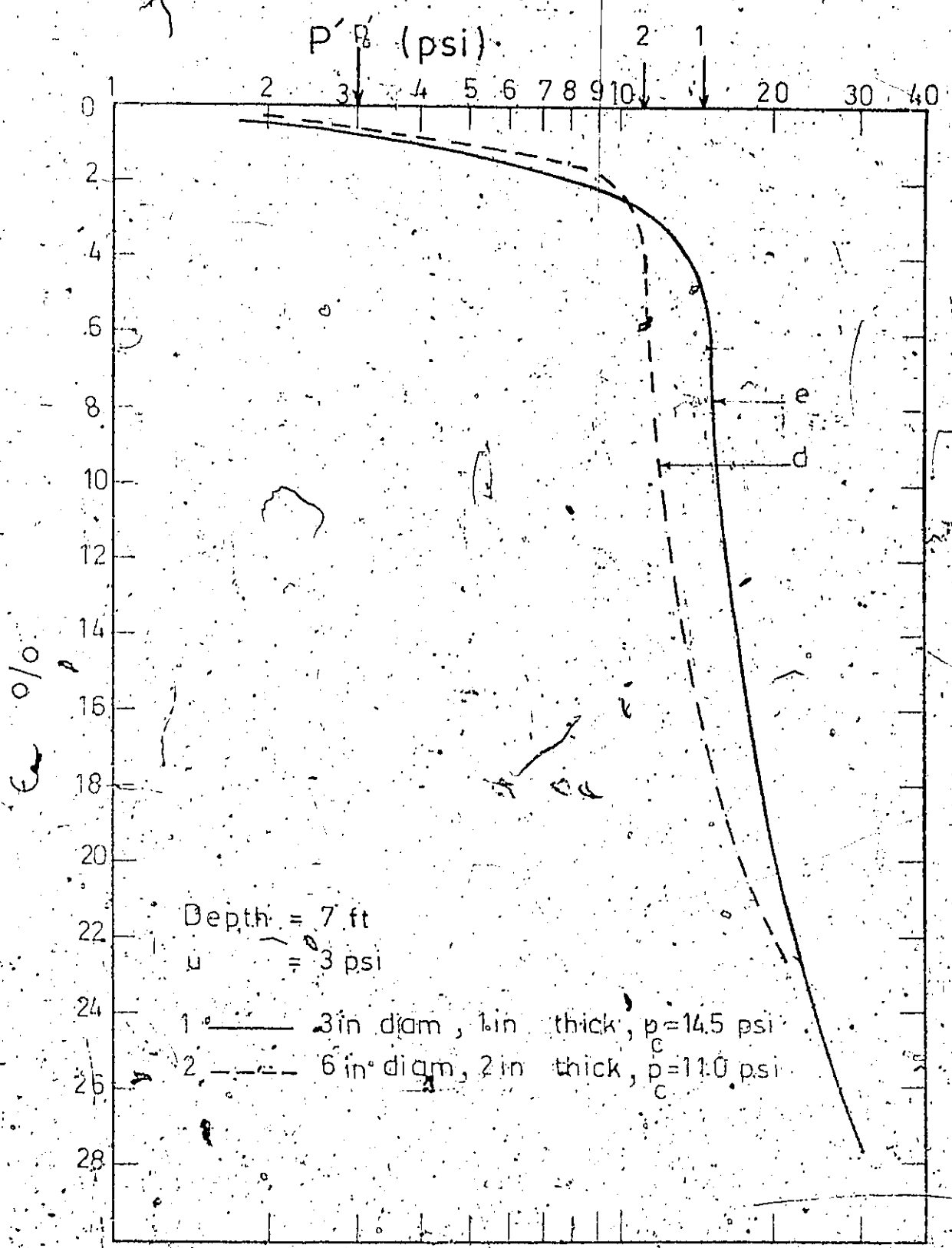
at the base, and all obtained from 5 feet (1.5 m) depth. It seems that all factors being equal, (diameter to thickness ratio,  $u$ , depth of the sample, etc.), the larger samples give a smaller  $p_c$ . This is also true for the samples from 7 feet (2.1m) depth, as shown in Fig. 4.11.

The difference in the  $p_c$  value obtained from tests on the two different sizes, could be due to any or a combination of three possible causes:

1. Disturbance: As Bozozuk (5) explains, the use of too large samples could introduce handling difficulties which would increase the depth of disturbance and account for the decrease in  $p_c$ . Using the same specimen thickness (0.78 in. = 2 cms), Bozozuk obtained a decrease in  $p_c$  from 0.62 kg/cm<sup>2</sup> to 0.60 kg/cm<sup>2</sup> (8.68 psi to 8.4 psi), by increasing the area of the specimen from 6.20 in.<sup>2</sup> to 9.30 in.<sup>2</sup> (40 cm<sup>2</sup> to 60 cm<sup>2</sup>).

On the other hand, with careful handling and trimming, the larger samples should suffer proportionally less disturbance. Care was taken during sample preparation, and in fact looking at curves (4-10) and (4-11) for example, disturbance does not seem to be a factor. Even if the larger samples were more disturbed, this would account only for small differences in  $p_c$  according to the order of values reported by Bozozuk.

2. Differences in hydraulic gradient: The effect of the hydraulic gradient will be discussed in the following



Effect of sample size

Controlled gradient consolidation test

FIGURE 4.11

section; however, it can be said that the differences in hydraulic gradient accounts only for small differences in the  $p_c$  values.

3. Stiffness of the rubber membrane: Swedish investigators report\* that the relatively stiff membranes supplied as standard with the Rowe cells may be at fault. They suggest that the 3 in. diameter membranes take relatively more force to extend than do the 6 in. diameter membranes. The true effective stress on the 3 in. diameter membrane samples would be less than shown on the figures. If the true effective stresses were plotted, the two curves would more nearly coincide.

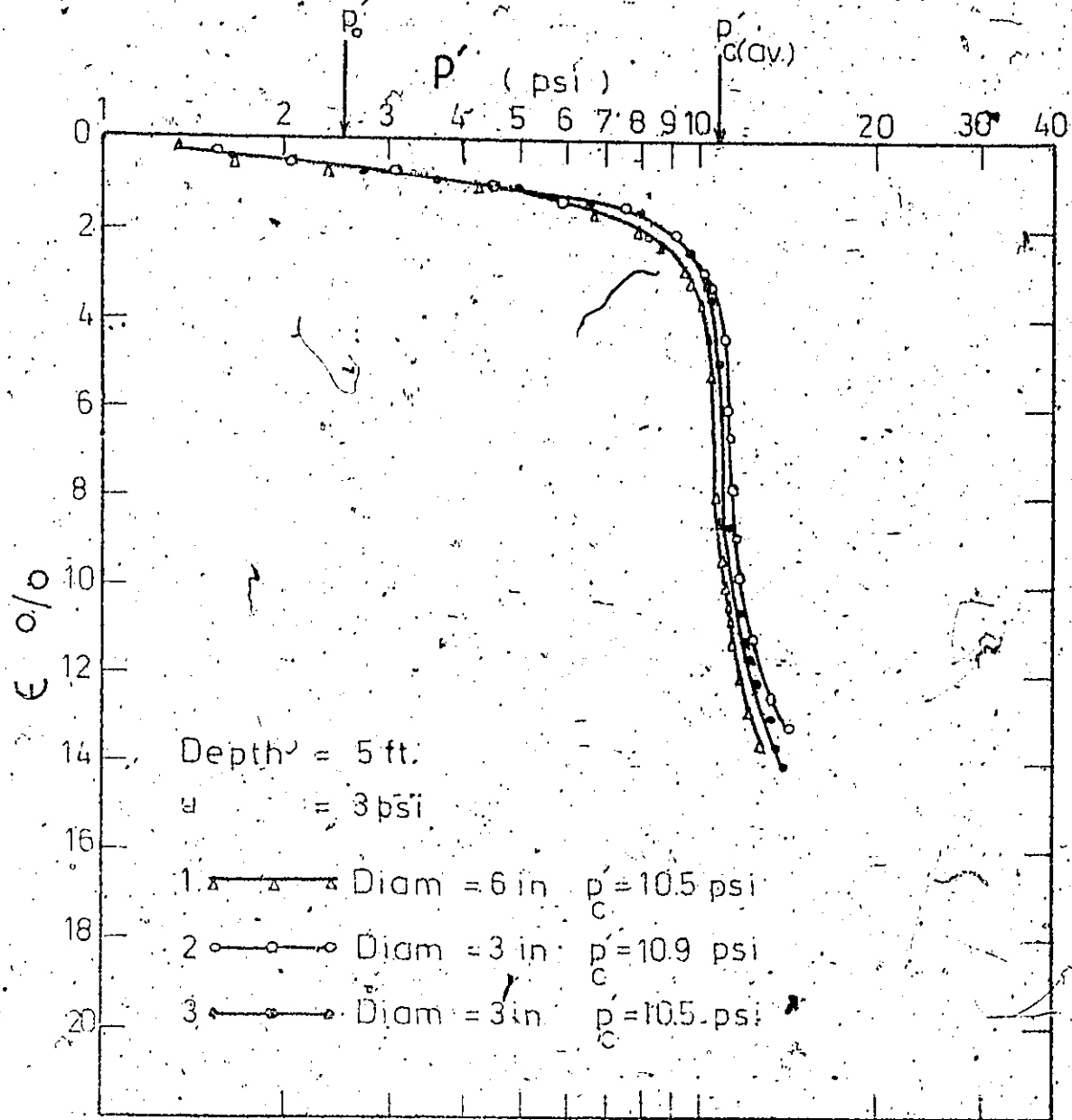
The Swedes have carried out tests on similar, soft, sensitive marine clay, and have shown that the use of thinner membranes removes the difference between the two curves.

To check the inference of membrane resistance for the particular Rowe cells used in this investigation, three tests were run using direct mechanical loading instead of the hydraulic system. The test results are reported in Figs. 4.12, 4.13 and 4.14.

It is seen that the curves obtained from the 6 in. diameter cells have moved to the left as compared to previously, while the curves from the 3 in. diameter remained

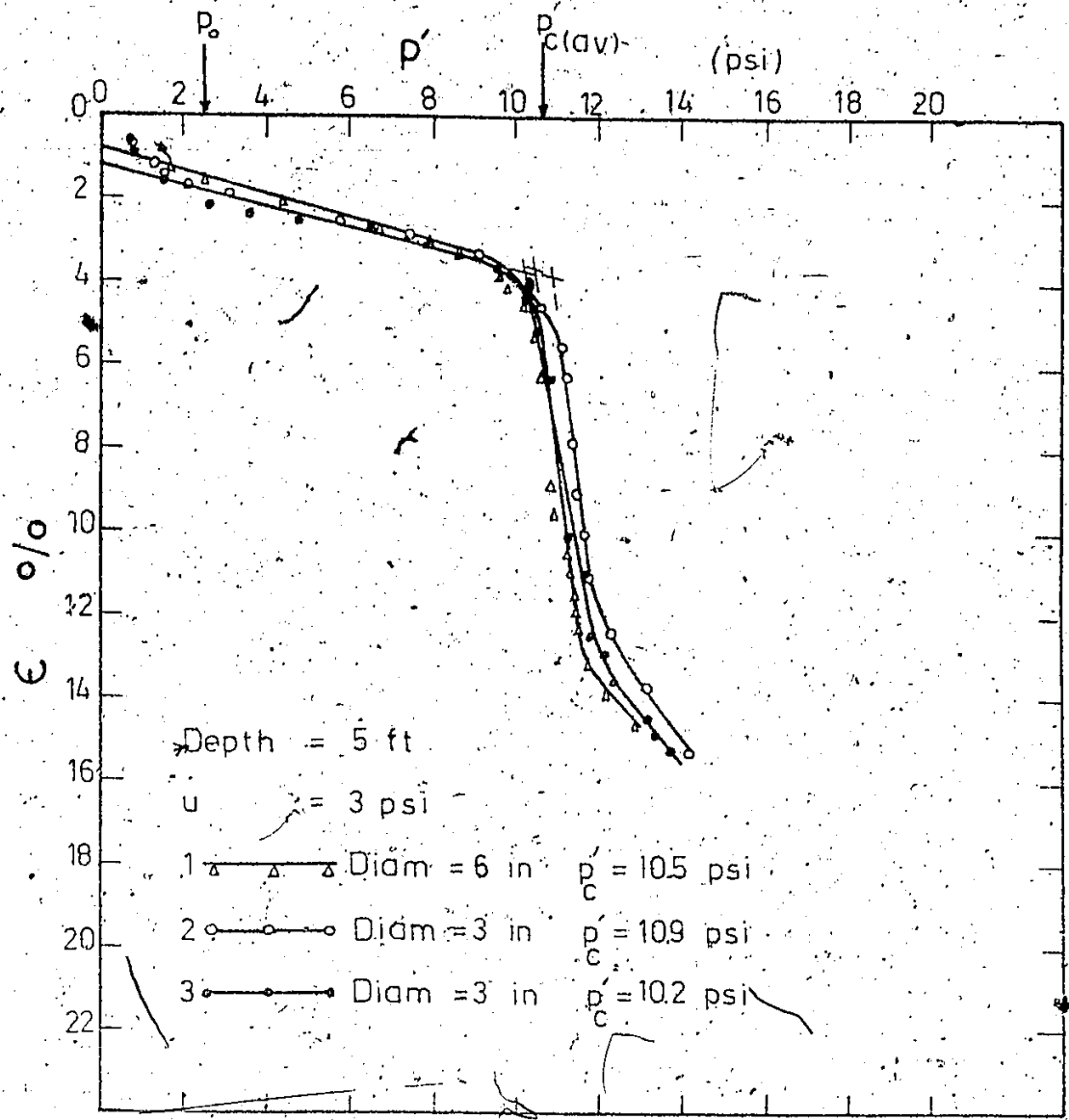
---

\* Private communication.



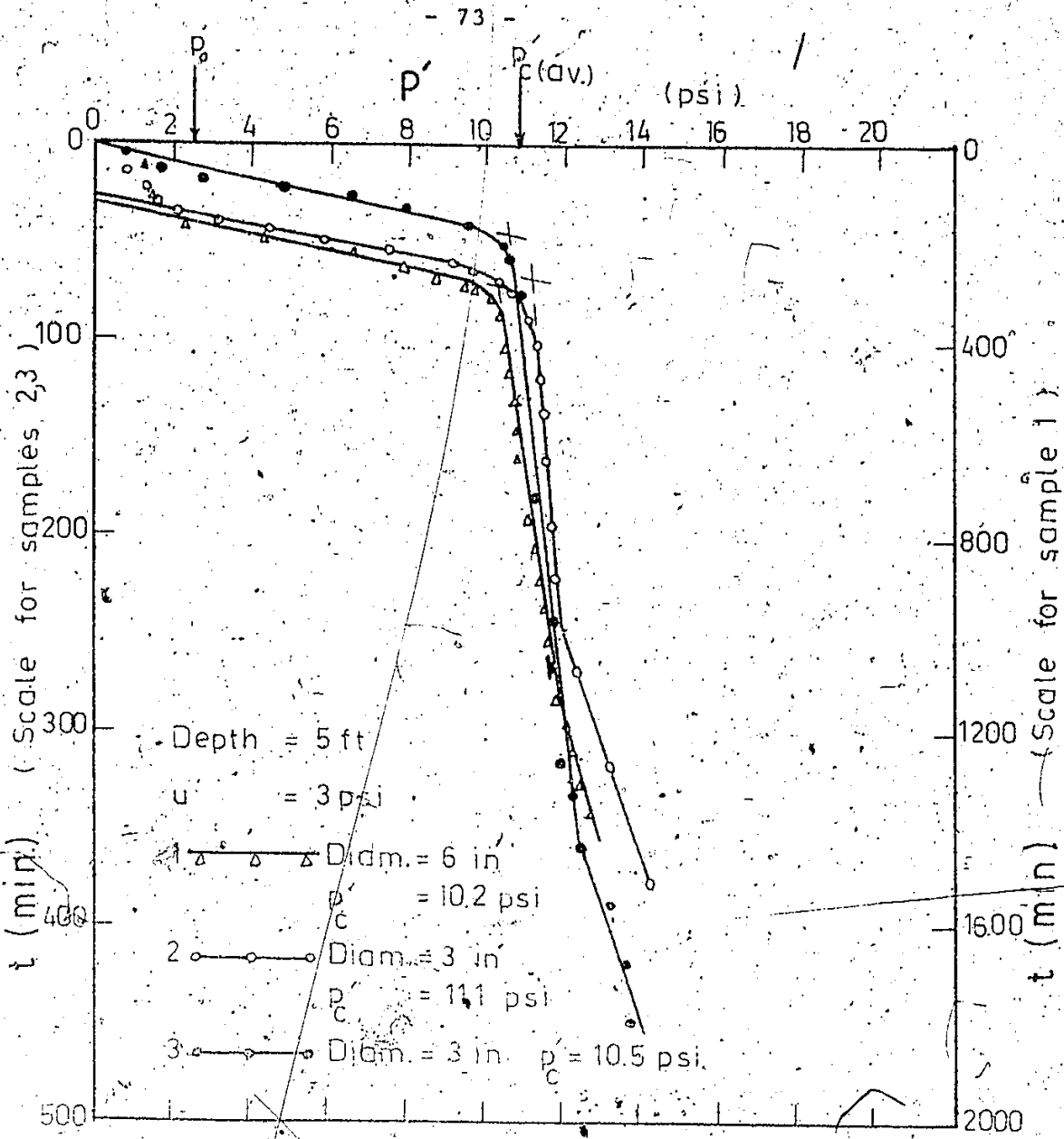
Controlled gradient consolidation tests using a mechanical loading system

FIGURE 4.12



Controlled gradient consolidation tests using a mechanical loading system.

FIGURE 4.13



Controlled gradient consolidation tests  
using  
a mechanical loading system

FIGURE 4.14

almost unchanged, so that the new  $p_c$  values almost coincide.

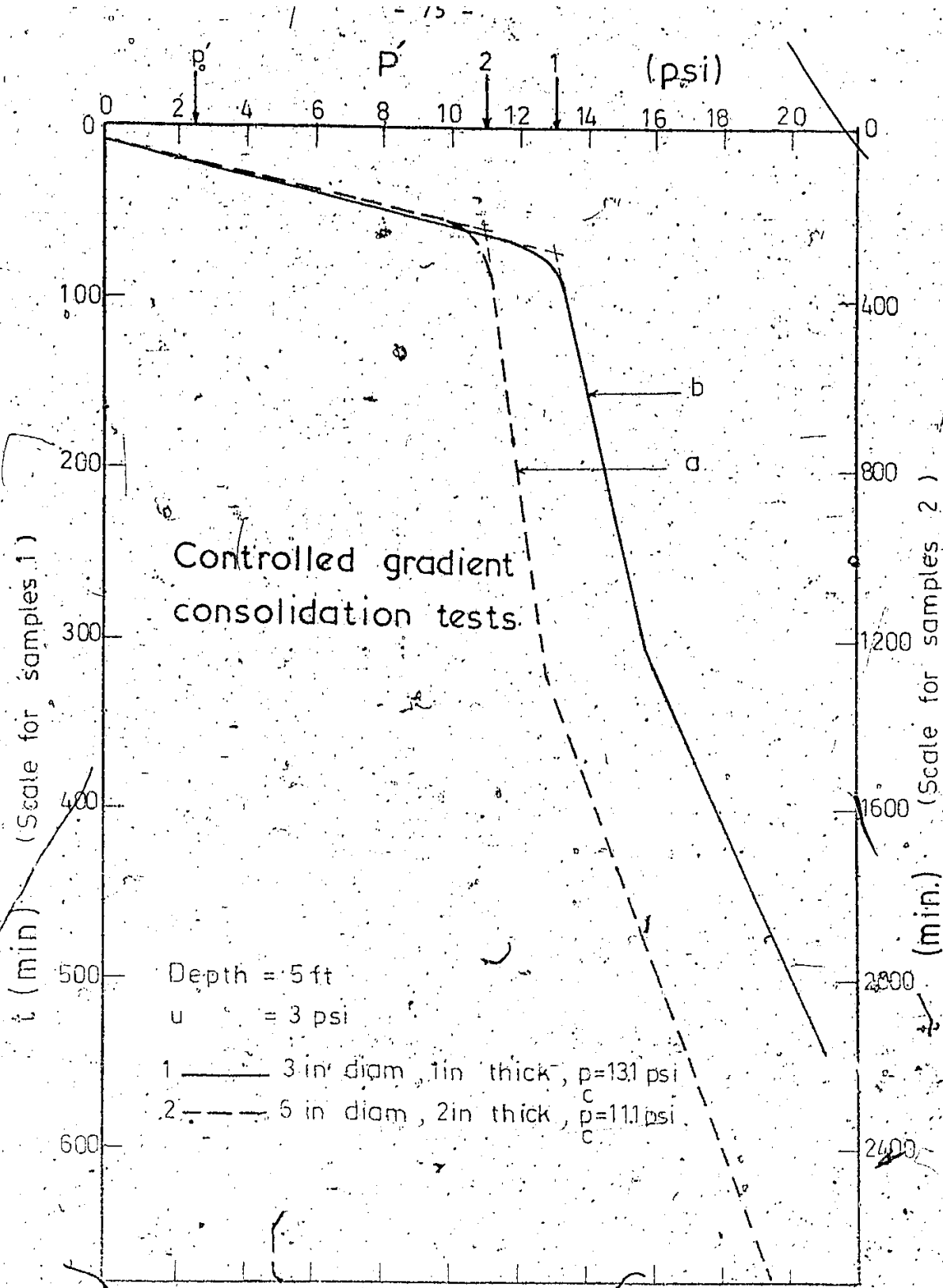
This should be further investigated at the first opportunity.

The effect of the sample size on the  $t-p'$  plot is shown in Figs. 4.15 and 4.16. From Lowe's expression for  $c_v$

$$c_v = \frac{\Delta p \cdot H^2}{\Delta t \cdot 2u} \quad (2.11)$$

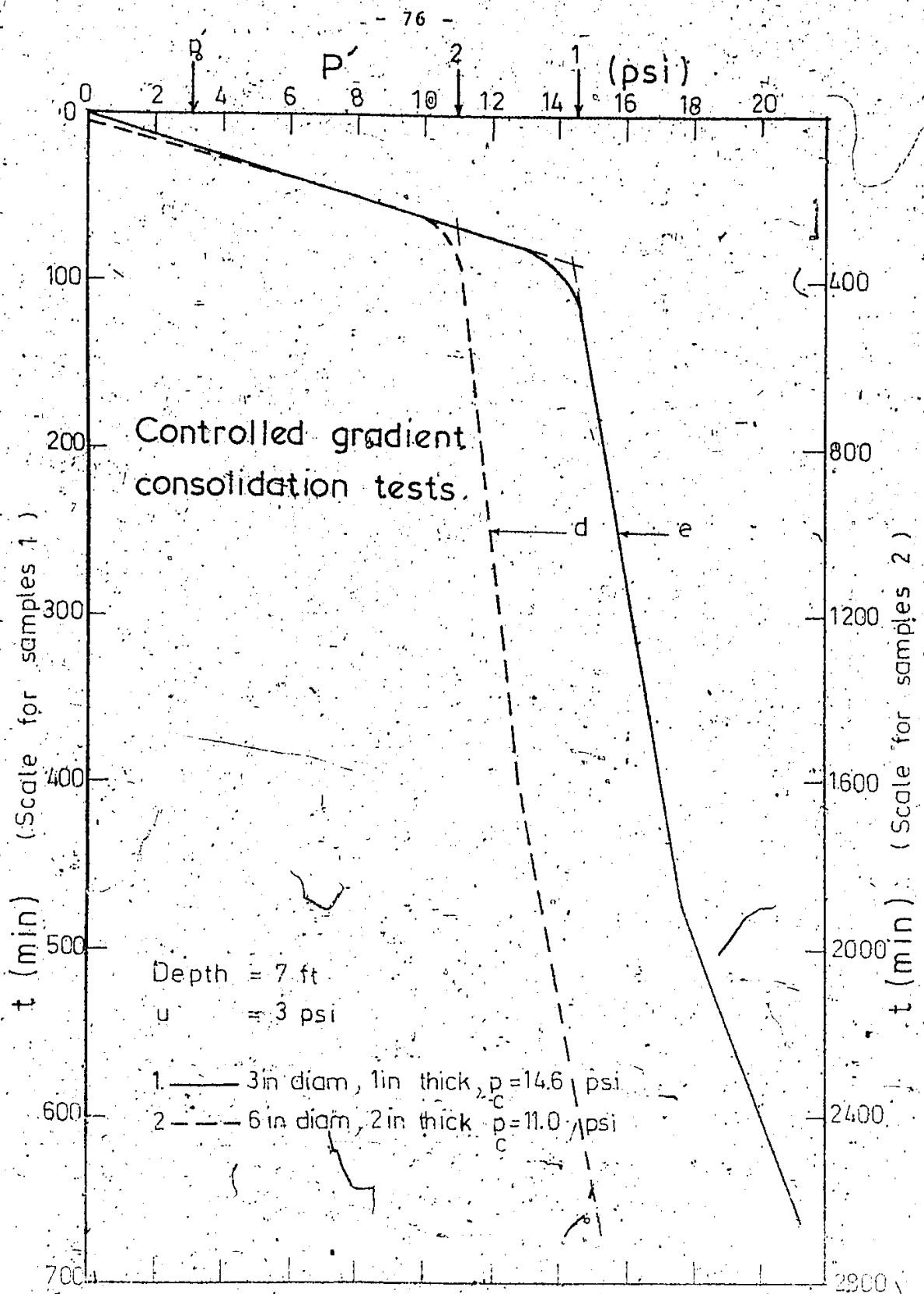
$c_v$  being the same for the same clay and  $u$  being the same, if  $H$  is doubled,  $\Delta t$  required to accommodate a particular value of  $\Delta p$  is quadrupled. That is,  $\Delta p / \Delta t$  should vary by a factor of four. In Figs. 4.15 and 4.16, the ordinate (time) scales, have a ratio of 4 between the 1 and 2 inch thick samples. It can be seen that by using these two scales, the slopes of the respective parts of the curves are about equal for the two sample sizes, but are displaced, (as are the  $\epsilon$ -log  $p'$  curves).

The effect of the sample size on the  $\epsilon-p'$  plot, and therefore on  $m_v$  is shown in Figs. 4.17 and 4.18. The slopes of the curves indicate good agreement in the  $m_v$  values for the two sizes. The value of  $c_v$  and  $k_v$  (Figs. 4.19 and 4.20), agree reasonably well although the curves are displaced with respect to each other. (If disturbance were a factor, such close agreement would not be expected. The displacement of the curves could be explained by the effect of the membrane stiffness or side friction.



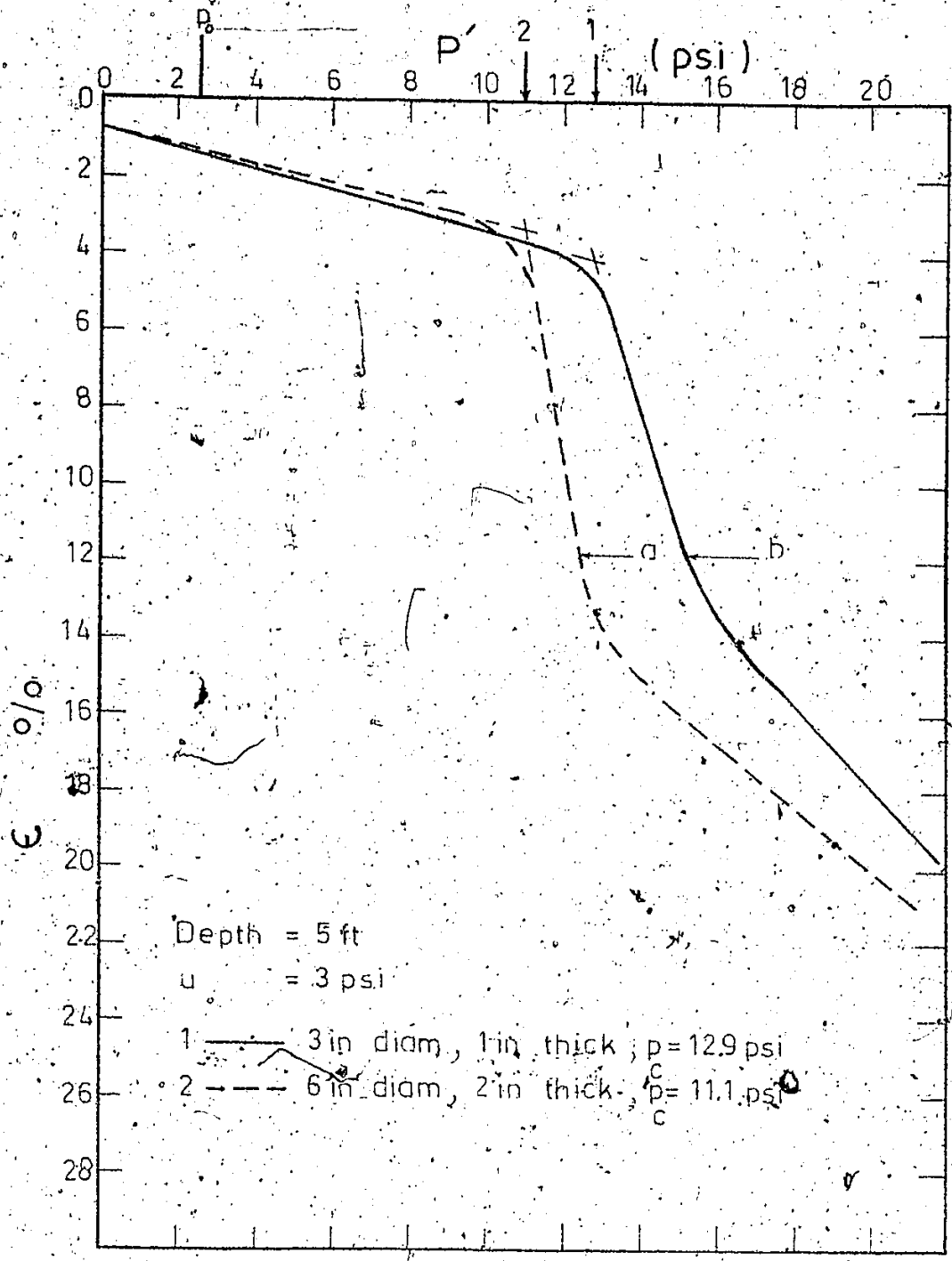
Effect of sample size.

FIGURE 4.15



Effect of sample size

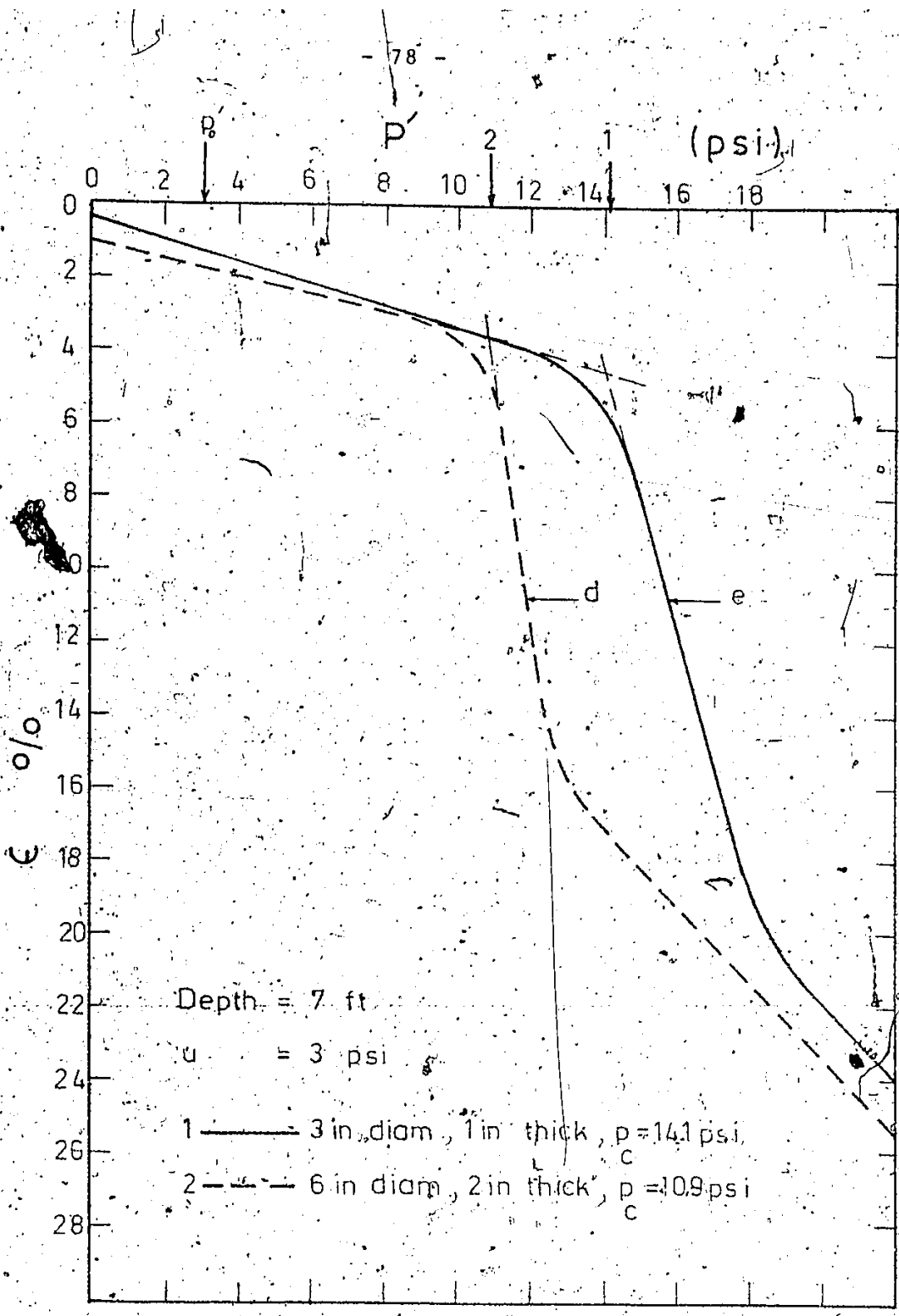
FIGURE 4016



Effect of sample size

Controlled gradient consolidation tests

FIGURE 4.17



Effect of sample size.

Controlled gradient consolidation tests.

FIGURE 4.13

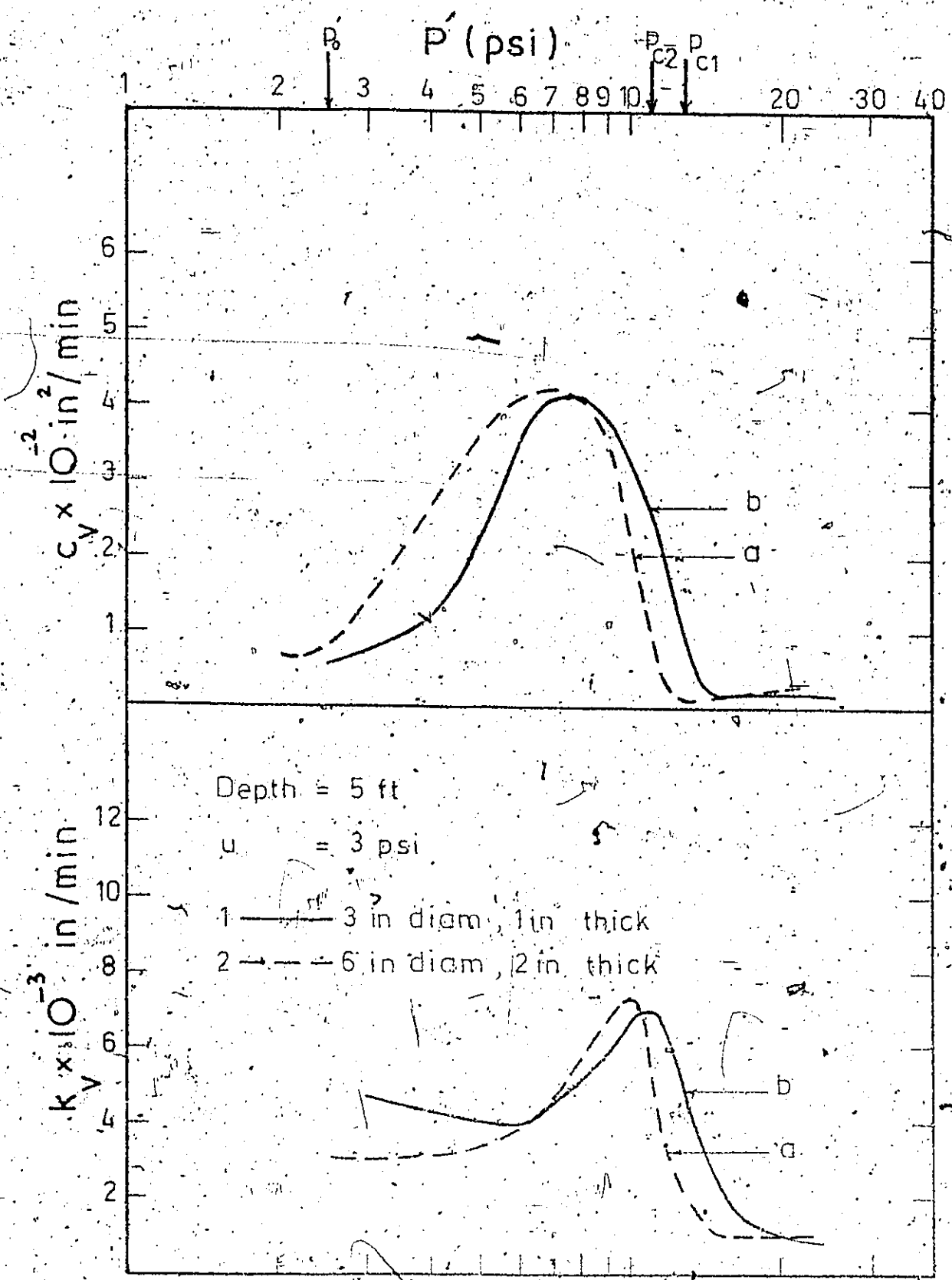
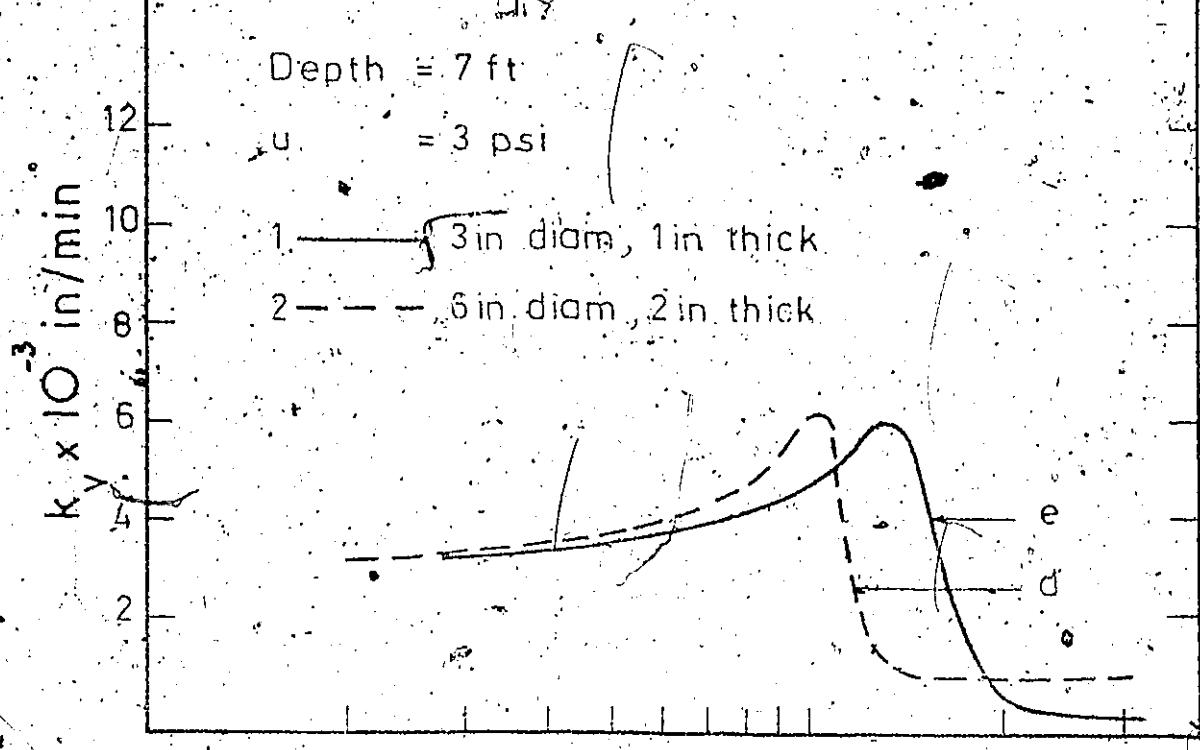
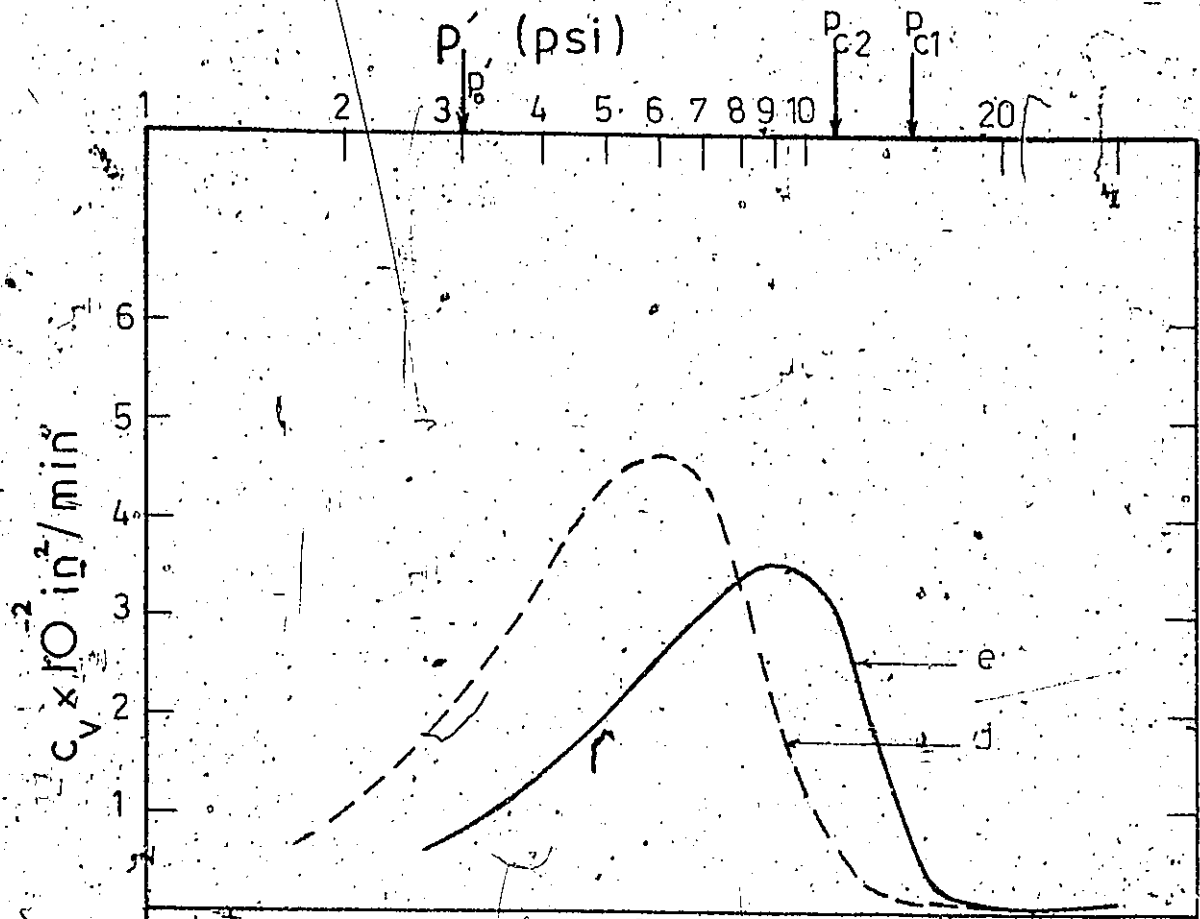


FIGURE 4.19

Effect of sample size

Controlled gradient consolidation

Tests



Effect of sample size

Controlled gradient consolidation tests

Figure 1.20

#### 4.2.3 Effect of the Hydraulic Gradient, $i$

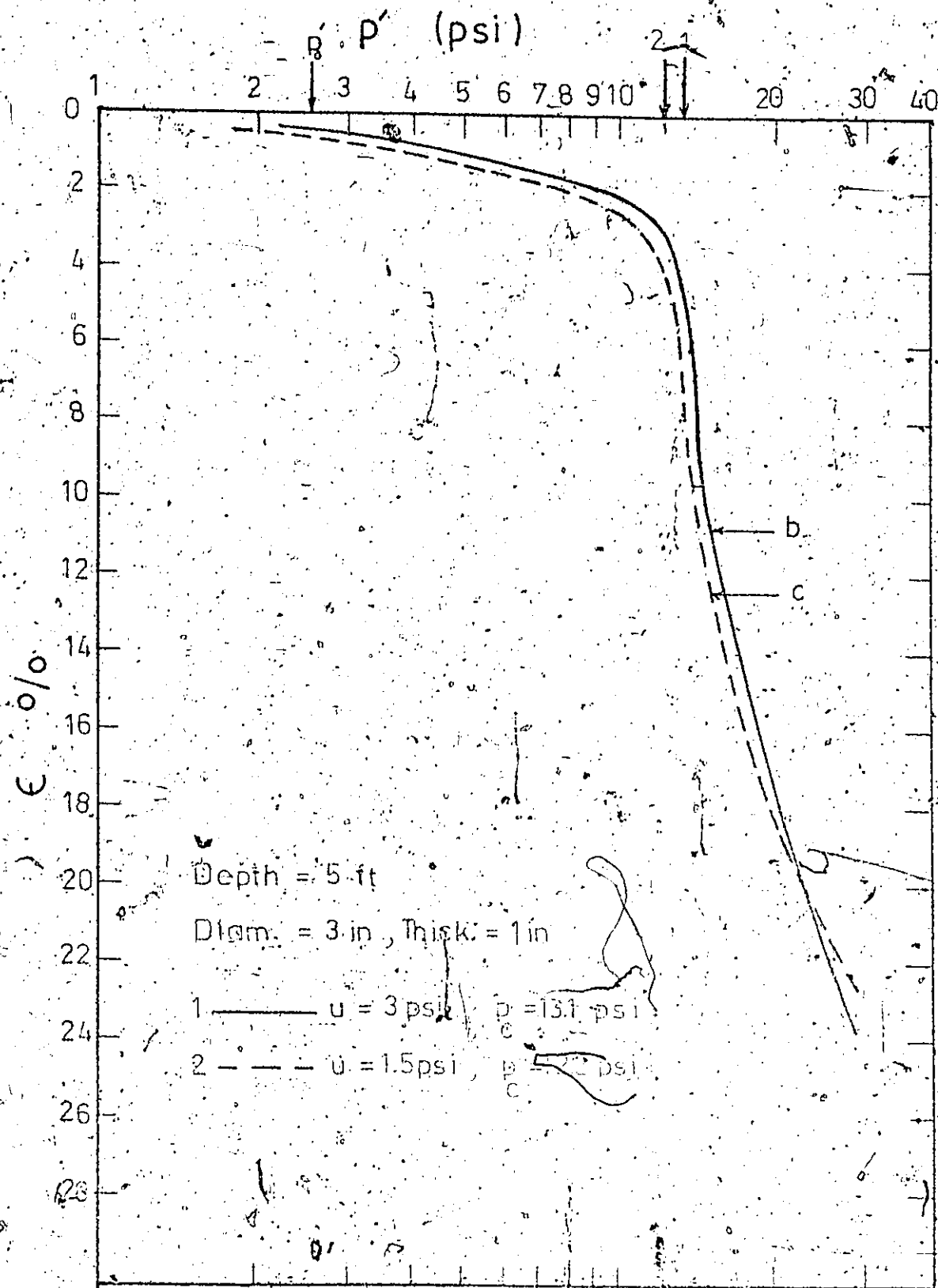
The effect of the hydraulic gradient,  $i$ , will be presented by comparing the results of tests on samples from the same depth, having the same size, but tested with different porewater pressures at the base.

Although Lowe et al did not measure that  $i$  had an effect on the  $e$ -log  $p'$  relationship for their clay, Figs. 4.21 and 4.22 show a distinct effect. From these figures and from Tables 4.8 and 4.9, it can be seen that the  $p_c$  value is higher for the larger  $u$  value at the base, that is, for the larger hydraulic gradient. This is in agreement with the work of previous investigators, e.g., Crawford (8), Hamilton and Crawford (15) and Jarrett (18), because the larger value of  $i$  means a shorter test duration, less secondary compression and a stress strain curve that is displaced to the right of longer time tests. Figures 4.23 and 4.24 show the effect of  $i$  on the  $t$ - $p'$  plots.

From the formula:

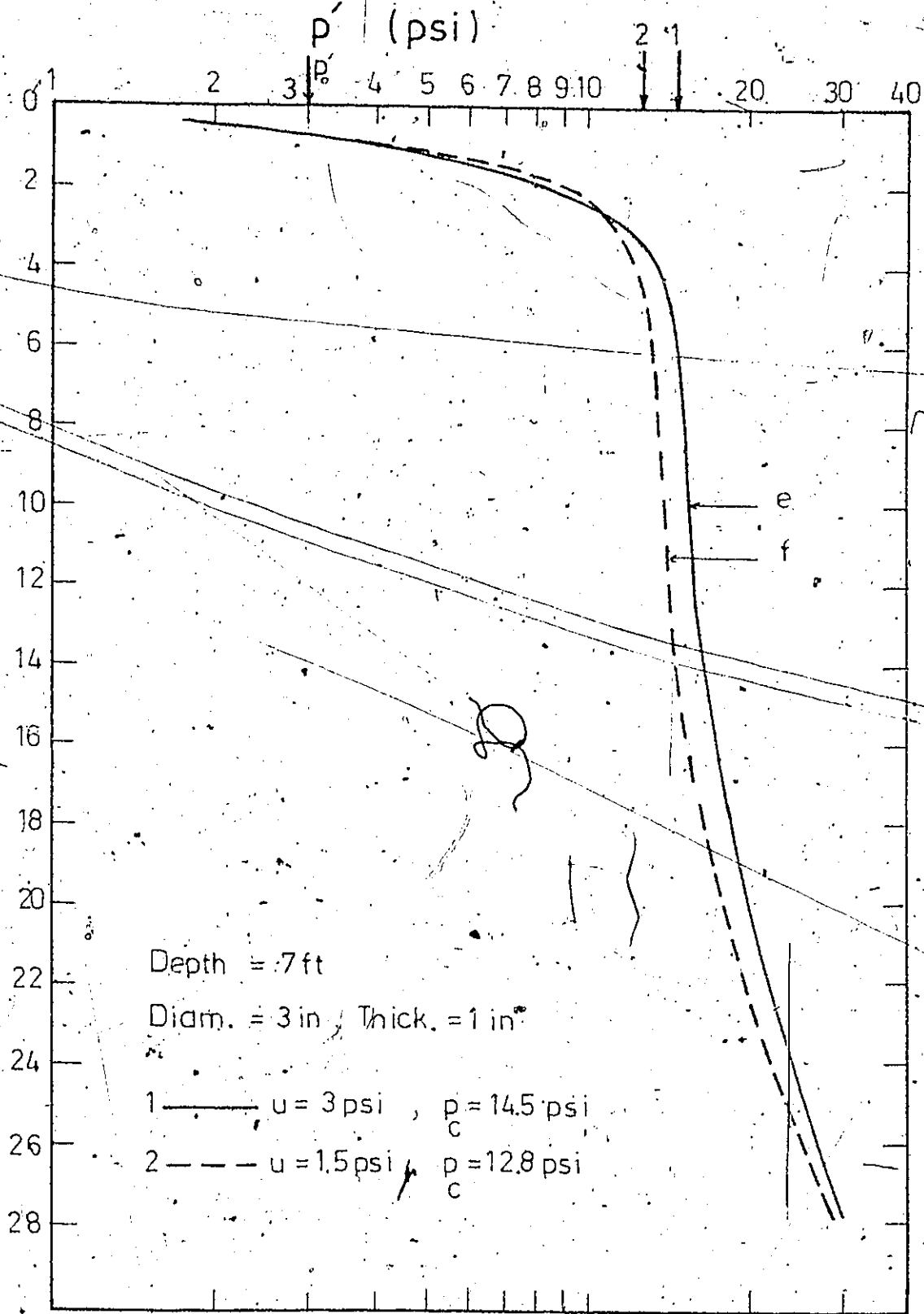
$$c_v = \frac{\Delta p}{\Delta t} \frac{H^2}{2u} \quad (2.11)$$

if  $u$  is doubled, all other factors being the same,  $\Delta t$  is halved. The time scale has been doubled for  $u = 1.5$  psi as compared to the scale for  $u = 3$  psi. For the samples from 7 ft depth, (Fig. 4.24), close agreement with the theory is found. For the samples from 5 ft depth, (Fig. 4.23), some discrepancy is noticed. One sample, represented



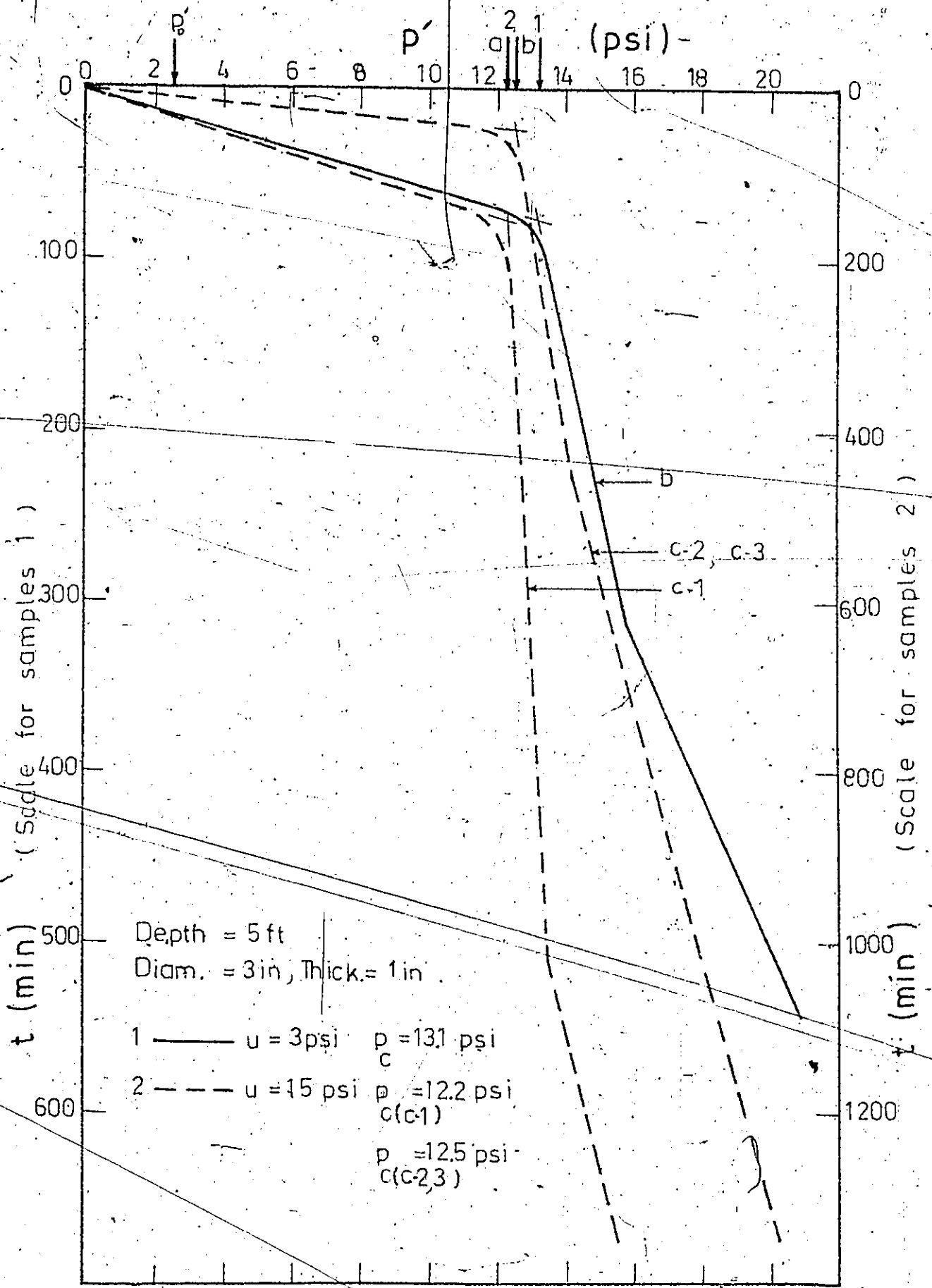
Effect of  
Controlled gradient consolidation tests.

FIGURE 4.11

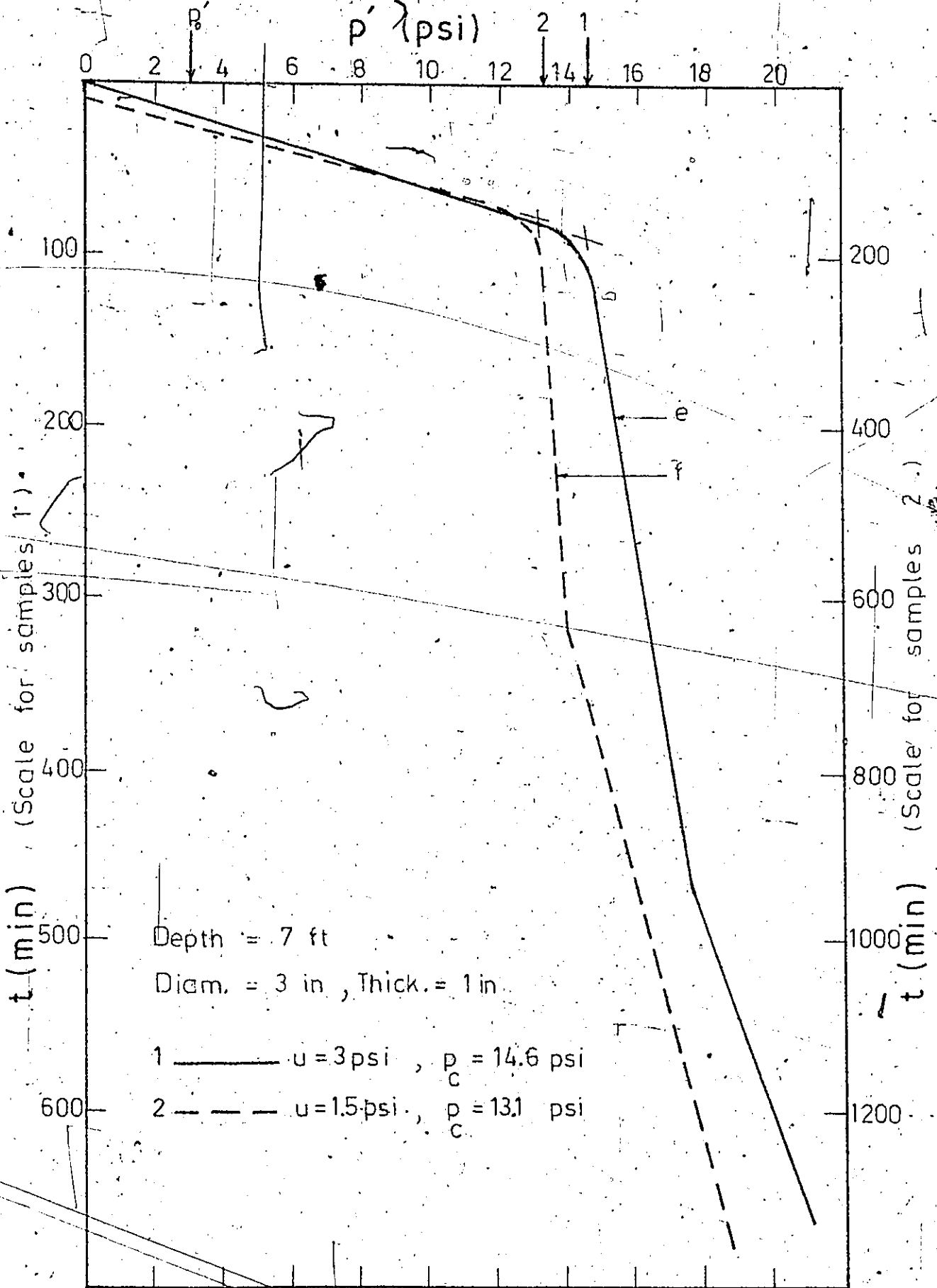


Effect of  $i$ :  
Controlled gradient consolidation tests.

FIGURE 4.22



Effect of  $i$ .  
 Controlled gradient consolidation tests.  
 FIGURE 4.23



Effect of  $i$ .

Controlled gradient consolidation tests.

by curve (a), closely follows the theory, while the other two samples, represented by an average curve (b), show a faster rate of stress application, (indicating a greater permeability), than predicted by the theory, especially in the stress range below the  $p_c$ . This difference could be due to a normal variation in the samples, although both the natural water content and the physical appearance of these two samples were no different. Figures 4.25 and 4.26, also prove that for a larger hydraulic gradient, a higher  $p_c$  is obtained. However, the curves are almost parallel; the variation in  $i$  does not seem to affect the values of  $m_v$  during the three phases of consolidation.

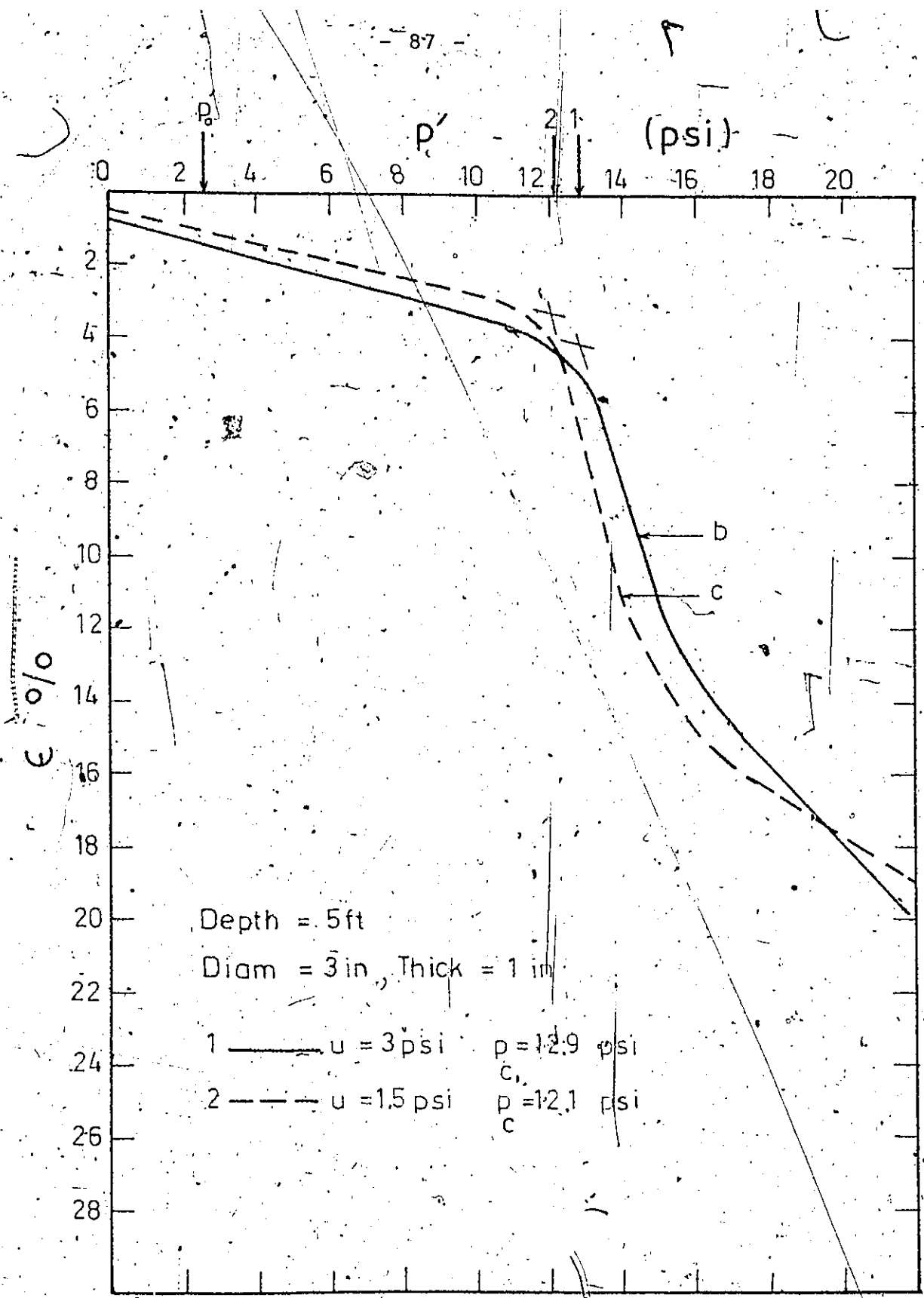
The curves showing  $c_v - \log p'$  and  $k_v - \log p'$  plots for various values of  $i$  are not presented because they are similar to those in Figs. 4.19 and 4.20 and do not show any particular trend as far as the effect of  $i$  on  $c_v$  or  $k_v$  is concerned.

#### 4.2.4 Effect of the Variation in $p_o$ and $p_c$

From the soil profile shown in Fig. 3.5,  $p_o'$  is calculated for the samples from 5 ft depth and 7 ft depth, assuming

$\gamma$ topsoil	=	90 pcf
$\gamma$ sand	=	110 pcf
$\gamma'$ sand	=	70 pcf

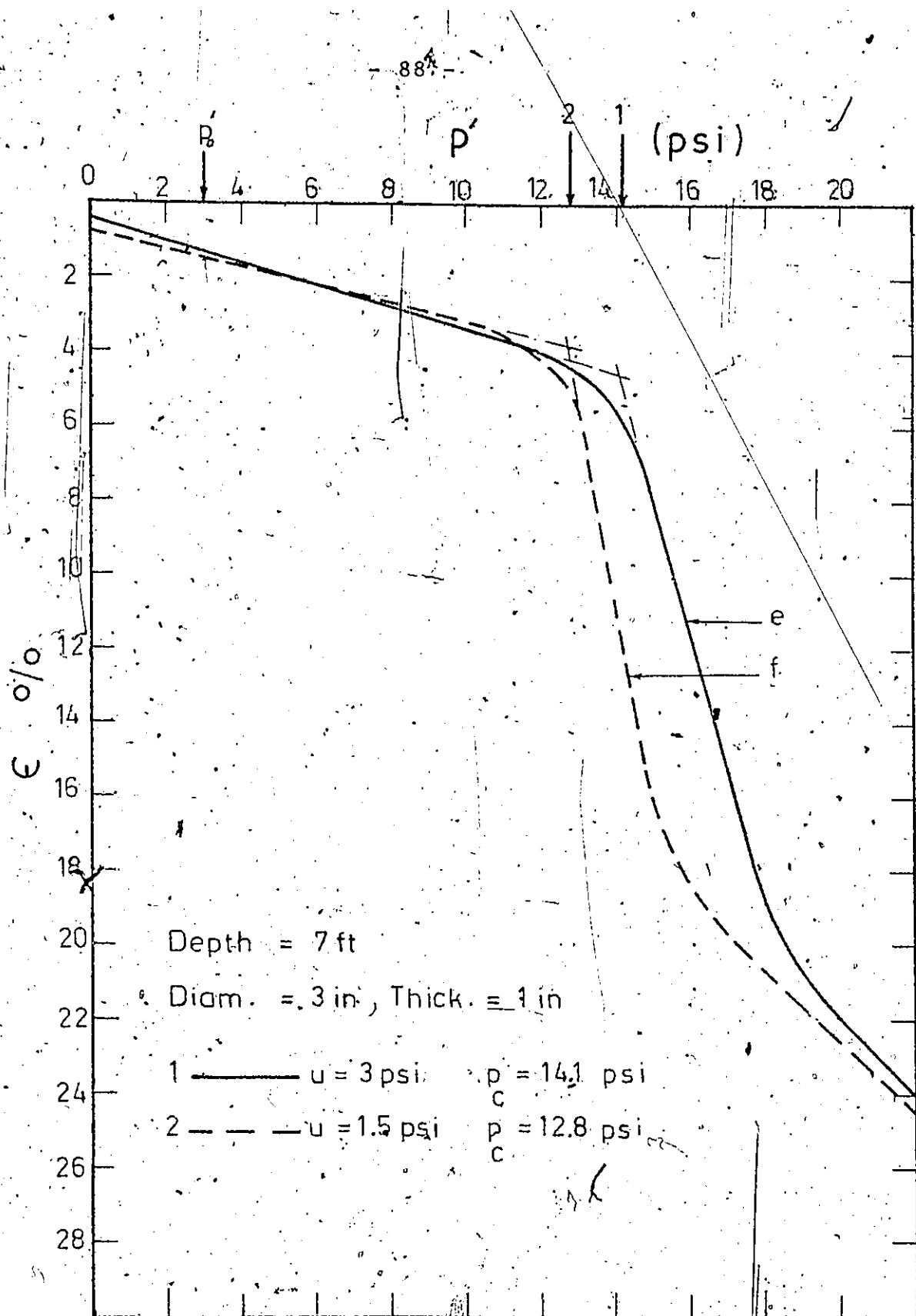
The average  $\gamma$  clay was found to be 100 pcf (as reported in Chapter 3).



Effect of  $i$ .

Controlled gradient consolidation tests.

FIGURE 4.25



Effect of  $i$

Controlled gradient consolidation tests.

FIGURE 4.26

$\gamma'$  clay  $\approx$  37 pcf.

The groundwater level was at 1.58 ft depth.

$$\begin{aligned} \text{Then } p'_o \text{ at 5 ft depth} &= 90 \times 1 + 110 \times 0.58 + 70 \times 2.42 + 37 \times 1 \\ &= 360 \text{ psf.} \\ &\approx 2.5 \text{ psi (17.35 kN/m}^2\text{)} \end{aligned}$$

$$\begin{aligned} \text{and } p'_o \text{ at 7 ft depth} &= 90 \times 1 + 110 \times 0.58 + 70 \times 3.42 + 37 \times 3 \\ &= 434 \text{ psf} \\ &\approx 3.0 \text{ psi (20.8 kN/m}^2\text{)} \end{aligned}$$

If we assume that any overconsolidation is due mainly to additional overburden that may have existed in the past or to a general lowering of the water table, then the difference between  $p_c$  at 7 ft and  $p_c$  at 5 ft should be equal to the difference between the  $p'_o$  values at these depths, i.e., equal to 0.5 psi.

The table in Fig. 4.27 compares the average values of  $p_c$  from each set of tests at 5 ft to the corresponding values at 7 ft. The large samples do not show any variation of  $p_c$  with depth. The small samples with  $u=3$  psi show an increase of  $p_c$  with depth, but this increase is larger than the expected amount. Only the small samples with  $u=1.5$  psi show a difference in  $p_c$  between the samples from the two depths, close to the expected 0.5 psi.

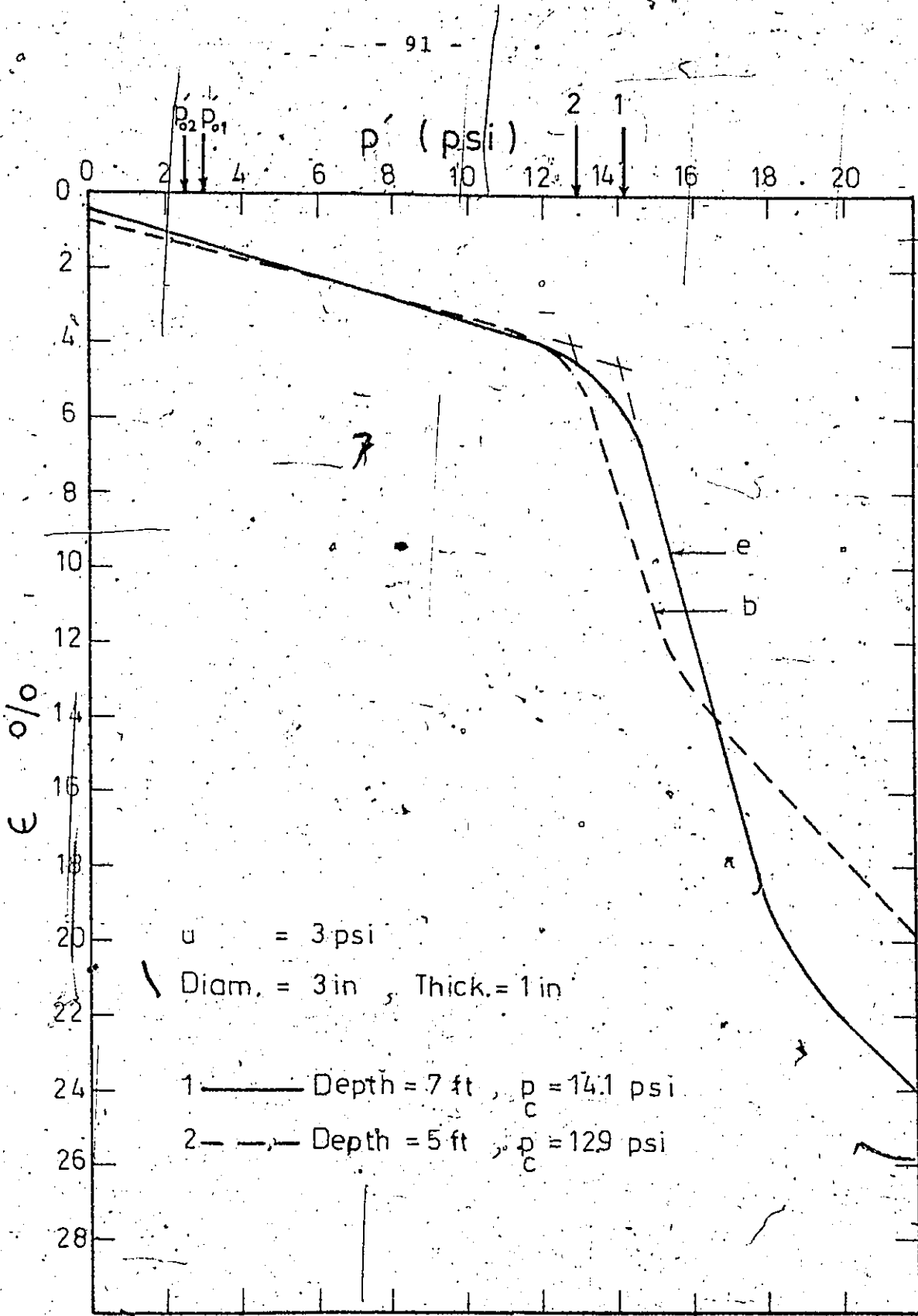
It is possible that other phenomena such as desiccation could result in a higher  $p_c$  value at 5 ft than 7 ft or in the same value of  $p_c$  as indicated by the 6 in tests.

Figures 4.28 and 4.29 are given as examples of the variation due to the depth of the samples. They are for tests on 3 in. diameter, 1 in. thick samples with  $u = 3$  psi.

FIGURE 4.27

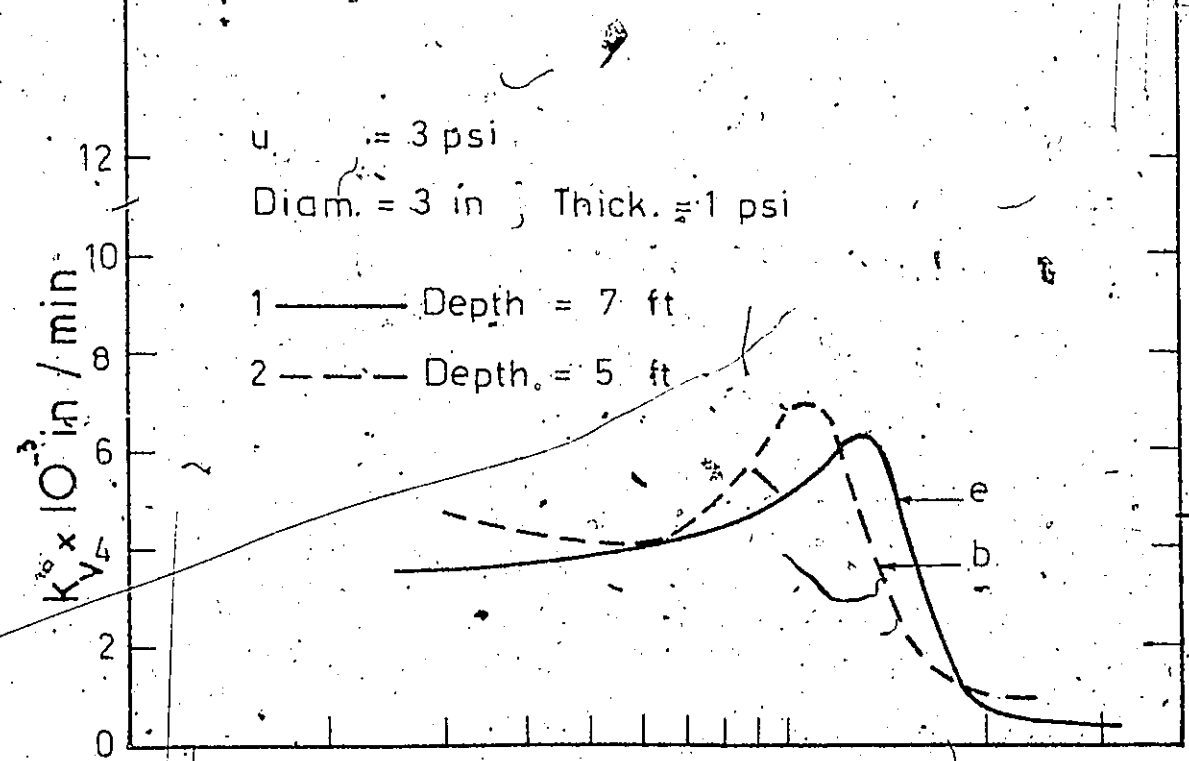
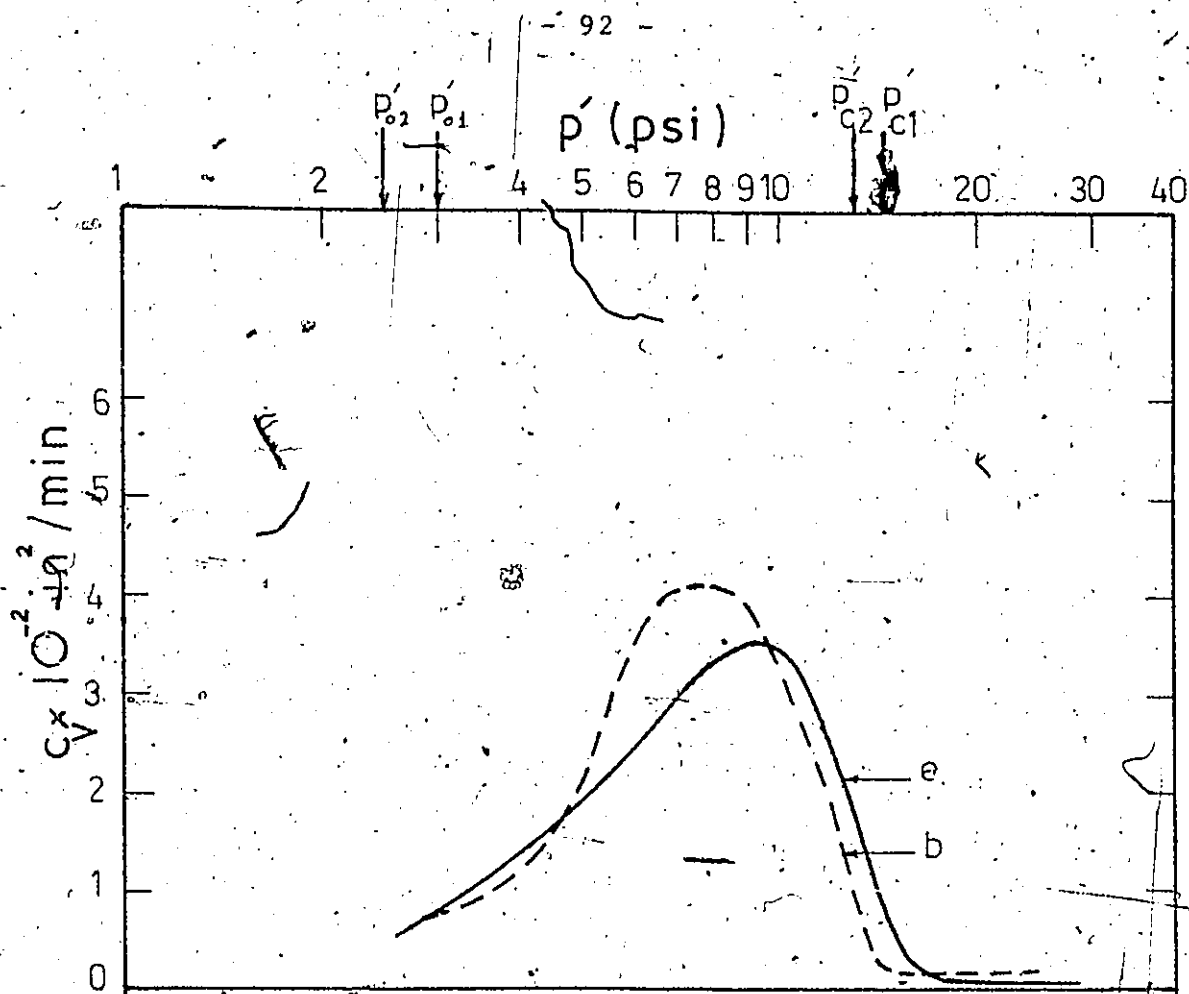
Variation of  $p_c$  with depth for  
different controlled gradient tests

Test No	Depth	sample size (in)		$\Delta u$ base psi	$P_c$ ( $\epsilon$ -log $p'$ curves)	$P_c$ t-p curves	$P_c$ t-p curves
		diam.	thick				
a	5	6	2	3	11.0	11.0	11.0
d	7	"	"	"	11.0	11.0	10.9
b	5	3	1	3	13.1	13.1	12.9
e	7	"	"	"	14.5	14.6	14.1
c	5	3	1	1.5	12.2	12.5	12.1
f	7	"	"	"	12.8	13.1	12.8



Effect of the depth of the sample  
Controlled gradient consolidation tests

FIGURE 4.28



Effect of the depth of the sample.  
 Controlled gradient consolidation tests.

FIGURE 4.29

Both Figs. 4.28 and 4.29 exhibit a translation in the results with depth. While this translation affects the values of  $p_c$  and the stress limits for the three phases of consolidation, it does not appear to affect the values of  $m_v$ ,  $c_v$  or  $k_v$  within the respective phases.

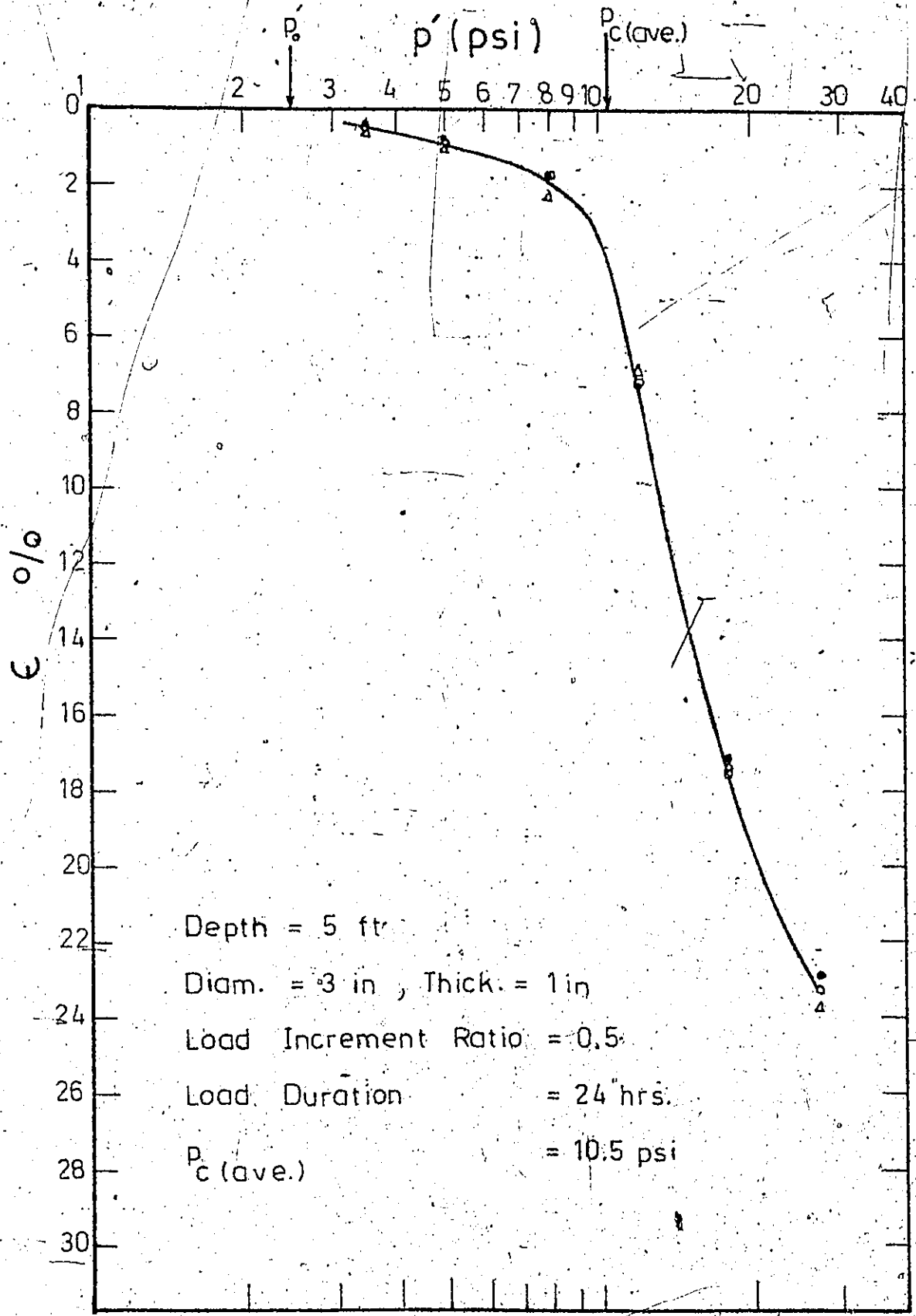
#### 4.3 The Conventional Consolidation Tests

As mentioned in the previous chapter, the conventional tests were only performed on 3 in. diameter, 1 in. thick samples. The tests were also performed in the same hydraulic cells as were the controlled gradient consolidation tests.

The repeatability for these tests was also satisfactory. As an example;  $\epsilon$ -log  $p'$  curves for samples from 5 ft. depth tested with a load increment ratio of 0.5 and a load duration of 24 hours, are presented in Fig. 4.30. The  $p_c$  values from  $\epsilon$ -log  $p'$  plots were obtained using the Casagrande construction.

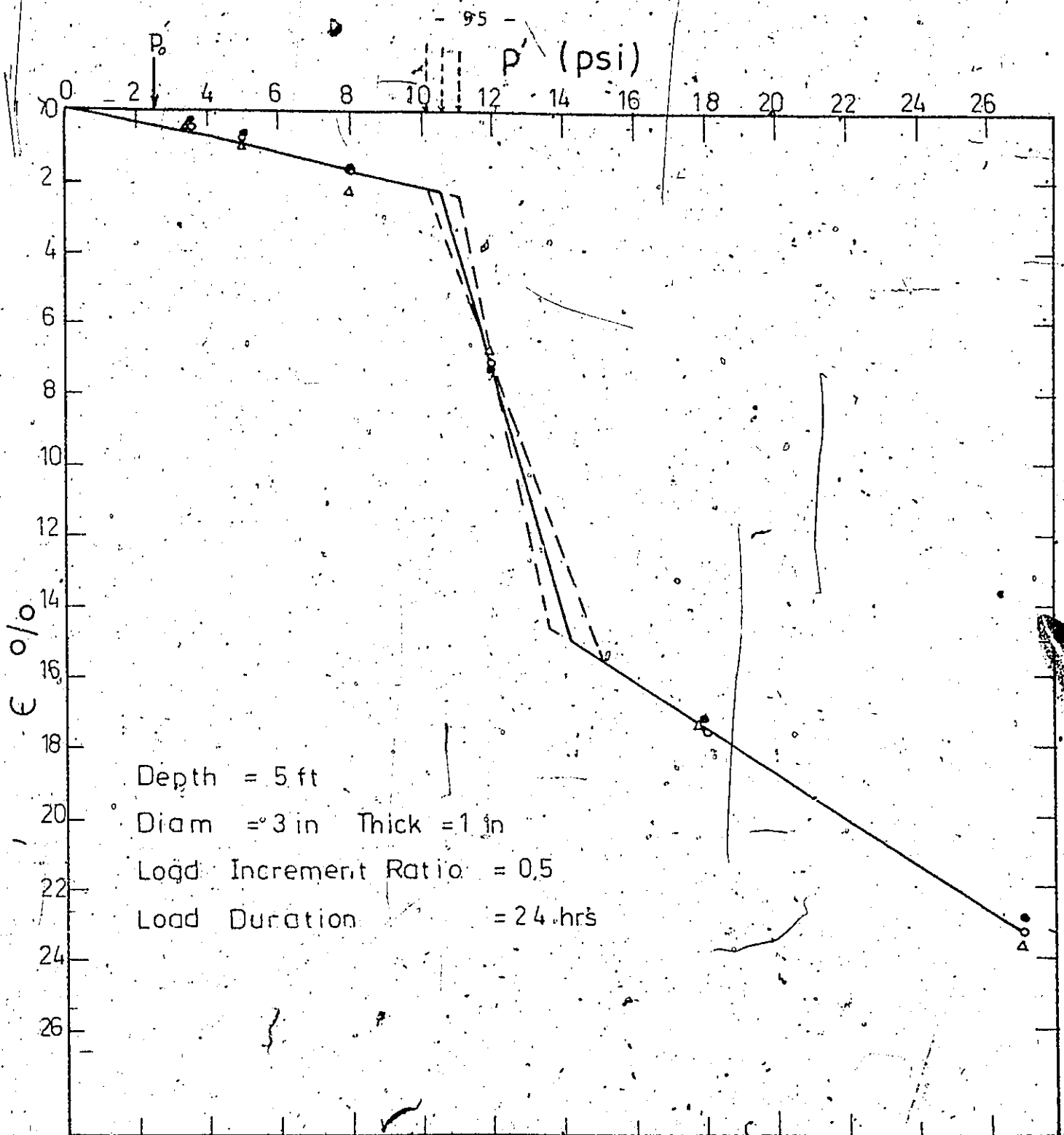
As shown in Fig. 4.31, the  $\epsilon$ - $p'$  plot can not give a reliable value of  $p_c$  because of the small number of points available in the range of phase II. Consequently,  $m_v$  values in this range are also not reliable.

Values of  $c_v$  were calculated using Taylor's fitting method whenever possible. The Casagrande method was not used because type I dial readings-log time curves (Fig. 2.9), were obtained only for loads past  $p_c$ .



E-Log  $p'$  Curve  
Conventional consolidation tests

FIGURE 4.30



E - P Plot

Conventional consolidation tests.

FIGURE 4.31.

For the short duration tests, (60 min, 30 min, 15 min load duration), it was noticed that for loads higher than the  $p_c$ , the samples did not reach 100% consolidation. A correction was made. It was assumed that at any load, the  $c_v$  calculated from the 24 hours load duration tests was the same as for the short duration tests. This  $c_v$  was used to find  $T_v$  for the short duration tests at the end of the particular load. From the  $T_v$ - $\bar{U}$  relationship, the degree of consolidation,  $\bar{U}$  was found. The compression under this load was then corrected for 100% consolidation.

Example: For a 60 min load duration test on a sample from 5 ft depth, the total compression,  $\Delta H$  of the sample at the end of the duration of the 16 psi load was 0.0930 in. Then the average drainage length during this load duration,  $H_{av}$  was

$$H_{av} = \frac{1-0.0930}{2} = 0.4585 \text{ in}$$

(The sample was draining from top and bottom).

The average  $c_v$  at 16 psi from the 24 hours load duration tests was found to be  $0.306 \cdot 10^{-2} \text{ in}^2/\text{min}$ .

Then for the 60 min duration test,

$$T_v = \frac{0.306 \cdot 10^{-2} \times 60}{0.4585^2} = 0.873$$

From the relation between  $T_v$  and  $\bar{U}$  as illustrated in Fig. 2.2,

$$\text{for } T_v = 0.873, \quad \bar{U} = 90.5\%.$$

Then for 100% consolidation, the compression under 16 psi should have been

$$\frac{(0.0930 - 0.0142) \times 100}{90.5} = 0.0870$$

where 0.142 is the total compression of the sample before the 16 psi load was applied. The total compression at 100% consolidation would have been

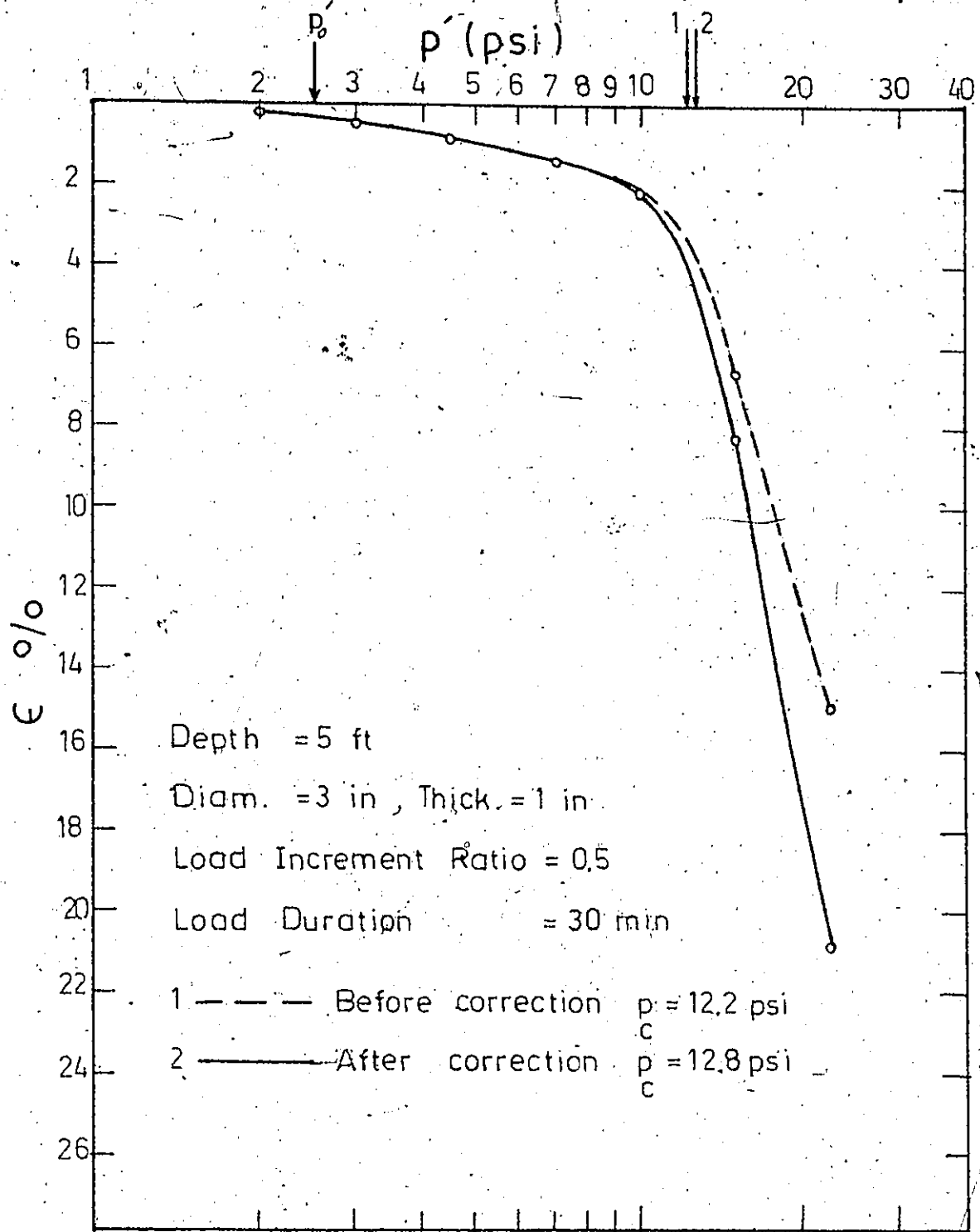
$$0.0870 + 0.0142 = 0.1012 \text{ in}$$

i.e., at 16 psi,  $\frac{\Delta H}{H}\%$  would be equal to 10.12%.

This correction is reliable for the first load which did not reach 100% consolidation (say 16 psi in this example). But it should be noted that for further loads, it does not give correct results. The reason is that some of the compression occurring under the next load (say 32 psi in this example) will be partly due to the primary consolidation of the 16 psi load still taking place, and differentiating between the effect of each load is not possible.

An example of the  $\epsilon$ -log  $p'$  curve before and after correction is given in Fig. 4.32.

From the tests of 24 hour duration it appears that load durations of the order of 150 minutes would be necessary to ensure 100% consolidation under each load increment. This was confirmed by single check tests of 12-hour duration which were carried out on samples for 5 ft and 7 ft depth.



$\epsilon$ -Log  $p'$  curve for a short duration test before and after correction.

FIGURE 4.32

The  $p_c$  values obtained from the incremental loading tests are presented in Fig. 4.33 for the samples from 5 ft depth and in Table 4.34 for those from 7 ft depth. An average curve was drawn for each set and an average  $p_c$  found for this curve. This was done only for the corrected curves, when correction was applied.

#### 4.3.1 Effect of the Load Duration

Figures 4.35 and 4.36 show  $\epsilon$ -log  $p'$  curves obtained from samples tested using the same load increment ratio (0.5), but with durations of 30 minutes and 24 hours. It is clear that for the longer duration test a smaller value of  $p_c$  is obtained. This is in agreement with results reported in the literature and quoted in Chapter 2.

#### 4.3.2 Effect of the Load Increment Ratio

From the number of tests performed, no study can be made of the effect of the load increment ratio alone, because in all cases, the load duration was also changed. However, examining Tables 4.33 and 4.34, and Figs. 4.37 and 4.38, summarizing all incremental test results, it can be deduced that the  $p_c$  increases when the load increment ratio and the load duration are decreased.

#### 4.3.3 Effect of the Variation in $p_o$ and $p_c$

The table in Fig. 4.39 compares the average  $p_c$

FIGURE 4.33

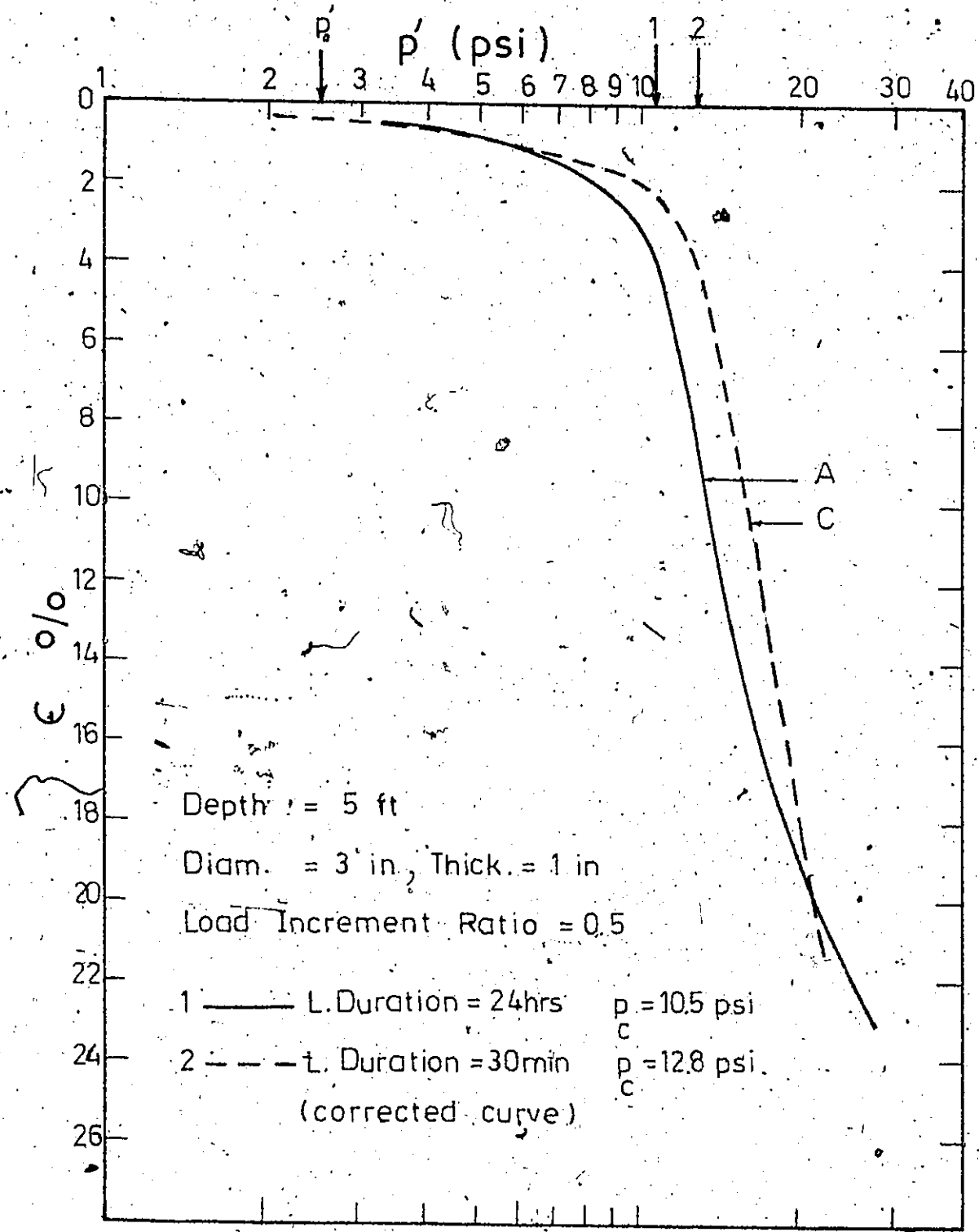
Summary of results of incremental  
loading tests on samples from 5 ft depth

Test No	Ratio	Duration	$P_c$ psi	$P_c$ corrected psi	$P_c$ average psi
A-1	0.5	24 hrs	10.2		10.5
A-2	"	"	10.8		
A-3	"	"	10.3		
B-1	1	60 min	11.0	11.0	11.0
B-2	"	"	11.0	10.9	
B-3	"	"	12.1	12.0	
C-1	0.5	30 min	12.2	12.8	12.8
C-2	"	"	11.9	12.5	
C-3	"	"	12.4	12.9	
D-1	0.25	15 min	14.5	14.0	13.7
D-2	"	"	14.0	13.5	
D-3	"	"	13.8	13.8	

FIGURE 4.34

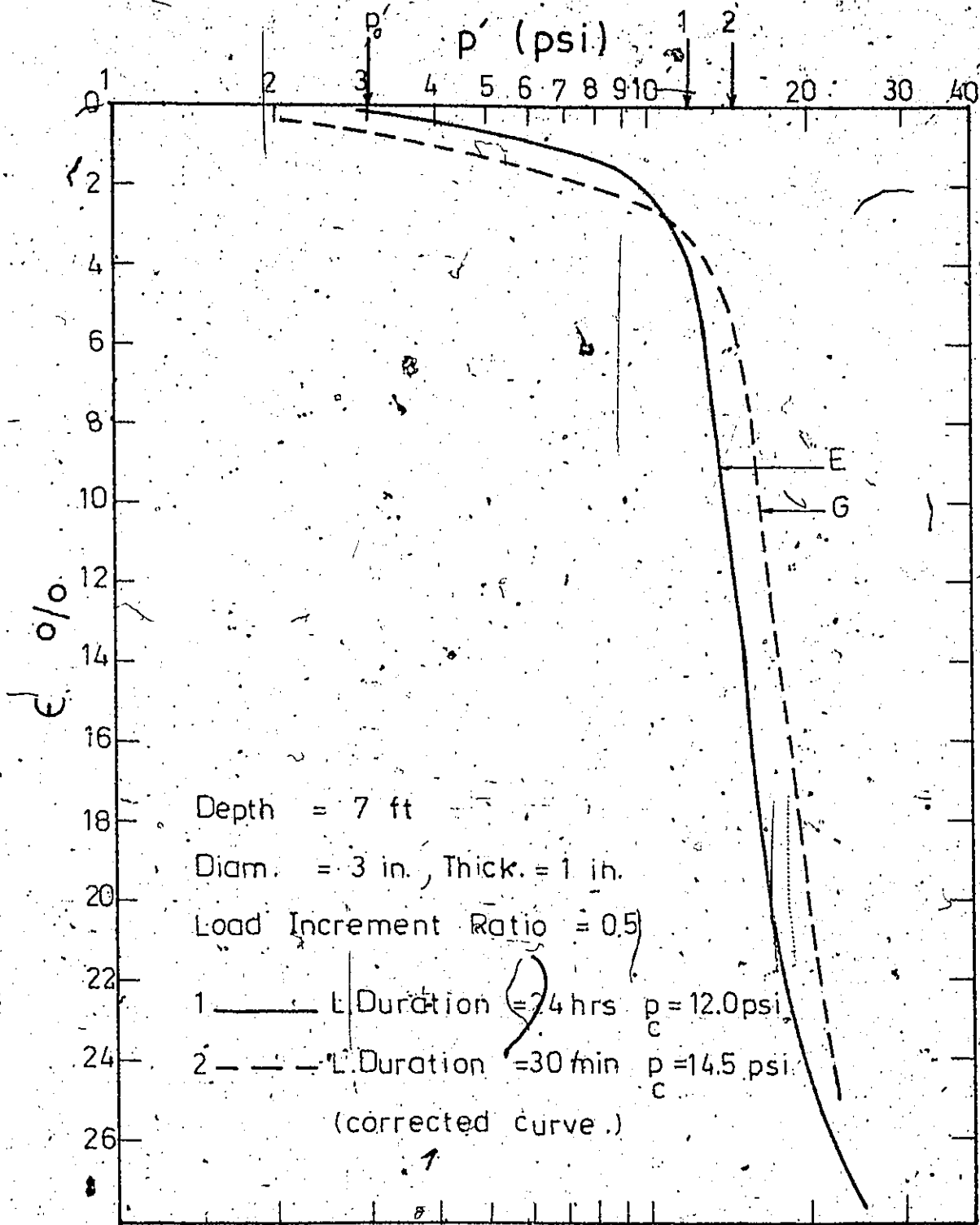
Summary of results of incremental loading  
tests on samples from 7 ft depth

Test No	Ratio	Duration	P <sub>c</sub> psi.	p <sub>c</sub> corrected psi	p <sub>c</sub> average psi
E-1	0.5	24 hrs	13.0		12.0
E-2	"	"	11.5		
E-3	"	"	12.2		
F-1	1	60 min	13.0	11.2	12.1
F-2	"	"	13.7	13.5	
F-3	"	"	12.0	11.2	
G-1	0.5	30 min	13.3	14.5	14.5
G-2	"	"	13.8	14.5	
G-3	"	"	13.9	14.5	
H-1	0.25	15 min	15.5	15.8	15.1
H-2	"	"	15.6	15.8	
H-3	"	"	13.6	14.5	



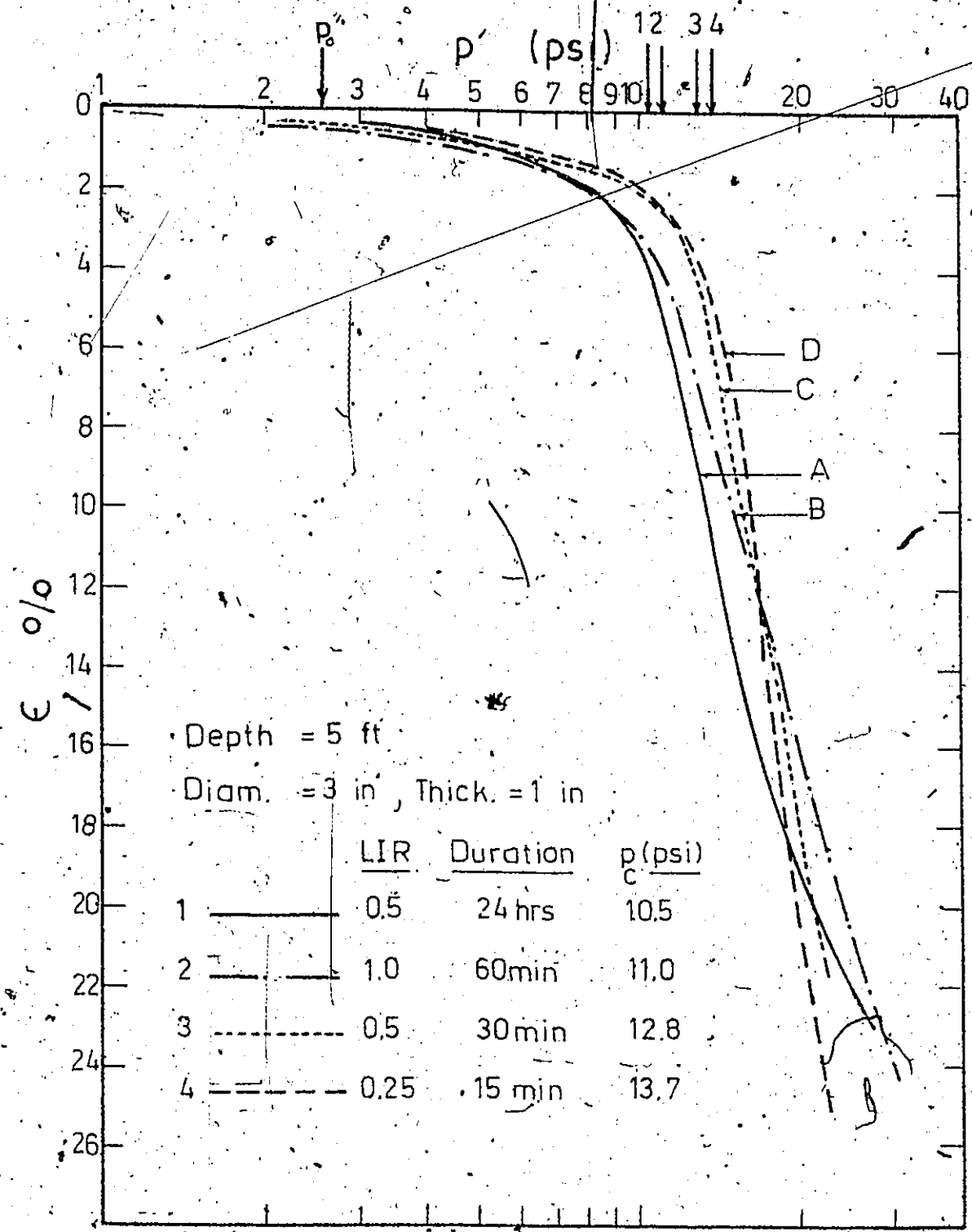
Effect of load duration.  
Conventional consolidation tests.

FIGURE 4.35



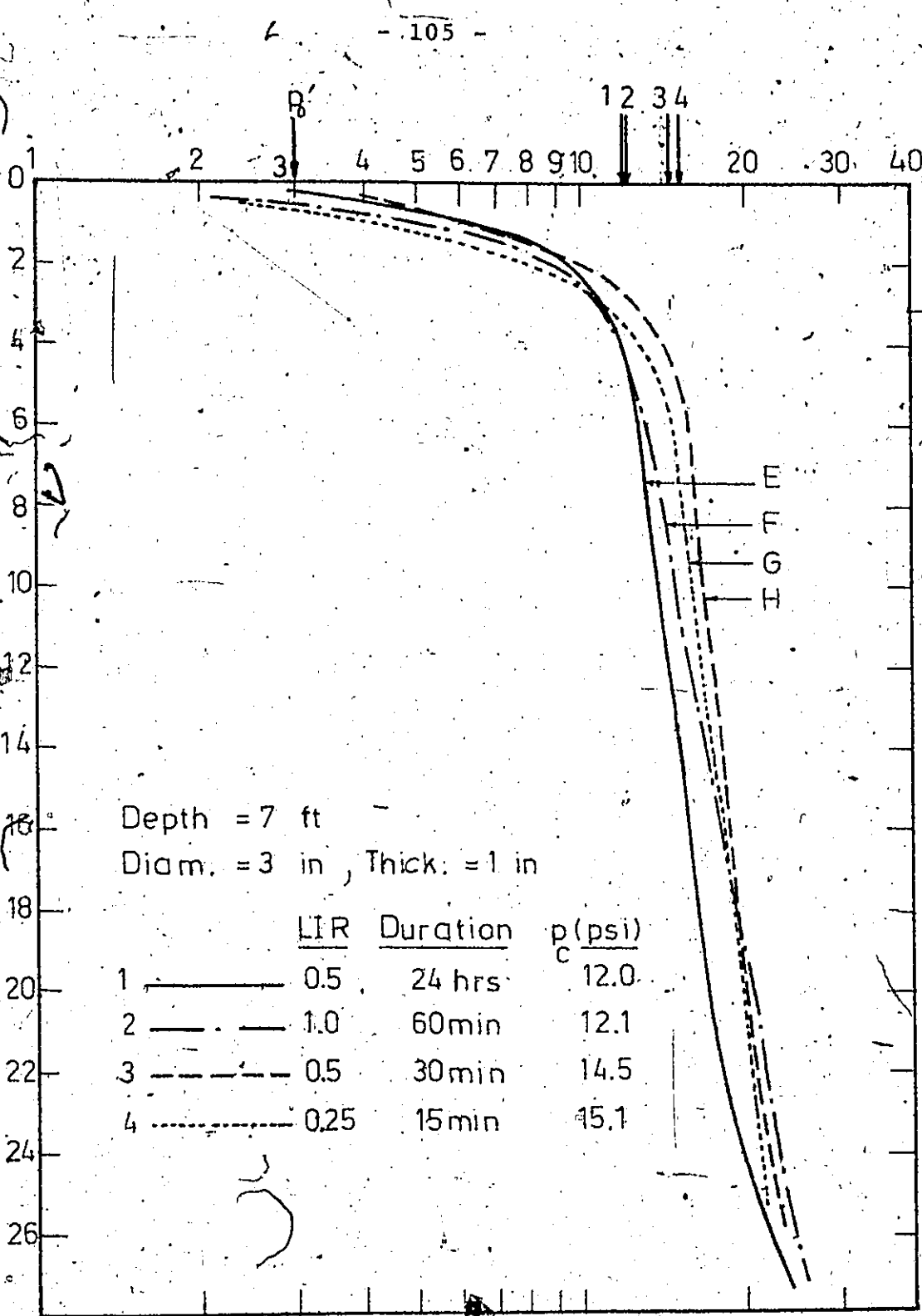
Effect of load duration  
Conventional consolidation tests

FIGURE 4.36



Effect of load increment ratio and duration.  
 Conventional consolidation tests.

FIGURE 4.37



Effect of load increment ratio  
and duration  
Conventional consolidation tests

FIGURE 4.38

FIGURE 4.39  
Variation of  $p_c$  with depth for  
incremental loading tests

Test No	Depth ft	Ratio	Duration	$p_c$ Average psi
A	5	0.5	24 hours	10.5
E	7	"	"	12.0
B	5	1	60 min	11.0
F	7	"	"	12.1
C	5	0.5	30 min	12.8
G	7	"	"	14.5
D	5	0.25	15 min	13.7
H	7	"	"	15.1

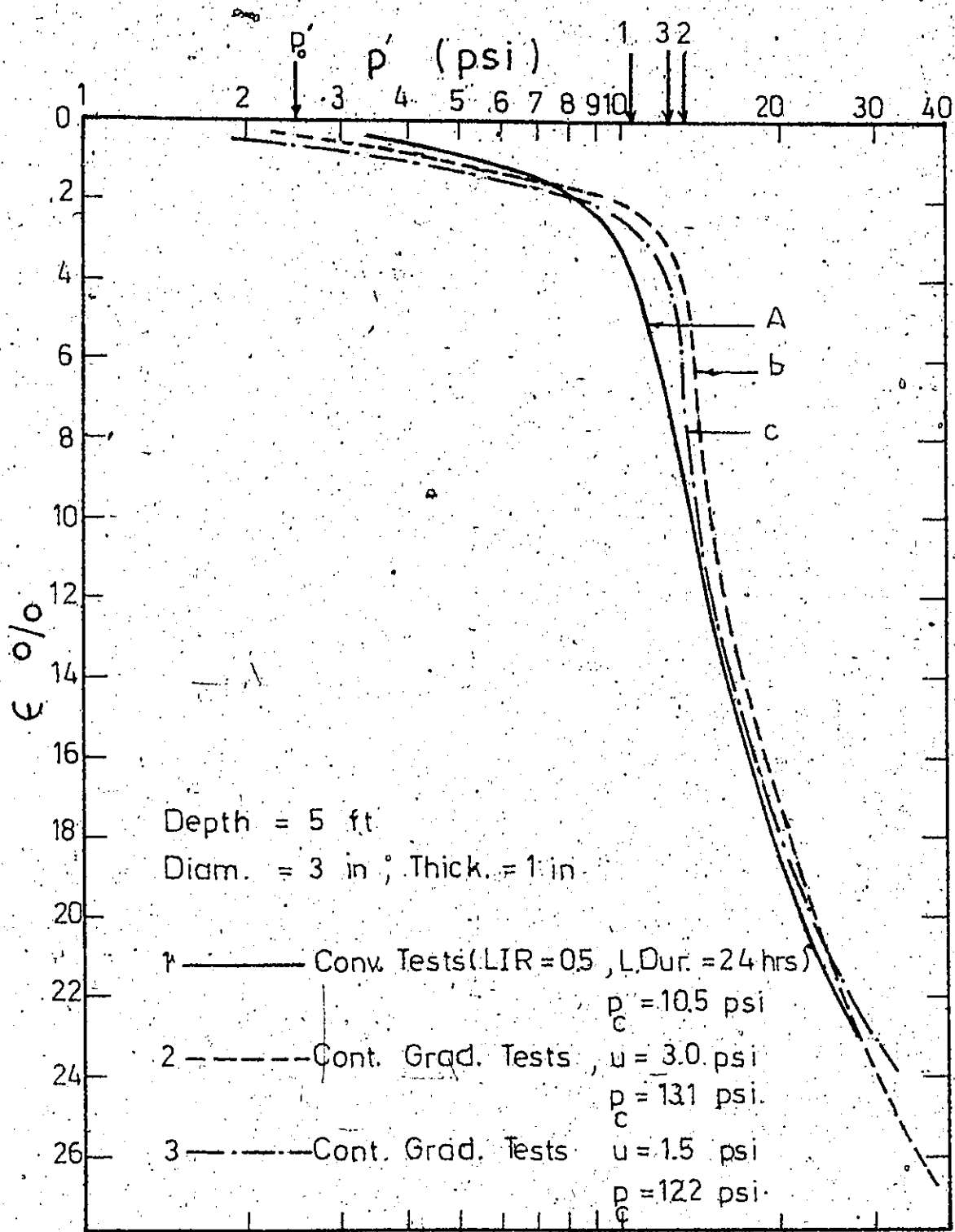
values from incremental loading tests on samples from 5 ft depth to the same tests on samples from 7 ft depth. The variation in  $p_c$  with depth, as shown, is larger than the expected 0.5 psi.

#### 4.4 Comparison of Results from the Controlled Gradient Consolidation Tests and the Conventional Tests

The comparison is made for the samples of the same size (3 in. diameter, 1 in. thick).

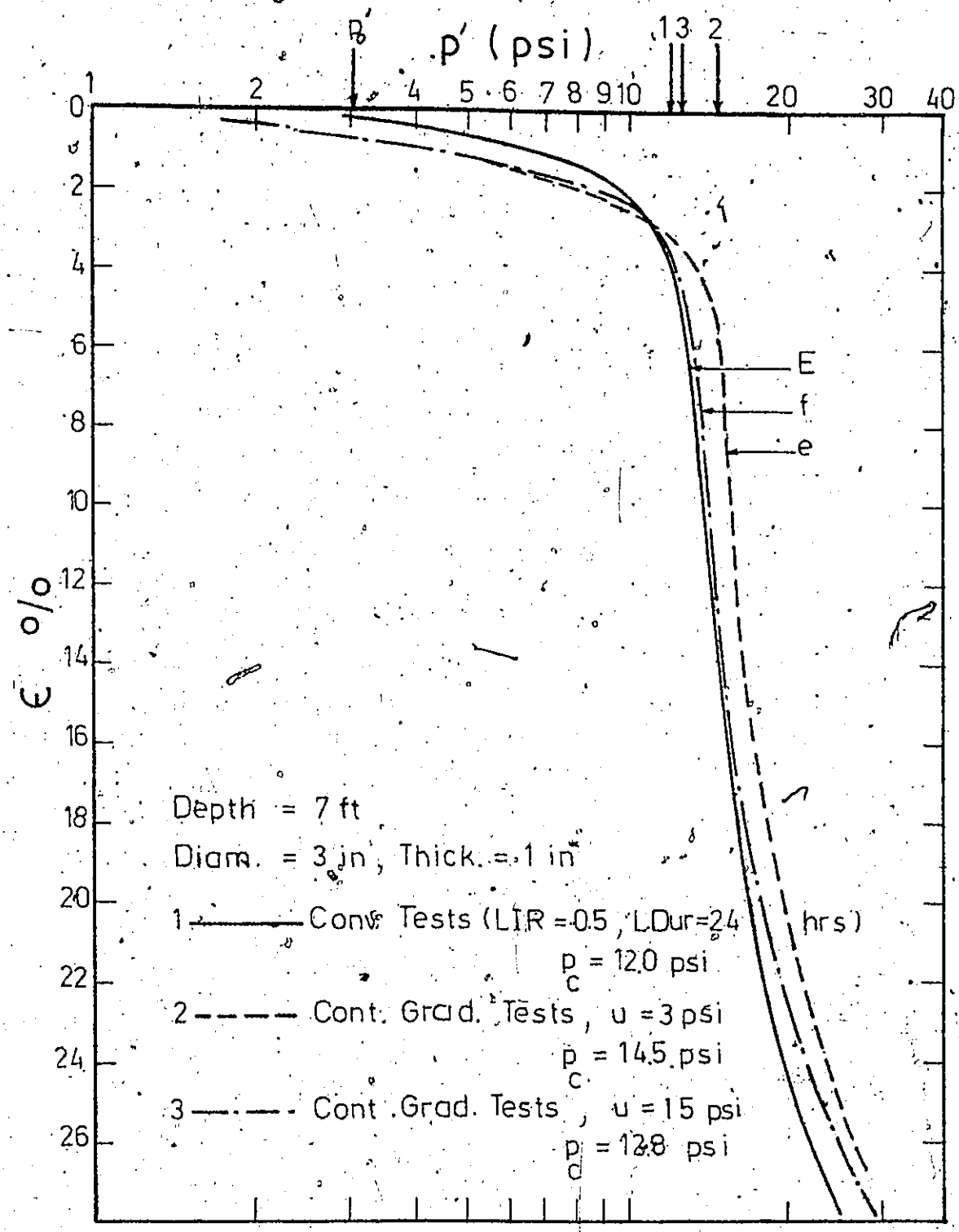
##### 4.4.1 The $\epsilon$ -log $p'$ curve

From Figs. 4.40 and 4.41, it appears that the conventional tests with load increment ratio of 0.5 and load duration of 24 hours, give a  $p_c$  smaller than the  $p_c$  from the controlled gradient tests with  $u$  1.5 psi or 3 psi. The  $\epsilon$ -log  $p'$  curves from the conventional tests fall below those from the controlled gradient tests for the range of stresses higher than the  $p_c$ . Comparing the total duration of the two types of tests, (6 days for the conventional, and 13 to 26 hours for the controlled gradient), this behaviour can be attributed to more secondary compression taking place in the 24 hours load duration tests. It can also be attributed to the effect of the shock loading on the soil structure as discussed in the following paragraph. But the fact that the curves from the conventional tests fall above those from the controlled gradient tests for the range of stresses less than the  $p_c$  cannot be explained.



Comparison between controlled gradient and conventional consolidation tests.

FIGURE 4.40



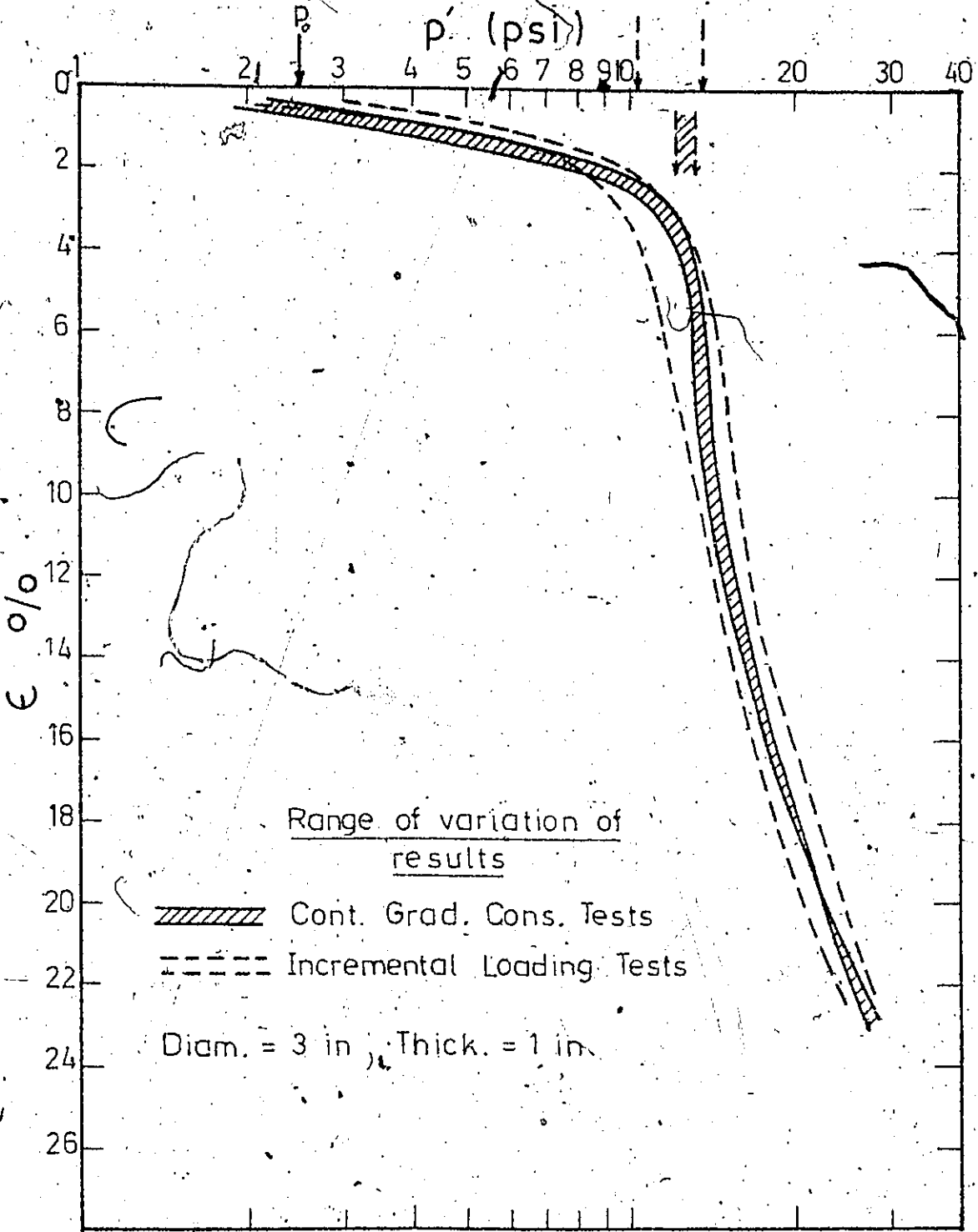
Comparison between controlled gradient and conventional consolidation tests.

FIGURE 4.41

When a load is applied suddenly to a soil sample, it is thought that the resulting "shock" breaks, at least partially, the cementation bonds of a sensitive clay. This leads to greater volume change under a particular load than would be the case for the same load applied more gradually, during the controlled gradient test for example. It is also thought that the higher hydraulic gradients which are set up in a conventional test lead to greater disturbance, along the lines of the hydraulic fracturing technique that is used in the field. This can be seen in Figs. 4.40 and 4.41.

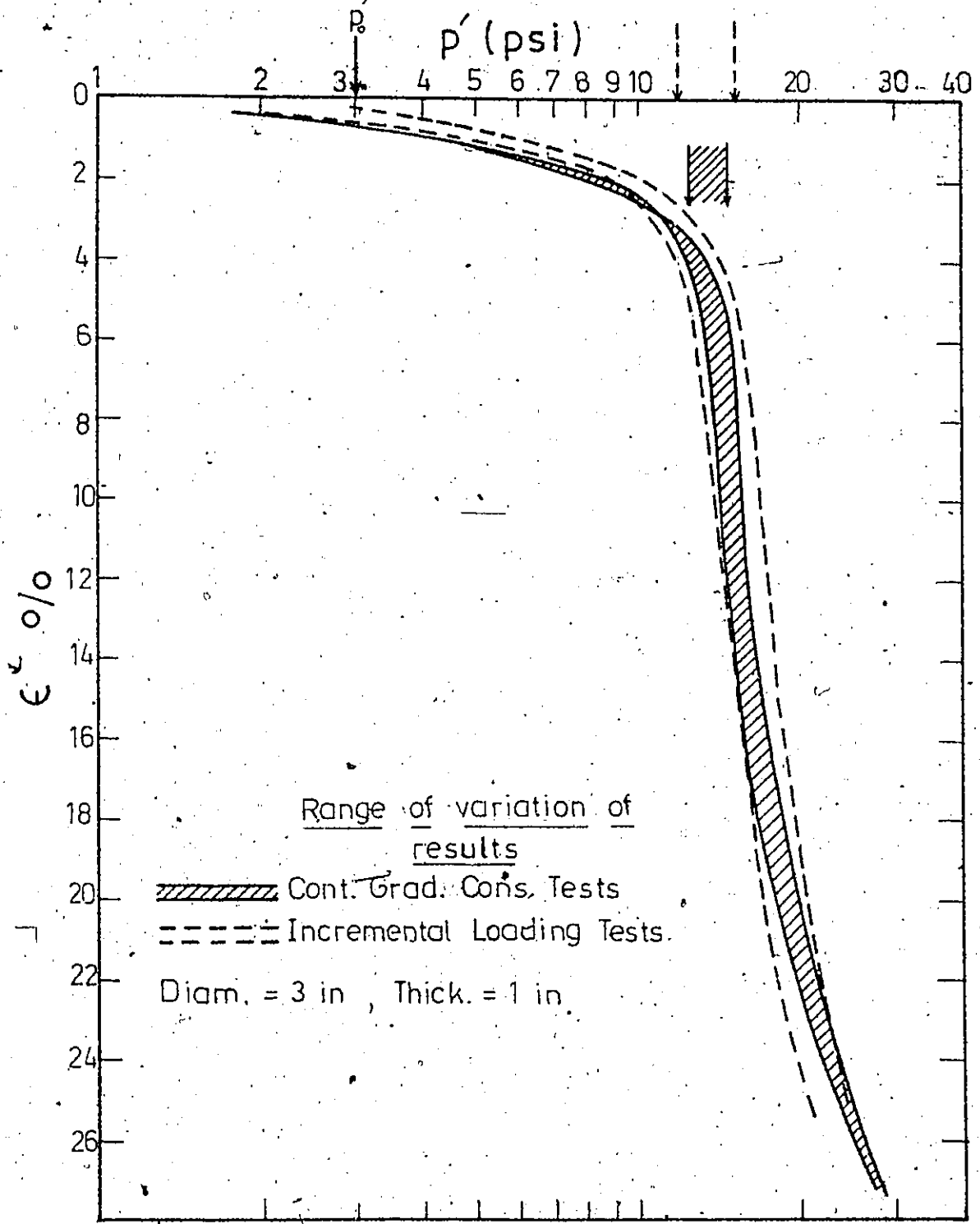
In Figs. 4.42 and 4.43, the  $\epsilon$ -log  $p'$  curves from the controlled gradient tests ( $u = 1.5$  psi and 3 psi) are represented by a shaded band. The dotted lines show the range of variation of the curves from incremental loading tests. The ranges in  $p_c$  values are also shown. The controlled gradient results proved to be more consistent.

It seems appropriate at this time to speculate on the engineering significance of the very steep, phase II part of the stress strain curves measured in the controlled gradient tests. There has been considerable speculation recently as to why pore pressures "refuse" to dissipate under some embankments constructed on soft clay. It could be that the loads created by these embankments lie in the range of or exceed phase II. If so, it stands to reason that very large settlements, with the concomitant expulsion of large volumes of water from the clay, will have to take



Range of variation of results for samples from 5 ft depth.

FIGURE 4.42



Range of variation of results for samples from 7 ft depth

FIGURE 4.43

place before the soil can carry additional effective stress. Until the soil can carry additional effective stress, there can be no reduction in the porewater pressure. Because of the low permeability of the clay this process will take many years leading a casual observer to conclude that "no consolidation is taking place" at any instant in time.

#### 4.4.2 The $\epsilon$ - $p'$ plot

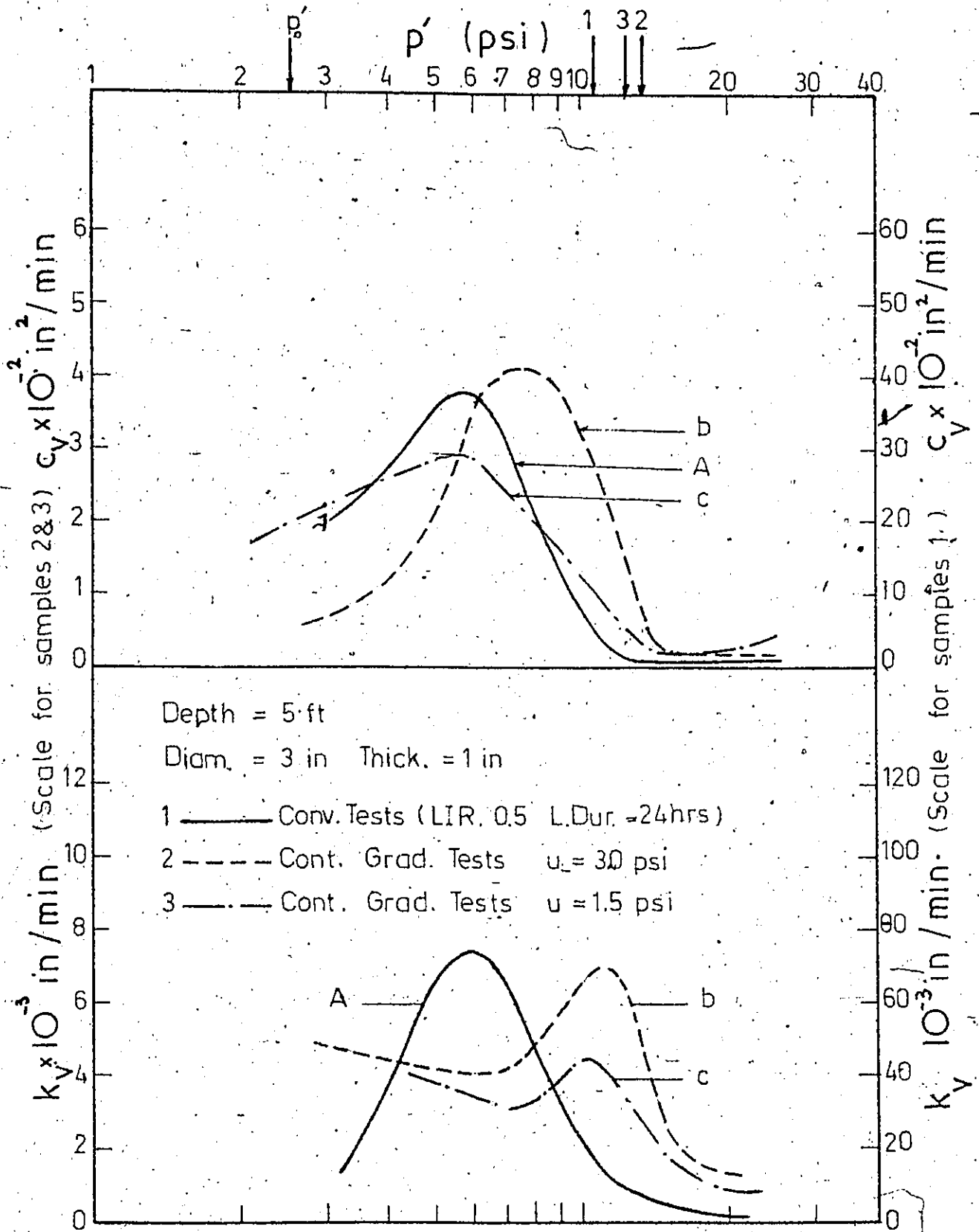
The  $\epsilon$ - $p'$  plot from conventional tests and controlled gradient tests compare favourably only in phases I and III. As discussed earlier, phase II from the conventional tests is not defined on an  $\epsilon$ - $p'$  plot and consequently this plot cannot be used for determining  $p_c$  or  $m_v$  during phase II.

#### 4.4.3 The $c_v$ - $\log p'$ and $k_v$ - $\log p'$ relationships

Figures 4.44 and 4.45 show the  $c_v$ - $\log p'$  and  $k_v$ - $\log p'$  plots for the incremental loading tests (load increment ratio 0.5, load duration 24 hours), and for the controlled gradient tests ( $u = 1.5$  psi and 3 psi). It can be observed that:

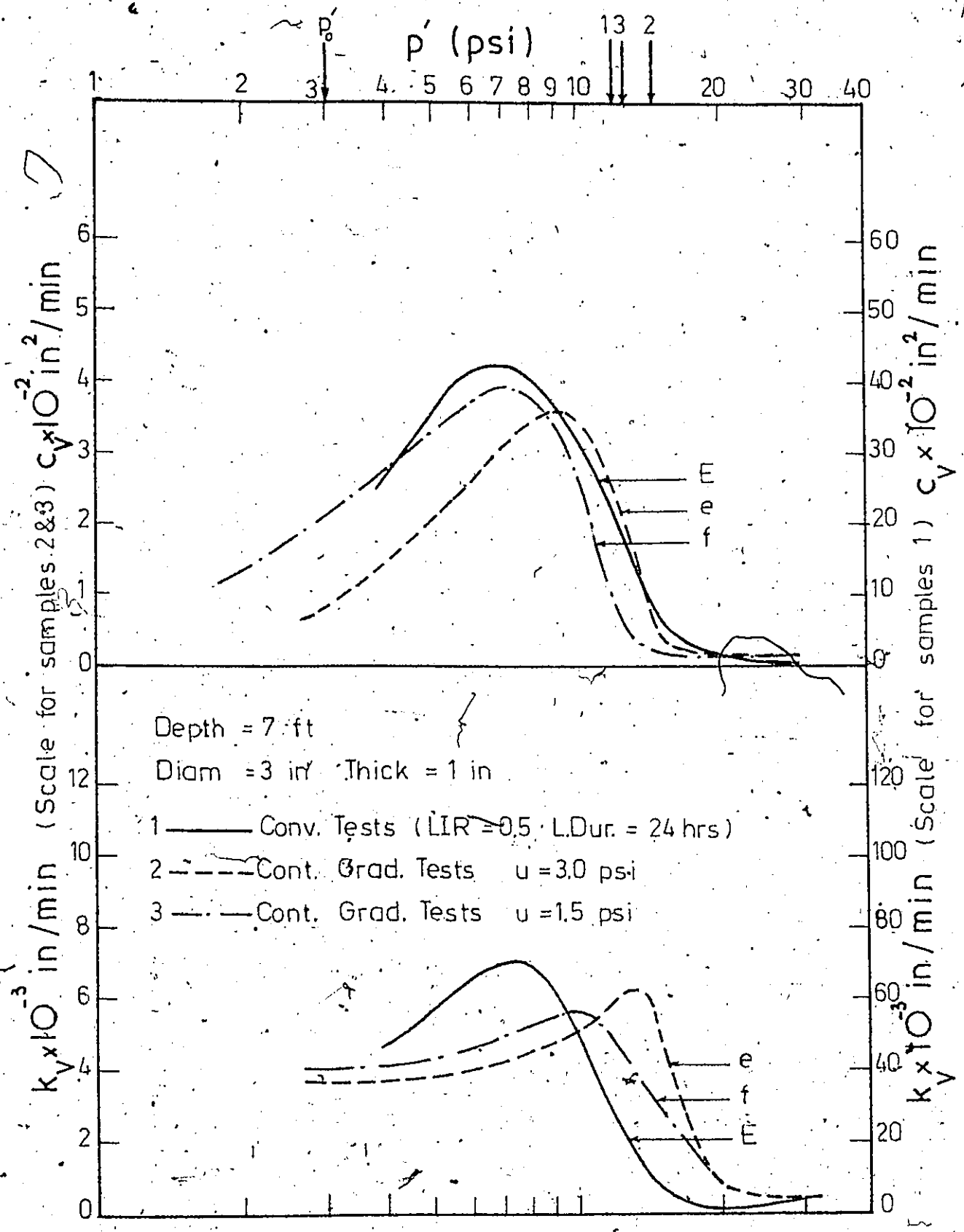
- The  $c_v$  and  $k_v$  scales for the conventional tests are ten times the scales for the controlled gradient tests.

- The peak values of  $c_v$  and  $k_v$  from the conventional tests are almost ten times those values from the controlled gradient tests.



Comparison between controlled gradient and conventional consolidation tests.

FIGURE 4.44



Comparison between controlled gradient and conventional consolidation tests.

FIGURE 4.45

- The peak of the  $k_v$ -log  $p'$  plots for the conventional tests does not seem to be related to the preconsolidation pressure. However, this can be due to an error in the calculation of  $m_v$  around the  $p_c$ , as explained earlier (Section 4.3).

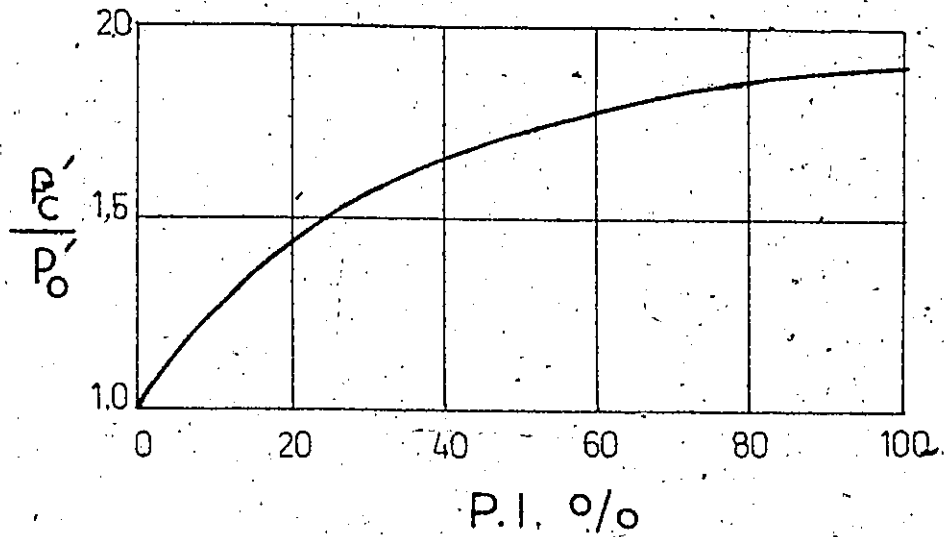
- The  $c_v$  values in the phase III parts of the tests agree quite well for the two types of tests. These  $c_v$  values vary between  $0.1 \times 10^{-2}$  in<sup>2</sup>/min and  $0.5 \times 10^{-2}$  in<sup>2</sup>/min. The discrepancy in phases I and II should be investigated, perhaps, by revising and modifying the assumptions of the consolidation theory.

(A note of caution should be interjected that due to the calibration difficulties with the Rowe cells, the values of  $m_v$ , particularly in phase I, can be in error).

#### 4.5 Comments Concerning the Clay

Comparing the  $p_c$  values obtained from the various tests to the existing overburden pressure  $p_o$  it is seen that this clay is overconsolidated. A question arises, which is whether the  $p_c$  values are an indication of a "true" preconsolidation pressure or a "quasi" preconsolidation pressure.

Figure 4.46 shows the correlation between the plasticity index and the ratio  $\frac{p_c'}{p_o}$  for normally consolidated clays which have aged over thousands of years. In this plot  $p_c'$  represents the "quasi" preconsolidation pressure due to delayed consolidation under the effective overburden



Correlation between  $\frac{P'_o}{C}$  ratio and the P.I. for normally consolidated clays.

(After Bjerrum)

FIGURE 4.46

pressure  $p'_o$ . The plot shows a maximum  $\frac{p'_c}{p'_o}$  of about 1.9.

In this study, the ratio  $\frac{p'_c}{p'_o}$  has a minimum value of 4.5.

This could prove that at least part of the preconsolidation pressure is due to the removal of overburden or the lowering of the water table (true overconsolidation). Whether or not delayed consolidation exists, and the magnitude of its influence cannot be determined from laboratory studies alone. Long term field studies would have to be carried out.

CHAPTER 5

CONCLUSIONS AND RECOMMENDATIONS FOR FURTHER RESEARCH

1. The controlled gradient consolidation test on Leda clay results in a well-defined  $\epsilon$ -log  $p'$  curve from which the  $p_c$  is easily obtained. In the past, such well-defined curves were only obtained with very small increment, conventional tests; with low rates of loading in constant rate of loading tests; or with low rates of strain in constant rate of strain tests.

2. The  $\epsilon$ - $p'$  plot obtained from the controlled gradient test results shows three straight lines, each defining one phase of the consolidation process. Extension of the first two lines intersect at the level of the pre-consolidation pressure. This plot can be used easily to define  $p_c$  as it does not require any judgement or complicated construction (such as with the Casagrande or Schmertmann methods).

This plot also clearly defines the stress level at which the Leda clay starts to gain strength at the end of phase II. This can be of practical importance in the case of stage construction of embankments on this type of clay, because when this stress level is reached the relative rate of construction can be accelerated. It also indicates that considerable settlement may occur with little or no increase in shear strength.

3. The  $t-p'$  plot from a controlled gradient test on Leda clay, shows two straight lines intersecting at the  $p'_c$  level, as was suggested by Lowe et al.

Further, for this particular clay, a third straight line, indicating an increase in the rate of stress application, seems to correspond to the third phase of consolidation.

4. The large strains which occur during phase II for very small stress changes may indicate the reason why some embankments on soft clay settle appreciably with no apparent decrease in the excess porewater pressure in the foundation soil.

5. The conventional, commercially obtainable Rowe cells used for this study were found to have serious shortcomings. In particular the cells could not be calibrated, and calibration deformations were excessive. Secondly, the rubber membranes used in the 3 in. cells were shown to reduce considerably the stresses applied to the soil specimens during the test. If these cells are to be used for further research, or even for commercial testing, these problems will have to be resolved.

6. For the samples tested, the  $c_v$  and  $k_v$  values from incremental loading tests were much higher than those from controlled gradient tests except in the region of phase III. This is in spite of the fact that both types

of test are based on the same Terzaghi theory. This may indicate that the assumptions made for the theory should be revised and the theory refined.

7. The variation in  $k_v$  during the incremental loading tests and the controlled gradient tests show an increase in  $k_v$  until a peak is reached. Afterwards,  $k_v$  decreases. This behaviour also indicates a deficiency in the theory as the real variation must be a continuous decrease in permeability due to the decrease in void ratio during consolidation. For the controlled gradient tests the decrease in  $k_v$  occurs sharply at a stress load close to the preconsolidation pressure.

8. From the tests performed, it also seems that the magnitude of the hydraulic gradient affects, to some extent, the results of the controlled gradient tests. It would also be of interest to find out if, for a given clay, there exists a certain value of the hydraulic gradient below which there is no further effect on the value of  $p_c$ .

9. The change in atmospheric pressure can affect the results of controlled gradient tests if "absolute" transducers are used. In the tests performed, this did not affect the  $p_c$  values because the  $p_c$  level was reached within a few hours before there could be any measurable change in the atmospheric pressure. But, in all cases where the test is of long duration (e.g., for stiff clays;

for very small hydraulic gradient; for very thick samples; ... ) the effect of the variation in atmospheric pressure should be eliminated by using a "gauge" transducer.

10. The Leda clay, which was tested, was shown to be overconsolidated with an overconsolidation ratio of from 4.5 to 5.5. There are indications that a fair proportion of the overconsolidation pressure is indeed due to true preconsolidation.

11. The test results indicate that stress increases of up to 90% of the difference between the  $p_c$  and  $p_o$  can be applied before appreciable straining commences. Information of this nature is valuable in the design of foundation and embankments on sensitive clay since undesirable settlement may result if stresses exceed this failure.

12. The major conclusion from the present work is that the controlled gradient consolidation test is applicable to engineering studies on a sensitive, marine clay. The test has a number of major advantages over other methods, but is hindered by the lack of development of a reliable oedometer.

LIST OF REFERENCES

1. Aboshi, H., Yoshikumi, H., and Marrayana, S.  
"Constant Loading Rate Consolidation Test".  
Soils and Foundations, The Japanese Society of Soil  
Mechanics and Foundation Engineering, Vol. 10, No. 1,  
March 1970. pp.43-56.
2. Barden, L.  
"Consolidation of Clay with Non-Linear Viscosity."  
Geotechnique, Vol. 15, No. 4, December 1965. pp.345-362.
3. Bjerrum, L., and Wu, T.H.  
"Fundamental Shear Strength Properties of the Lilla  
Edet Clay."  
Geotechnique, Vol. 10, No. 3, September 1960. pp.101-109.
4. Bjerrum, L.  
"Engineering Geology of Norwegian Marine Clays as  
Related to Settlements of Buildings,"  
(Rankine's Lecture 1967),  
Geotechnique, Vol. 17, No. 2, June 1967. pp.83-117.
5. Bozozuk, M.  
"Effect of Sampling, Size and Storage on Test Results  
of Marine Clays."  
Am. Soc. Testing Mat., Special Technical Publication,  
No. 483, 1971, pp.121-131.
6. Casagrande, A.  
"The Determination of the Preconsolidation Load and  
its Practical Significance."  
Proceedings, First Internatl. Conf. on Soil Mechanics,  
Cambridge, Mass., 1936, Vol. 3. pp.60-64.
7. Crawford, C.B.  
"Engineering Studies of Leda Clay".  
Soils in Canada, Special Publication N:3, Royal Society  
of Canada, 1961, pp.200-217.
8. Crawford, C.B.  
"Interpretation of the Consolidation Test."  
Journal of Soil Mechanics and Foundations Division,  
A.S.C.E., Vol. 90, No. SM5, September 1964. pp.87-102.  
or 'Research Paper' No. 239 of the Division of Building  
Research.
9. Crawford, C.B.  
"The Resistance of Soil Structure to Consolidation."  
Canadian Geotechnical Journal, Vol. 2, No. 2, May 1965.  
pp.90-97.

10. Crawford, C.B.  
"Quick Clays of Eastern Canada."  
Engineering Geology, Vol. 2, N:4, 1968. pp.239-265.
11. Crawford, C.B., and Eden, W.J.  
"A Comparison of Laboratory Results with In-Situ Properties of Leda Clay."  
Proceedings, 6th Internatl Conf. on Soil Mechanics, Montreal, 1965, Vol. 1, pp.31-35.
12. Gadd, N.R.  
"Surficial Geology of the Ottawa Map Area."  
Geological Survey of Canada, Paper, 12-16.
13. Gillot, G.E.  
"Fabric of Leda Clay Investigated by Optical, Electron-Optical and X-ray Diffraction Methods."  
Engineering Geology, Vol. 4, N:2, April 1970, pp.133-153.
14. Gillot, G.E.  
"Mineralogy of Leda Clay."  
Canadian Mineralogist, Vol. 10, No. 5, May 1971, pp.797-811.
15. Hamilton, J.J., and Crawford, C.B.  
"Improved Determination of the Preconsolidation Pressure of a Sensitive Clay."  
Am. Soc. Testing Mat., Special Technical Publication, No. 254, 1959, pp.254-271.
16. Hansbo, S.  
"Consolidation of Clay with Special Reference to the Influence of Vertical Sand Drains."  
Proceedings, Swedish Geotechnical Institute, No. 18, 1960.
17. Janbu, N.  
"Consolidation of Clay Layers Based on Non-Linear Stress-Strain."  
Proceedings, 6th Internatl Conf. on Soil Mechanics, Montreal, 1965, Vol. 14. pp.83-87.
18. Jarret, P.M.  
"Time Dependent Consolidation of a Sensitive Clay."  
Material Research and Standards, Vol. 7, No. 7, 1967. pp.300-304.
19. Langer, K.  
"The Influence of the Speed of Loading Increments on the  $e$ -log  $p$  Diagram of Undisturbed Soil Samples."  
Proceedings, 1st Internatl Conf. on Soil Mechanics, Cambridge, Mass., 1936, Vol. 2, pp.116-118.

20. Leonards, G.A., and Ramiah, B.K.  
"Time Effects in the Consolidation of Clays."  
Am. Soc. Testing Mat., Special Technical Publications,  
No. 254, 1959. p.116-130.
21. Leonards, G.A., and Girault, P.  
"A Study of One Dimensional Consolidation Test."  
Proceedings, 5th Internatl Conf. on Soil Mechanics,  
Paris, 1961, Vol. 1, pp.213-218.
22. Leonards, G.A., and Altschaeffl, A.G.  
"Compressibility of Clay."  
Proceedings, American Society of Civil Engineers,  
Vol. 90, No. SM5, September 1964, pp.133-155.
23. Lowe, J., Jonas, E., and Obrician, V.  
"Controlled Gradient Consolidation Test."  
Proceedings, American Society of Civil Engineers,  
Vol. 95, No. SM1, January 1969, pp.77-97.
24. Narain, N., and Singh, B.  
"Quasi-Preconsolidation Effects and Pore Pressure  
Dissipation during Consolidation."  
Proceedings, 7th Internatl Conf. on Soil Mechanics,  
Mexico, 1969, Vol. 1, pp.311-315.
25. Newland, P.L., and Allely, B.H.  
"A Study of the Consolidation Characteristics of a Clay."  
Geotechnique, Vol. 10, No. 2, June 1960, pp.62-74.
26. Northey, R.D.  
"Rapid Consolidation Tests for Routine Investigations."  
Proceedings, 2nd Australian-New Zealand Conf. on  
Soil Mechanics, Christchurch, 1956, pp.20-26.
27. Penner, E.  
"A Study of Sensitivity in Leda Clay."  
Canadian Journal of Earth Sciences, Vol. 2, No. 5,  
October 1965, pp.425-441.
28. Quigley, R.M., and Thompson, C.  
"The Fabric of Anisotropically Consolidated Marine Clay."  
Canadian Geotechnical Journal, Vol. 3, 1966, pp.61-73.
29. Rowe, P.W., and Barden, L.  
"A New Consolidation Cell."  
Geotechnique, Vol. 16, No. 2, June 1966, pp.162-170.
30. Sangrey, D.A., and Paul, M.J.  
"A Regional Study of Landsliding Near Ottawa."  
Canadian Geotechnical Journal, Vol. 8, No. 2, 1971,  
pp.315-335.

31. Sangrey, D.A.  
"Naturally Cemented Clays."  
Geotechnique, Vol. 22, No. 1, 1972, pp.139-152.
32. Schiffman, R.L.  
"Consolidation of Soil under Time-Dependent Loading and Variable Permeability."  
Bulletin No. 248, Highway Research Board, Vol. 37, 1958, pp.584-617.
33. Schmertmann, J.H.  
"The Undisturbed Consolidation Behaviour of Clay."  
Transactions, American Society of Civil Engineers, Vol. 120, 1955, pp.1201-1233.
34. Shields, D.H., and Rowe, P.W.  
"Radial Drainage Oedometer for Laminated Clays."  
Proceedings, American Society of Civil Engineers, Vol. 91, No. SM1, January 1965, pp.15-23.
35. Simons, N.E., and Beng, T.S.  
"A Note on the One Dimensional Consolidation of Saturated Clays."  
Geotechnique, Vol. 19, No. 1, 1969, pp.140-149.
36. Smith, R.E., and Wahls, H.E.  
"Consolidation Under Constant Rates of Strain."  
Proceedings, American Society of Civil Engineers, Vol. 95, No. SM2, March 1969, pp.519-539.
37. Tatsuro Okumura and Fumiko Ogawa.  
"Influence of Loading Duration on the Consolidation Indices."  
Soils and Foundations, Vol. 11, No. 2, March 1971, pp.52-61.
38. Taylor, D.W.  
"Research on Consolidation of Clays."  
Department of Civil & Sanitary Engineering, Mass. Inst. of Technology, Cambridge, Mass., Serial 82, August 1942.
39. Terzaghi, K.  
"Theoretical Soil Mechanics."  
J. Wiley and Sons, Inc., New York, 1943.
40. Van Zelst, T.W.  
"An Investigation of the Factors Affecting Laboratory Consolidation of Clays."  
Proceedings, 2nd Internatl Conf. on Soil Mechanics, Rotterdam, 1948, Vol. 7, p.53.

41. Wahls, H.E.  
"Analysis of Primary and Secondary Consolidation."  
Proceedings, American Society of Civil Engineers,  
Vol. 88, No. SM6, December 1962, pp.207-231.
42. Wissa, A., Christian, T., Davis, E.H. and Heiberg, S.  
"Consolidation at Constant Rate of Strain."  
Proceedings, American Society of Civil Engineers,  
Vol. 97, No. SM10, October 1971, pp.1393-1413.
43. A.S.T.M. Standards, 1973, Part 11, A.S.T.M. designation  
D.2435.  
One Dimensional Consolidation Properties of Soils.  
pp.738-741.

APPENDIX A

ADDITIONAL REFERENCES

Barden, L.

"The Relations of Soil Structure to the Engineering Geology of Clay Soil."  
Quarterly Journal of Engineering Geology, Vol. 5, No. 1/2, 1972, pp.85-102.

Bene, Schjetne, Sollie

"Sampling Disturbance of Soft Marine Clays"  
Norwegian Geotechnical Institute, Report No. 85, 27

Hvorslev, M. J.

"Subsurface Exploration and Sampling of Soils for Civil Engineering Purposes"  
Report in a Research Project of the Committee of Sampling and Testing of the American Society of Civil Engineering, Waterway Experimental Station, Vicksburg, 1949.

Jarret, P. M.

"The Effect of Soil Structures on the Engineering Behaviour of a Sensitive Clay"  
Quarterly Journal of Engineering Geology, Vol. 5, No. 1/2, 1972, pp.103-109.

Lambe, T. W.

Soil Testing for Engineers  
J. Wiley & Sons, Inc., New York. 1951

Larochelle, P. and Lefebvre, C.

"Sampling Disturbances in Champlain Clays,"  
American Society Testing Material, Special Technical Publication No. 483, 1971, pp.143-163.

Lowe, J., III.

"New Concepts in Consolidation and Settlement Analysis"  
The Eighth Terzaghi Lecture, Proceedings American Society of Civil Engineers, Vol. 100, No. GT6, June 1974.

Foundation Engineering

Edited by G. R. Leonards,  
McGraw-Hill Company Inc. 1962

Shields, D. H.

"The Influence of Vertical Sand Drains and Natural Stratification on Consolidation"  
Thesis presented to the University of Manchester, in 1963, in partial fulfillment of the requirements for the degree of Doctor of Philosophy.

## APPENDIX B

### OTHER TESTS PERFORMED

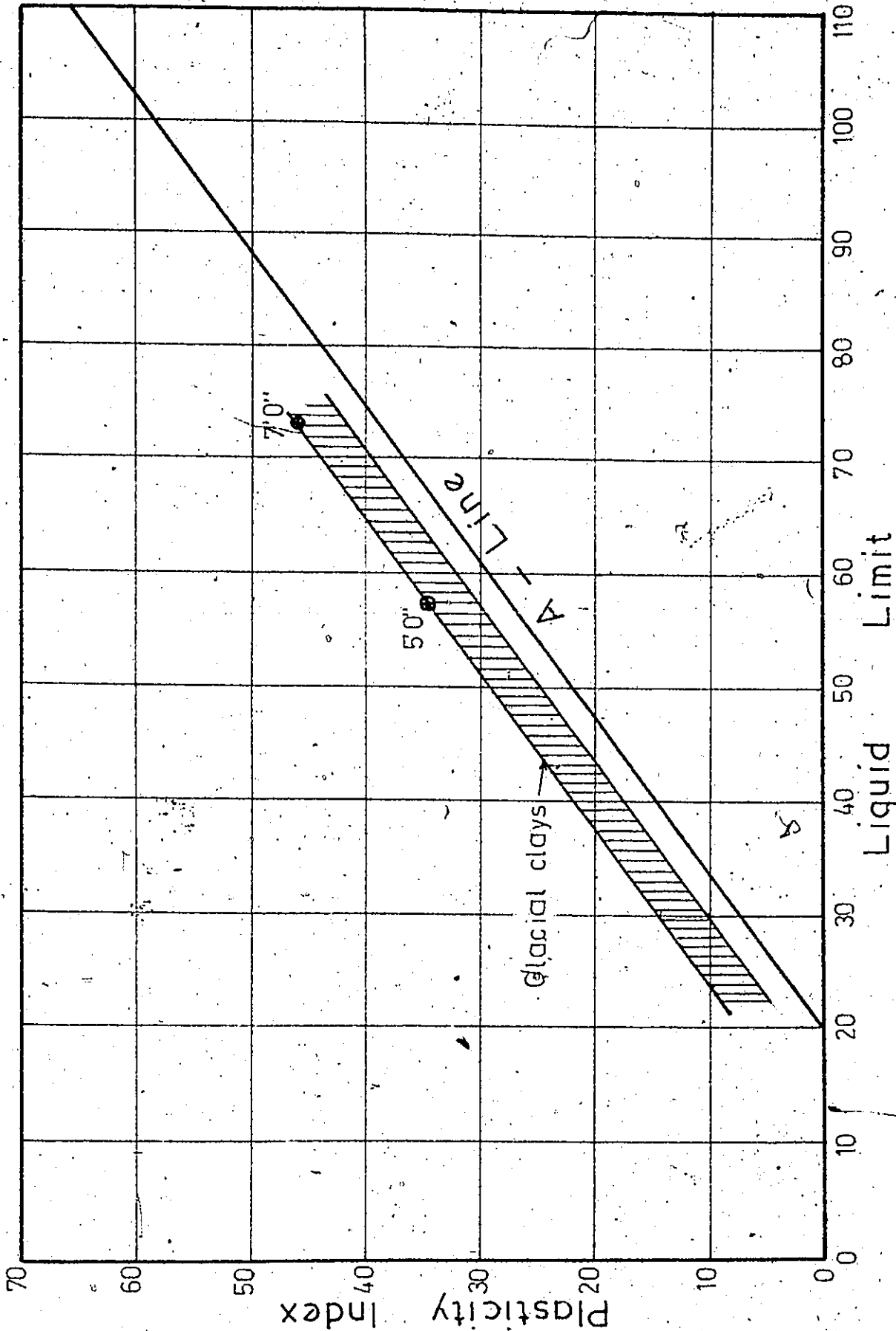
The following tests were performed according to the A.S.T.M. Standards (1973), and the procedures described by Lambe (1951).

#### B.1 Moisture Content and Atterberg Limits

During the trimming of each specimen tested, three samples were taken for moisture content determination. The average water content was found to be  $70\% \pm 2\%$  at 5 ft depth. At 7 ft depth, more variation in the moisture content was found and the values ranged between 85% and 95%. Two points representing the Liquid Limit versus Plasticity Index for the two depths are shown on the plasticity chart (Fig. B.1). The points fall above the A-line, and within the zone representing the glacial clays. It should be noted that the water content at the two levels was higher than the liquid limit.

#### B.2 Particle Size Analysis

Hydrometer analysis were performed. The results are given in Fig. 3.6. The clay content was found to be 74% at 5 ft depth and 78% at 7 ft depth. The activity of the clay was found to be 0.46 at 5 ft depth and 0.59 at 7 ft depth.



Plasticity Chart

FIGURE B.1

### B.3 Specific Gravity Tests

Specific gravity tests were performed on two samples from 5 ft depth and two other from 7 ft depth. The average specific gravity of the soil particles,  $G$ , in both cases was found to be 2.79. This compares with values of 2.8 reported by Lambe.

### B.4 Unit Weight

The unit net weight was calculated for each sample tested by weighing a known volume of clay. The average value was found to be 100 pcf at 5 ft and 95 pcf at 7 ft. These values are constant with the moisture contents and specific gravity reported above.

### B.5 Degree of Saturation

The degree of saturation is equal to the ratio of the volume of water to the total volume of voids. The values of  $S$  calculated were in the range of 99.46% with a standard deviation of 2%. In fact, because the groundwater level was above the sampling depths, all the samples are expected to have been saturated. The small variation could be due to experimental errors.

### B.6 Salt Content Analysis

This analysis was performed on a sample from 7 ft depth according to the procedure described by the National Research Council of Canada (Division of Building Research).

The porewater was extracted by applying a pressure of about 75 psi to the sample in the Rowe cells. The porewater was collected from the bottom drainage line. Three samples of 20 ml each were taken, using a pipette, and put in a pyrex recipient for which the weight had been previously obtained to 1 milligram. The porewater was then evaporated and the residue treated with hydrogen peroxide (30%) solution to eliminate any organic matter. The residue was put back into the oven to dry once more, then weighed.

The salt content,  $S_c$ , is given by the formula

$$S_c = \frac{W_r}{V} \times 1000 \quad \text{in g/l}$$

where  $W_r$  = dry weight of the residue in grams  
 $V$  = volume of the porewater evaporated.

An average  $S_c$  for the three samples was calculated and found to be 1.17 g/l.

B.7 Summary

The following table compares the results of the foregoing tests to those reported in the literature for clay from the same area (Gloucester).

Depth ft	W%	LL%	PL%	PI%	%clay	Salt Content g/l	Unit Weight pcf	Reference
5	70	60	25	35.1	74		100	
7	85-95	73	27	46	78	1.17	95.0	
10	72			23	71	0.5	99	Crawford & Eden (1965)
5.5	70	43	23.5	19.5	66			Gillot (1970)
7.2	80	50	22	27	58			Bozozuk (1971)

18

APPENDIX C

AUTOMATIC CONTROL SYSTEM

C.1 Theory of Operation

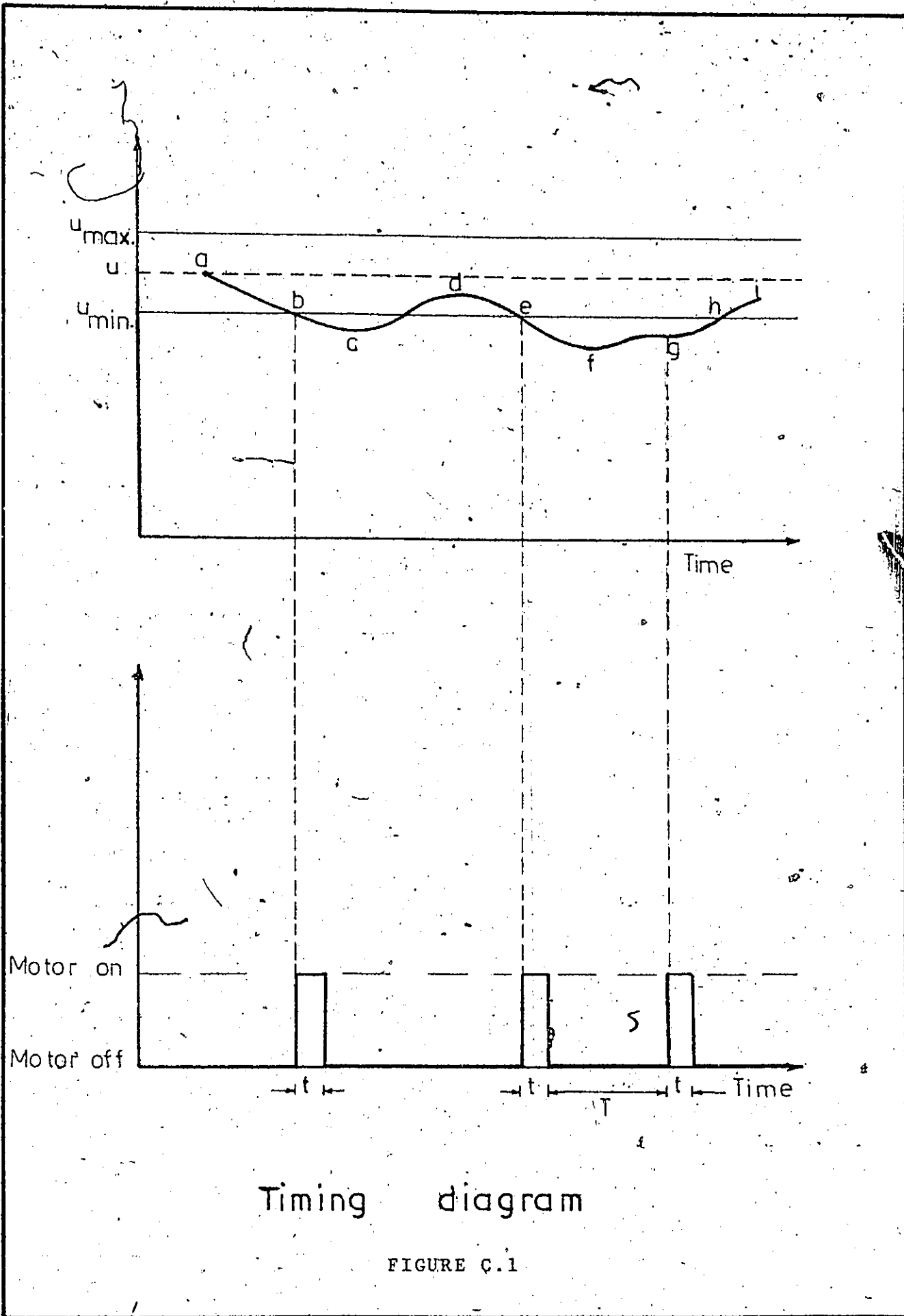
The function of this system is to keep the base porewater pressure constant within certain limits. A maximum value ( $u_{max}$ ), and a minimum value ( $u_{min}$ ) for the base porewater pressure are selected and applied to the system. If  $u$  is the nominal porewater pressure required at the base, and  $\delta u$  is the tolerance allowed, then

$$u_{max} = u + \delta u$$

$$u_{min} = u - \delta u$$

A pressure transducer continuously monitors the actual porewater pressure at the base ( $u_{act}$ ). If the value of  $u_{act}$  decreases below that of  $u_{min}$ , a control circuit activates a motor to raise the mercury pots and thus increases the load on the soil sample. Similarly, if the value of  $u_{act}$  increases to a value above that of  $u_{max}$ , the control circuit activates the motor to reduce the load on the soil sample.

A timing diagram is shown in Fig. C.1. The actual base porewater pressure is represented by the curve abcdefghi. At point a,  $u_{act}$  is very close to the nominal value, but due to consolidation of the soil sample,  $u_{act}$  tends to decrease. As soon as  $u_{act}$  becomes equal to  $u_{min}$  (at point b), the



Timing diagram

FIGURE C.1

motor is activated, and an increment of pressure is applied to the sample. However, due to the low permeability of the clay, a time delay exists, and it is only at point c that  $u_{act}$  starts increasing until point d is reached.

Curve efghi is supplied to illustrate the conditions when the rate of consolidation is faster than the case illustrated by curve abcd. The only difference between the two curves is that, if a time T elapsed after the application of the pressure increment at point e, and  $u_{act}$  is still less than  $u_{min}$ , another incremental pressure is applied. The operation is repeated until  $u_{act}$  becomes greater than  $u_{min}$ .

During the time t, the mercury pots move upward a distance of 0.035 in., corresponding to an increase of 0.0175 psi. The time T is the time between successive additions of incremental pressure in the case where one increment is not enough to bring the value of  $u_{act}$  in between  $u_{max}$  and  $u_{min}$ .

The time periods t and T are related to the permeability and the thickness of the soil sample. Preliminary tests were run and the values of t and T were varied until the right values could be found to suit the type of soil tested, and the sample thicknesses used. T and t were finally set to be 5 and 0.2 sec., respectively.

## C.2 Description of the System

### C.2.1 Pressure transducer

A pressure transducer of the type APT 25 manufactured by Microdot Inc. was used to measure the base porewater pressure.

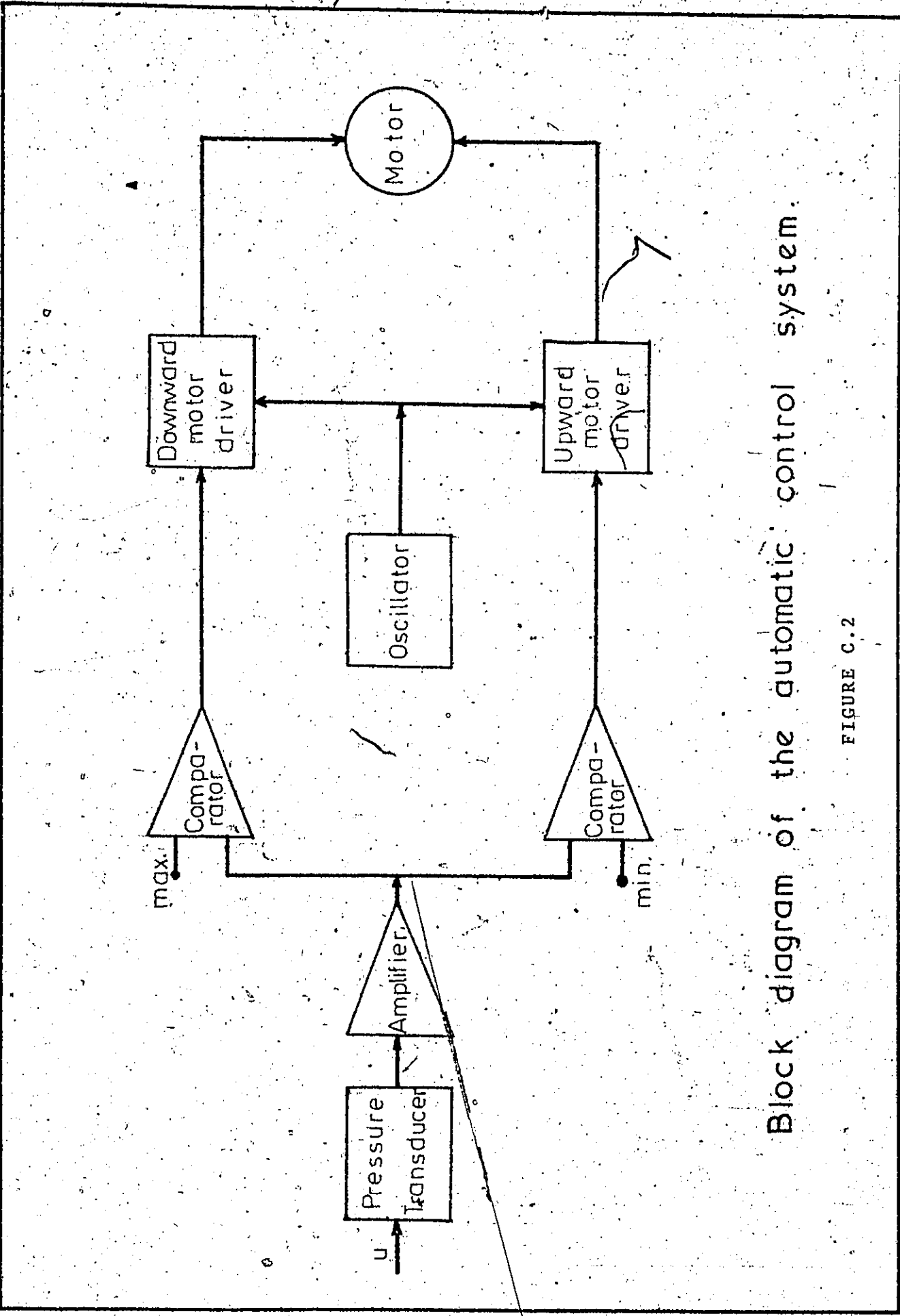
### C.2.2 Control circuits and motor

A block diagram is shown in Fig. C.2. The pressure transducer output is amplified, and the amplifier's output feeds two comparators. The first compares the amplifier's output to the maximum value  $u_{\max}$ , and the second compares it to the minimum value  $u_{\min}$ . The result of the comparison controls the direction of the motion of the motor, through upward/downward motor drivers. An oscillator giving a continuous train of pulses of duration  $t$ , and at intervals  $T$ , controls the timing of the motion of the motor, through the upward/downward motor drivers.

### C.2.3 Mercury pot system

The Bishop mercury pot system was used to apply the pressure on the sample. The only variations applied to the system were the elimination of the springs and the use of the motor to operate the system.

The springs were eliminated for two reasons: first, their function of maintaining a constant pressure to compensate for the decrease in volume of the sample was no



Block diagram of the automatic control system.

FIGURE C.2

longer needed in this case, and second because their presence would induce oscillations into the control system, and alter its correct functioning.



grey  
soft silty clay

brown to yellow  
fine silty sand

top soil and sand

Figure D.1 Soil Profile at the Site



Figure D.2 Block Samples Cut Out of a Bench



Figure D.3 Clay Bench After Block Samples Were Cut Out

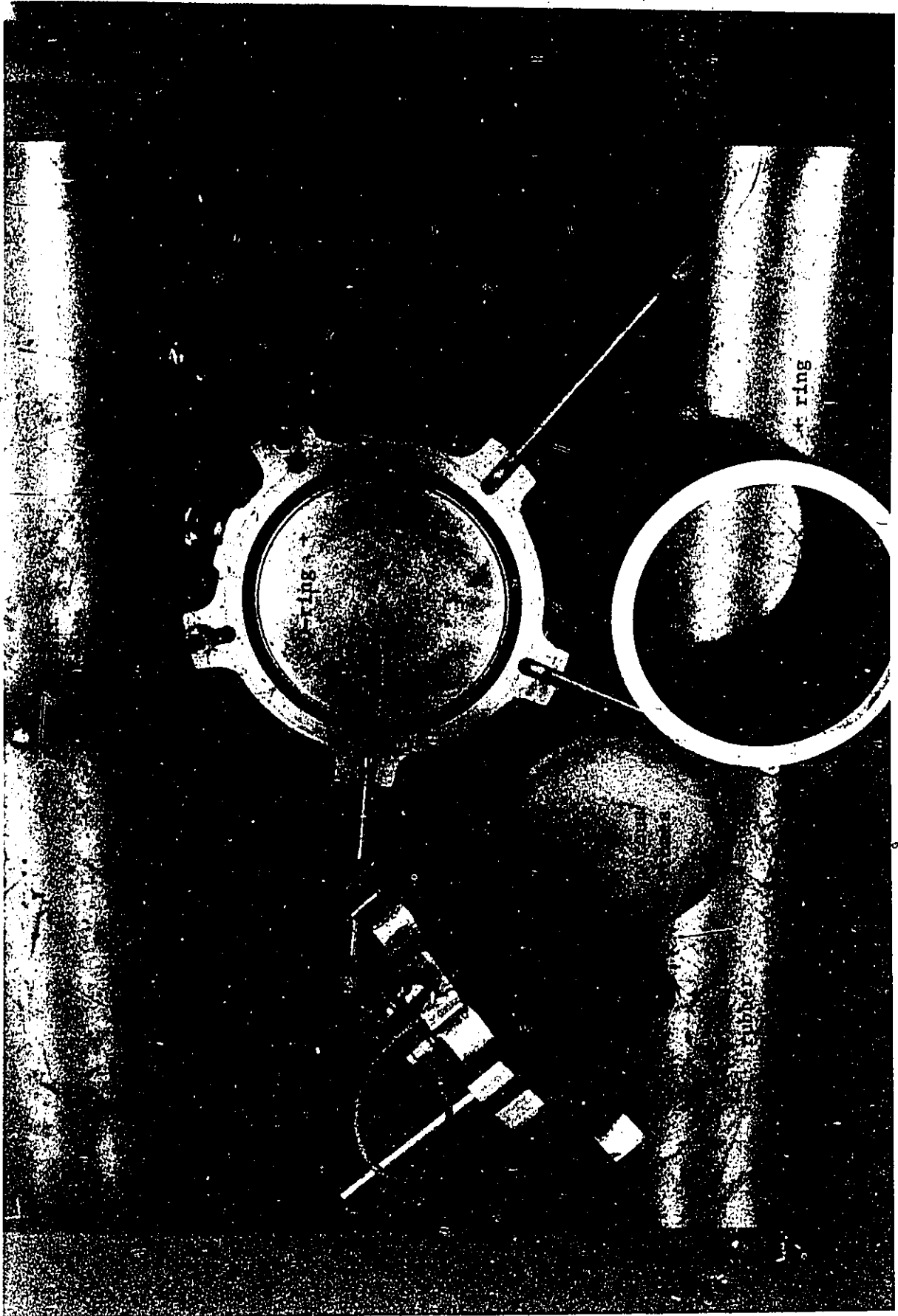


Figure D.4 Display of the Consolidated Cell Components

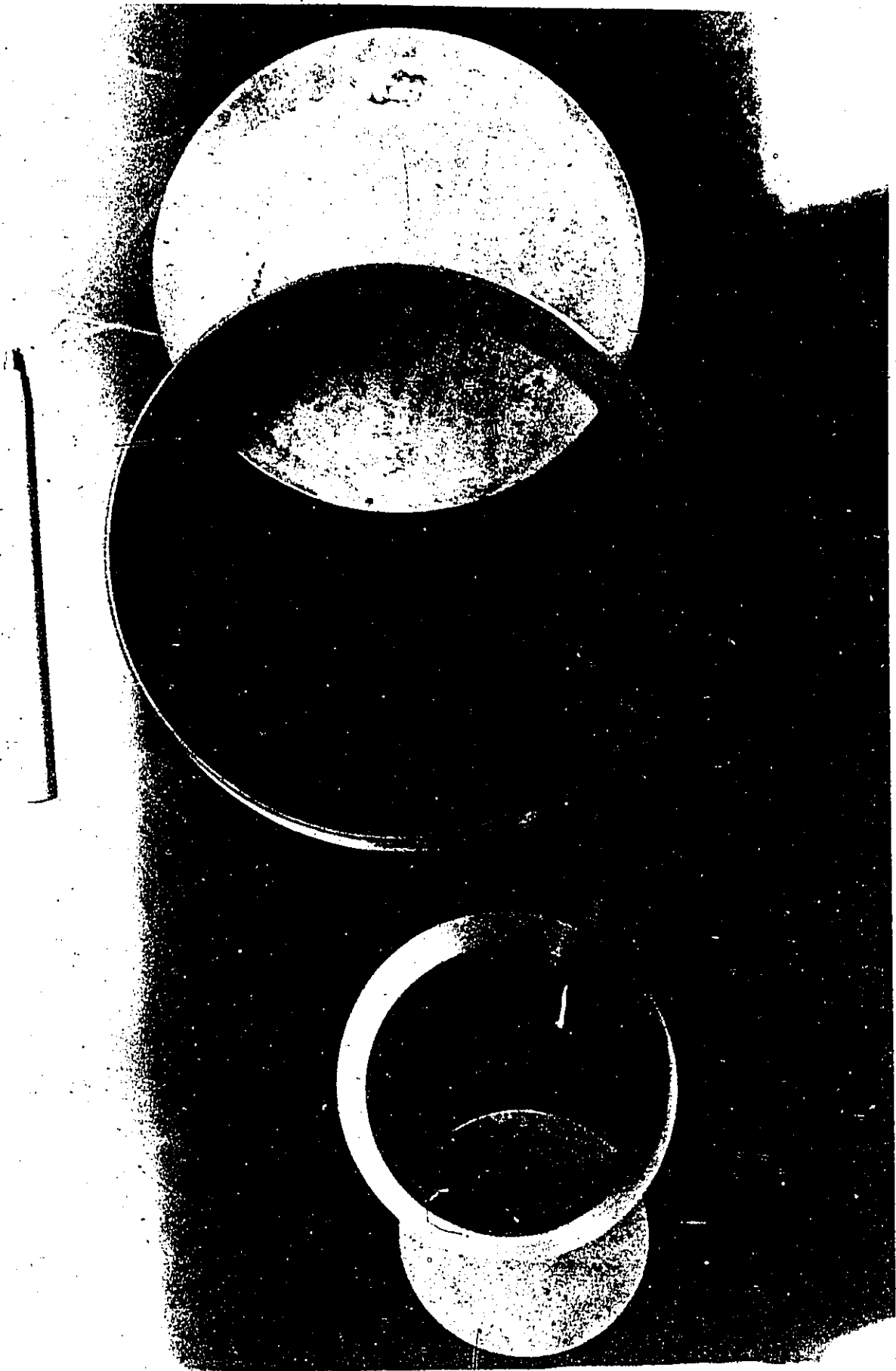


Figure D.5 Sample Cutting Rings and Extruding Plates for 3 in and 6 in diameter Samples

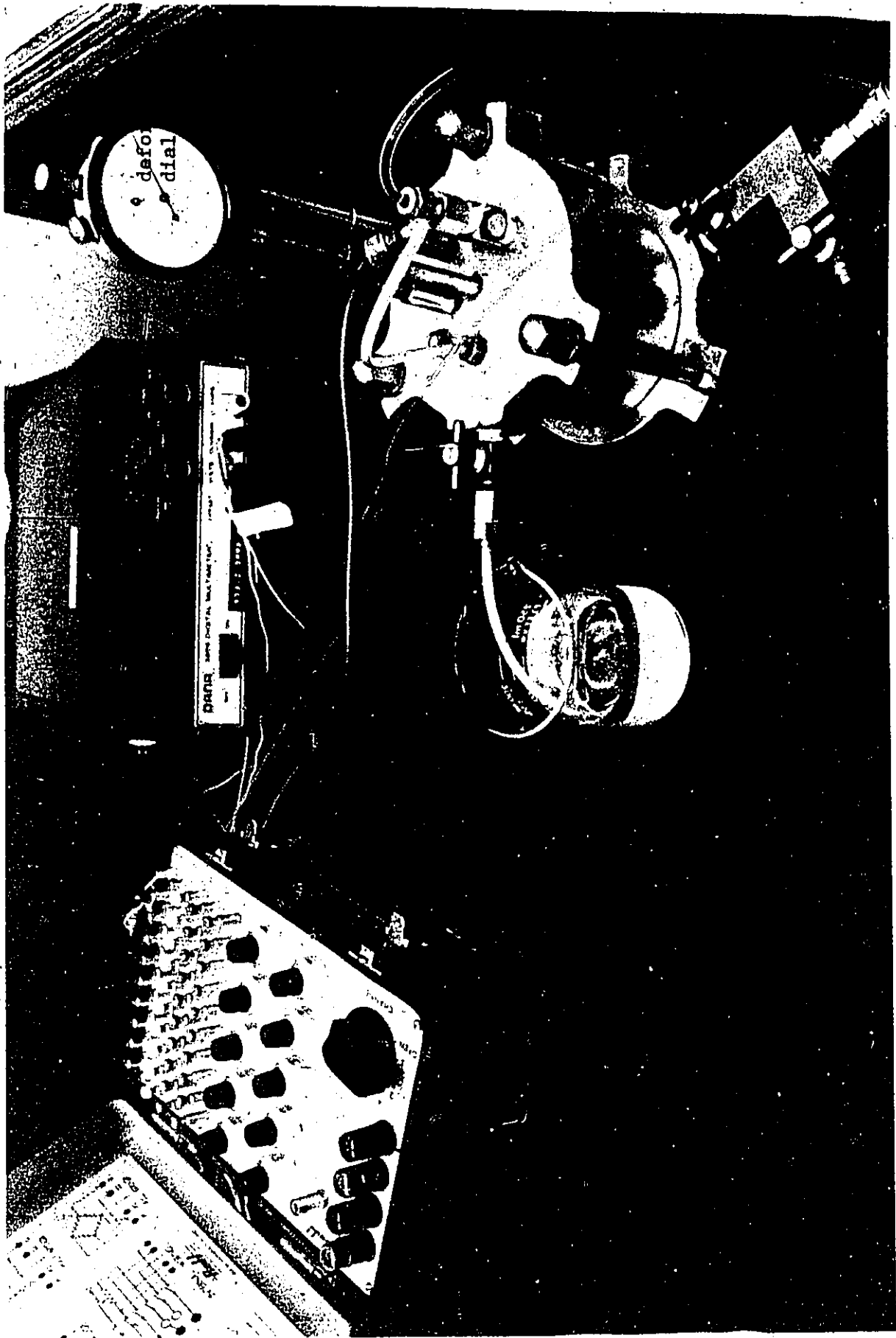


Figure D.6 Experimental Set Up for a Controlled Gradient Consolidation Test

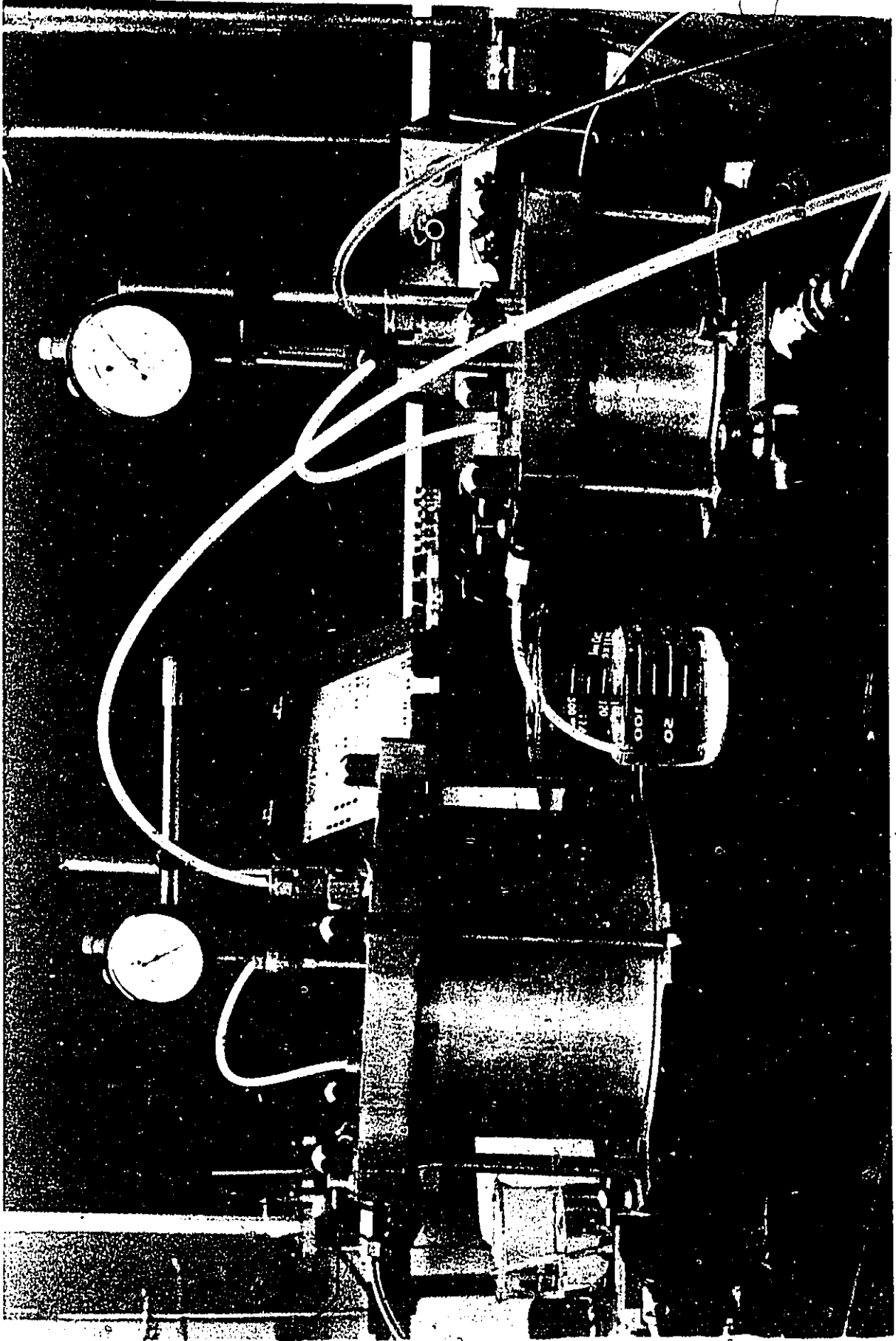


Figure D.7 Controlled Gradient Consolidation Tests in Progress in 3 in and 6 in diameter cells

4

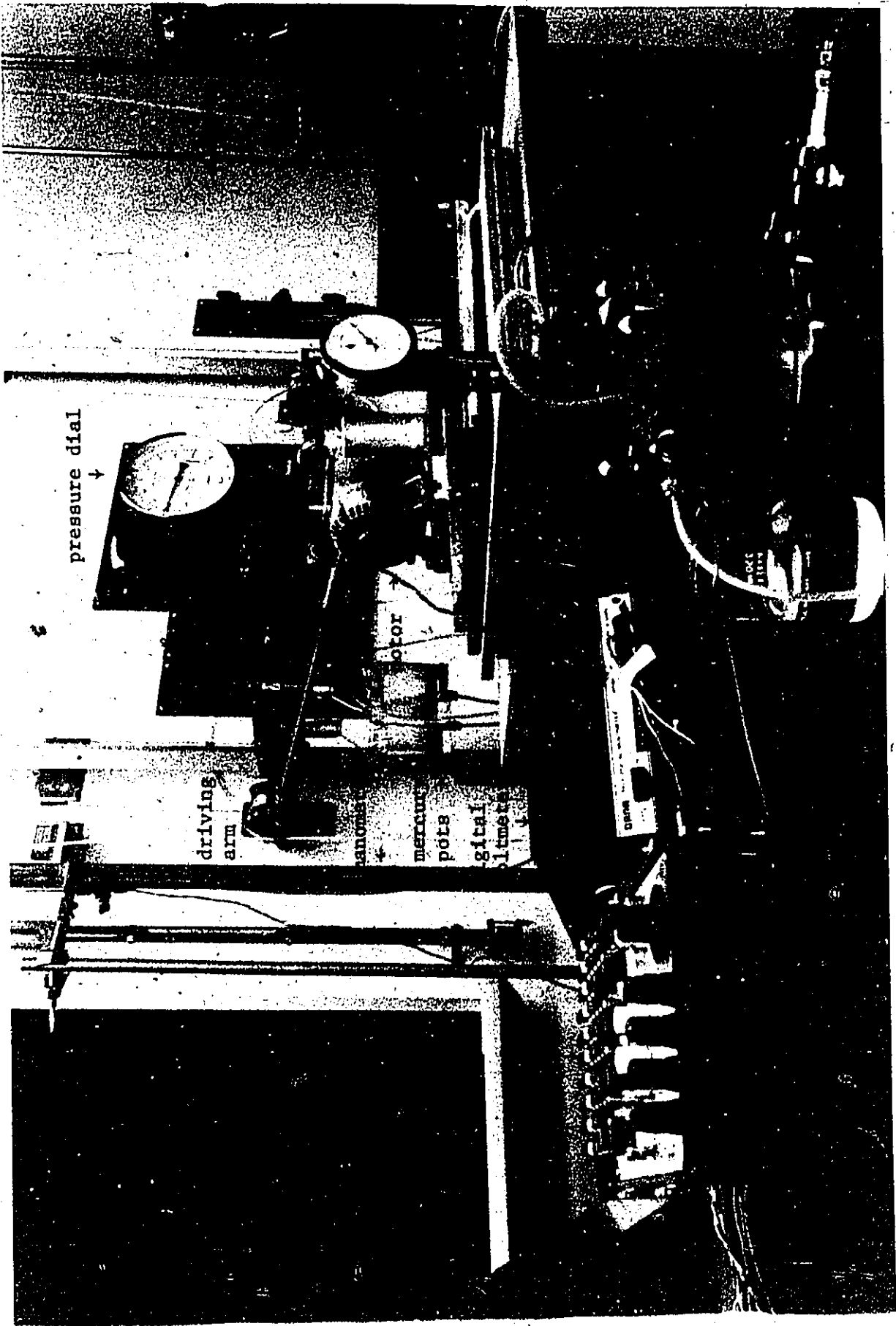


Figure D.8 Automatic Control System used to run the Controlled Gradient Tests